

Beam Orientation Selection in Radiotherapy Treatment Planning

ISBN: 90-8559-199-6

Druk: Optima Rotterdam

© Copyright: 2000 IOP Publishing Ltd. (chapter 2)

© Copyright: 2003 Elsevier Inc. (chapter 3)

© Copyright: 2005 Elsevier Ireland Ltd. (chapter 4)

© Submitted (chapter 5)

Beam Orientation Selection in Radiotherapy Treatment Planning

Bundelhoek keuze bij het maken van een bestralingsplan.

PROEFSCHRIFT

ter verkrijging van de graad van doctor
aan de Erasmus Universiteit Rotterdam
op gezag van de rector magnificus

Prof.dr. S.W.J. Lamberts

en volgens het besluit van het College voor Promoties.

De openbare verdediging zal plaatsvinden op
woensdag 20 september 2006 om 13:45 uur

door

Evert Woudstra

geboren te Den Haag

Promotiecommissie

Promotoren: Prof.dr. B.J.M. Heijmen
Prof.dr. P.C. Levendag

Overige Leden: Prof.dr. W.J. Niessen
Prof.dr.ir. A.W. Heemink
Prof.dr. S. Vynckier

This thesis has been prepared at the Department of Radiation Oncology, Division of Medical Physics, Erasmus MC/Daniel den Hoed Cancer Center, Rotterdam, The Netherlands.

Address for correspondence:

E. Woudstra, Department of Radiation Oncology, Division of Medical Physics, Erasmus MC/Daniel den Hoed Cancer Center, Groene Hilledijk 301, 3075 EA Rotterdam, The Netherlands.

Phone: +31.10.4391381. Fax: +31.10.4391012. E-mail: e.woudstra@erasmusmc.nl

*Sarah said: 'God hath made me to laugh,
so that all that hear will laugh with me.'
Holy Bible, Genesis 21:6*

Contents

Chapter 1	Introduction	3
1.1	Radiation therapy	4
1.2	Sequential orientation selection used in daily forward treatment planning.....	5
1.3	Automated sequential orientation selection with ‘Cycle’	8
Chapter 2	Constrained treatment planning using sequential beam selection	11
Abstract.....		12
2.1	Introduction	12
2.2	Method	13
2.3	Results	19
2.4	Discussion	28
Chapter 3	Automated beam angle and weight selection in radiotherapy treatment planning applied to pancreas tumors.....	33
Abstract.....		34
3.1	Introduction	34
3.2	Methods and Materials	36
3.3	Results	43
3.4	Discussion	48
3.5	Conclusions	51
Chapter 4	Automated selection of beam orientations and segmented intensity modulated radiotherapy (IMRT) for treatment of oesophagus tumors	53
Abstract.....		54
4.1	Introduction	55
4.2	Methods and Materials	56
4.3	Results and discussion.....	60
4.4	Conclusions	65

Chapter 5	Comparison of an algorithm for automated sequential beam orientation selection with exhaustive search and simulated annealing	69
Abstract.....		70
5.1	Introduction.....	70
5.2	Methods.....	72
5.3	Results.....	80
5.4	Discussion	84
5.5	Conclusion.....	86
Chapter 6	General discussion.....	89
6.1	Introduction.....	90
6.2	Sequential beam selection	90
6.3	Hard constraints.....	91
6.4	IMRT and beam orientation selection	92
6.5	Clinical implementation	93
Summary		95
Samenvatting.....		99
Acknowledgements.....		103
Curriculum vitae		106

CHAPTER 1
INTRODUCTION

1.1 Radiation therapy

Radiation therapy is a treatment modality using ionising radiation in the treatment of patients with cancer. The treatment aims to deliver a precisely specified quantity of radiation dose to a defined target volume with as minimal as possible damage to the healthy surrounding tissues. The clinical aim with curative intention is the eradication of the tumour, resulting in prolonged survival with good quality of life. The total radiation dose is administered in up to 40 daily fractions. This fractionation scheme reduces the occurrence of severe treatment related morbidity. During the successive fractions, the number of tumour cells is gradually reduced.

Nevertheless, radiation therapy will inevitably result in some early and late complications. In a curative setting, a significant level of side effects may be acceptable as long as the aim to deliver the highest possible dose to the target volume to ensure local control can be achieved. In practice, the therapy is aimed at minimisation of side effects while simultaneously maximising the probability of tumour control. Trade-off decisions are based on clinical experience with dose delivery to large patient groups as e.g. reported in the literature.

In the treatment preparation phase, patient immobilisation devices may be produced to assure reproducibility in the daily set-up of the tumour relative to the treatment beams. CT and/or MRI scans are then acquired. These scans are used as a three-dimensional anatomical patient model for the design of a treatment plan, i.e.: the optimal beam orientations, beam intensities, etc. and the corresponding calculated dose distribution.

Both the target volume (the so-called ‘planning target volume’ or PTV) and the organs at risk (OAR) are delineated in the scans. The PTV contains the volume of visible tumour, volumes suspect for tumour cells, and finally an additional margin to account for possible errors in reproducibility of patient position and movement of the tumour during the treatment sessions.

A standard method used in treatment plan design is to select radiation beams from several directions. As a consequence, the PTV receives a dose contribution from all beams and organs at risk are (partially) avoided, resulting in a substantial reduction in the volume receiving a high dose. For tumour sites such as e.g. prostate, rectum and mamma this approach has resulted in more or less standardized beam configurations, the so-called ‘class solutions’, that are applied to the majority of the patients with only small adjustments regarding beam orientation and beam intensity. For other tumour sites, position and size of the delineated PTV and the organs at risk may be very

different between patients. For such tumour sites class solutions with fixed beam orientations may result in treatment plans of sub-optimal quality and customisation of treatment plans is unavoidable.

Daily experience in treatment planning reveals difficulties to meet dose prescriptions for cases where small and sensitive organs at risk are in close proximity of a large PTV or in cases where many sensitive organs at risk enclose the delineated PTV. E.g. for a pancreas tumour with kidneys, liver and small bowel in close proximity or oesophagus tumours in between the lungs and near the spinal cord, it may be very time consuming to find an acceptable solution with the common manual trial-and-error method for beam orientation selection. Moreover, if a suitable solution cannot be found, one can never guarantee that an acceptable plan really does not exist. The reason is that the final dose distribution is largely dependent on the number of beams, the orientation of each beam and the applied beam intensity profile. This generates a large degree of freedom in treatment planning that can hardly be overviewed by a human planner. During the last decade, much effort has been put into mathematical optimisation of these treatment plan parameters.

Development of optimisation techniques was greatly influenced by the introduction of intensity-modulated radiation therapy (IMRT). IMRT optimises the beam intensity profiles for a selected combination of beam orientations. IMRT offers a greater dose shaping potential than conventional uniform and wedged beam therapy. This dose shaping is of particular interest when the high dose region should be conformed more closely to a concave shaped PTV because of an organ at risk situated in the cavity. Because of the huge number of degrees of freedom, the modulation of the intensity profiles can only be derived using an optimisation algorithm. A remaining question is whether the selected beam combination is optimal for a specific treatment planning case and whether customisation of orientation selection is required to further improve the quality of the treatment plan.

1.2 Sequential orientation selection used in daily forward treatment planning.

As mentioned above, for some tumour sites a class solution approach may result in acceptable treatment plans. Other tumour sites need customisation of beam directions, mainly caused by the patient dependent position and size of the PTV. The treatment planning problem for these sites becomes even more complex when the PTV is

enclosed by many sensitive OARs having substantially different tolerance levels. Some examples are:

- the mediastinum or oesophagus enclosed by lungs and the spinal cord,
- stomach and pancreas enclosed by kidneys, liver, small bowel and spinal cord,
- the nasal cavity enclosed by the eyes, optical nerve and chiasm.

In these cases, one beam direction is largely preferred. From clinical experience with forward treatment planning of such cases it was concluded that the best way to find a promising dose distribution is to carefully select the orientation of this first beam and to enhance the existing distribution by sequential addition of beams with significantly lower beam weight. This method was applied in our radiotherapy department with substantial benefit. Two clinical examples are given below:

In Figure 1.1, a large stomach tumour was to be irradiated to 50 Gy and special attention was asked for the kidneys. In order to maintain the dose to the kidneys as low as possible the best direction to start with, is from the left lateral direction. The

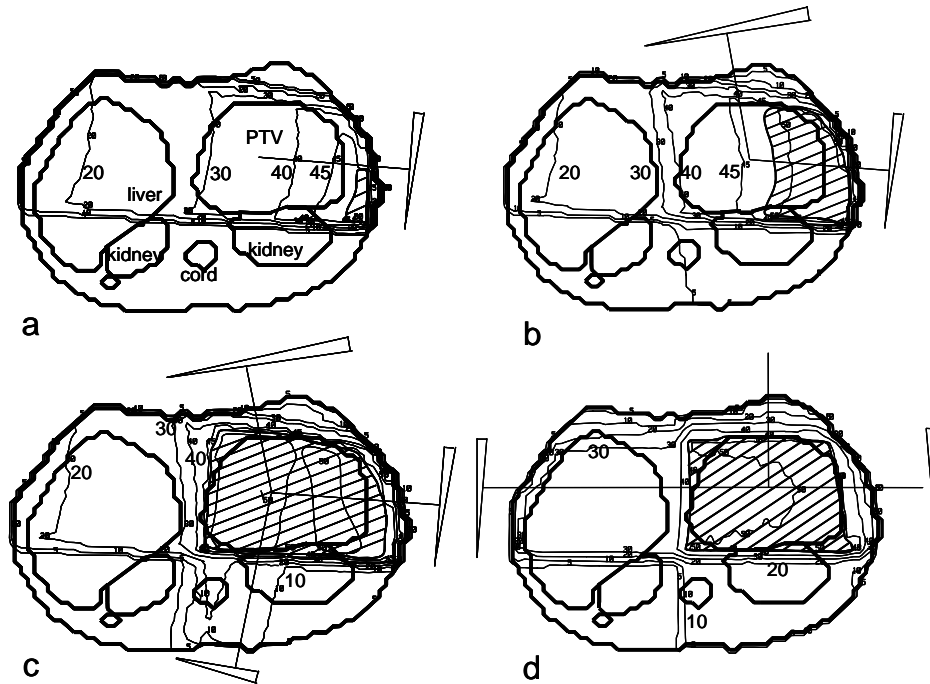


Figure 1.1 Sequential search of beam orientations and beam weights. The shaded areas have a dose larger than 95% of the prescribed tumor dose. Isodoselines: 5, 10, 20, 30, 40, 45 and 50 Gy.

corresponding dose distribution is shown in Figure 1.1a. This beam delivers 73% of the prescribed mean PTV dose and largely avoids both kidneys. The shaded area in Figure 1.1a shows a small area with a dose larger than 95% of the prescribed tumour dose. A large part of the remaining prescribed PTV dose is added through a beam with much lower beam weight from almost anterior direction (Figure 1.1b). In this beam a wedge is applied to change the beam intensity profile for improved dose uniformity in the PTV. Because of the low PTV dose contribution (16%) of this second beam, also the dose level to the left kidney is limited. The PTV dose contribution from the second beam is visualised by the extension of the shaded area (Figure 1.1b). As after addition of the second beam only the medial part of the PTV is still slightly under-dosed, the third beam does not need to completely cover the PTV. In a compromise between PTV dose homogeneity and the dose to the left kidney, an orientation is selected more or less between the kidneys. A dose contribution to the PTV of only 11% of the prescribed dose finalises the required PTV dose uniformity (Figure 1.1c).

Figure 1.1d provides the comparison with a distribution using equal beam weights and more traditional beam orientations. The comparison shows that the dose levels in the

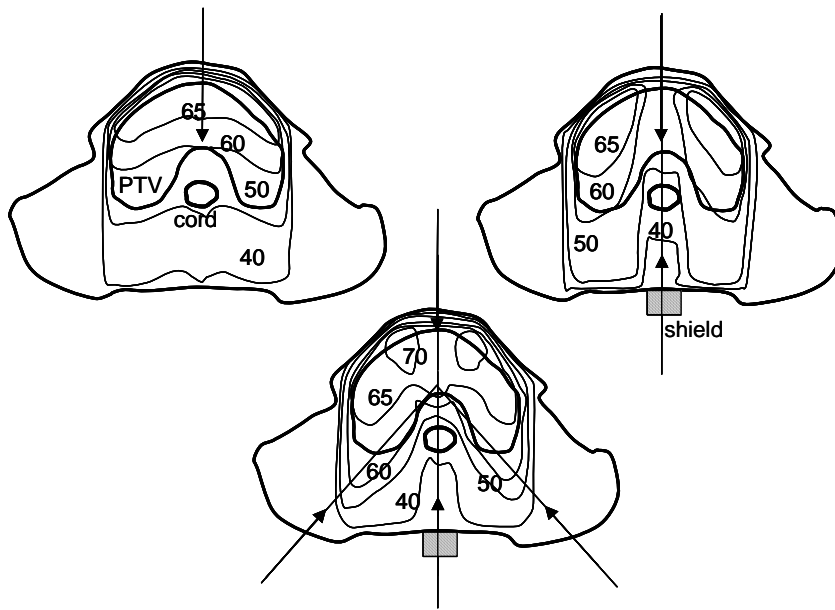


Figure 1.2 Sequential selection of beam orientations and beam weights for a hoarse-shoe like target volume.

organs at risk from sequential selection plan are lower for the left kidney and the liver.

Figure 1.2 presents a second, somewhat more generalised, example of sequential treatment planning in practice. A thyroid tumour with concave shape should receive 70 Gy, while the spinal cord dose should be kept below 50 Gy. Because the PTV extends to almost the surface of the patient and the organ at risk is behind the PTV, the beam for application of the largest dose is the anterior beam (68% of the prescribed PTV dose). The dose level is increased further in the lateral parts of the PTV through a low weight posterior beam with the spinal cord shielded (16% of the prescribed PTV dose). The remaining underdosage in the medial part of the PTV is ‘corrected’ through two laterally oblique beams with low weight (16% of the prescribed PTV dose). Although this distribution is far from optimal, compared with current IMRT-results, this example emphasises that the sequential selection approach appears to be able to design non-standard dose distributions even when only simple means are available.

The sequential selection method has proven to be effective and favourable for many non-standard cases through years of treatment planning experience. This method, using dose addition to improve the depth dose of a single beam dose distribution, was mentioned already long ago by Kahn (1) and potential and variables of influence were investigated and described by Woudstra (2).

The favourable dose distributions from this approach raised the question whether this idea of ‘sequential beam selection’ could be worked out in a more general way and could be generalised in an algorithm and be applied for computerised generation of treatment plans.

1.3 Automated sequential orientation selection with ‘Cycle’

In this thesis an algorithm, designated Cycle, has been developed to automatically generate an ‘acceptable’ plan for each patient. An acceptable plan delivers the prescribed PTV dose while strictly obeying imposed hard constraints for organs at risk and for dose homogeneity in the PTV. Only dose and dose-volume based constraints have been used, e.g. on the maximum dose in an OAR, or on the maximum volume of an OAR that may receive a defined dose level. Starting with an empty plan (no beams), Cycle sequentially adds beams until the target dose has been reached within the imposed hard constraints. Beams are selected from a large set of input orientations. Using Cycle, it is not required to define the number of beams for the plan in

advance. Only the most efficient orientations from the input set will survive the selection procedure. Selection from a larger set of input orientations does not necessarily result in a plan with more orientations but in a more proper orientation selection. A priori assumptions regarding beam orientations are not required.

Chapter 2 describes the basic features of Cycle. Here, beams are assumed to have a uniform intensity profile. For each patient, the input set consists of pre-calculated three-dimensional dose distributions for generally 36 coplanar, equi-angular beams (10 degrees intervals). Starting with an empty plan (no selected beams), the algorithm generates a treatment plan by sequentially adding beams/dose from the potential input orientations until the prescribed target dose has been reached, and as long as none of the imposed hard constraints has been violated. For the selection of each new beam to be added, all available 36 orientations are reviewed; the orientation to be selected has the best compromise between the PTV dose increase, and the unavoidable further approach towards the imposed hard constraints. To avoid generation of sub-optimal plans, each new beam is added with a low weight. Favorable beam directions are then selected several times.

Sequential selection of beams is performed using a ‘dynamic’ score function. The meaning of the word ‘dynamic’ is twofold. Firstly, after each new beam selection the total dose distribution delivered so far is updated by adding the dose contribution from the new beam. Before selection of the next beam the score function is adapted to the updated dose distribution. Secondly, at the start of the beam selection process, the score function has equal penalty factors for approaching each of the various constraints. In case these initial factors do not result in a plan that delivers the prescribed tumour dose without violating constraints, the algorithm calculates new factors and generates a new plan. The new penalty factors favour selection of orientations that better avoid constraints that were violated in the previous run.

Chapter 3 describes investigations on the value of Cycle for 3DCRT in pancreas patients. Apart from the beam with a uniform profile, for each input beam orientation there are now also beams with wedges in four wedge directions. Cycle has been extended with options to minimise the selected number of beams, and to escalate the PTV dose. For five patients, comparisons were made between clinical plans and plans obtained by Cycle with the same beam number. The influence of beam number reduction on the plan quality was studied. For each patient the potential for dose escalation was investigated. The escalated plans obtained by selection from the full input beam set with 36 input directions were compared with the escalation results

from equi-angular subsets of the full input set.

Chapter 4 describes the extension of Cycle for segmented IMRT and the application for irradiation of oesophagus tumours. Segmented IMRT means that apart from the uniform and wedge beams that cover the full PTV projection, beam segments are added to each input direction, to allow dose delivery with (partial) shielding of organs at risk. For five oesophagus cases, Cycle was used to investigate the value of beam orientation selection in combination with segmented IMRT. Some commercial IMRT algorithms did unexpectedly yield increased mean lung dose values, when the number of input orientations was increased from four to nine. Because these commercial algorithms applied DVH-points as constraints, Cycle was also used to investigate whether this observation was caused by the indirect mean lung dose reduction by means of DVH-point minimisation.

Chapter 5 investigates whether Cycle does indeed find an acceptable solution if such a solution exists. To study this question, for 10 patients the prescribed PTV dose was stepwise increased, each time followed by a plan generation by Cycle. This process was stopped when Cycle was no longer able to generate an acceptable plan, i.e. deliver the (escalated) prescribed PTV dose while not exceeding the prescribed hard constraints. Plans were then generated with an exhaustive search algorithm (ES) and with Fast Simulated Annealing (FSA) to find out whether acceptable solutions with this maximum PTV dose did indeed not exist.

References

- 1 *F.M. Kahn, The Physics of Radiation Therapy, 2nd edition 1994, pp 254*
- 2 *E. Woudstra, Improvement of depth dose distributions by addition of small doses from laterally incident beams. Radiother Oncol 1988; 13: 31-39*

CHAPTER 2
CONSTRAINED TREATMENT PLANNING USING SEQUENTIAL BEAM
SELECTION

E. Woudstra and P.R.M. Storchi: Phys. Med. Biol. **45**, 2133-2149, 2000

ABSTRACT

In this paper an algorithm is described for automated treatment plan generation. The algorithm aims at delivery of the prescribed dose to the target volume without violation of constraints for target, organs at risk and the surrounding normal tissue. Pre-calculated dose distributions for all candidate orientations are used as input. Treatment beams are selected in a sequential way. A score function designed for beam selection is used for the simultaneous selection of beam orientations and weights. In order to determine the optimum choice for the orientation and the corresponding weight of each new beam, the score function is first redefined to account for the dose distribution of the previously selected beams. Addition of more beams to the plan is stopped when the target dose is reached or when no additional dose can be delivered without violating a constraint. In the latter case the score function is modified by importance factor changes to enforce better sparing of the organ with the limiting constraint and the algorithm is run again.

2.1 Introduction

The goal of conformal radiotherapy is to shape the 3-dimensional high dose region as close as possible to the target volume in order to minimise dose delivery to healthy tissues. This can be achieved by selection of appropriate beam orientations, adequate field shapes, beam weights and modulated intensity patterns. Especially if a clinical target volume is surrounded by a large number of organs at risk, the determination of these parameters may be very difficult for a human planner and will generally take a large amount of time. Therefore, extensive research has been performed on computer optimisation of treatment plans. Brahme (1988), Bortfeld *et al* (1990), Spirou and Chui (1998), Wang *et al* (1995) and Xing *et al* (1999) have developed methods for optimisation of beam intensity profiles for previously selected beam orientations. Webb (1989, 1991, 1992 and 1994), Morrill *et al* (1991 and 1995), Bortfeld and Schlegel (1993), and Mageras and Mohan (1993) have investigated the use of simulated annealing for automated selection of beam angles and beam weights or intensity modulated profiles. Söderström and Brahme (1993) searched for the best orientations using inverse planning and explored the P^+ space for a large number of beam combinations. Rowbottom *et al* (1998 and 1999) have studied customisation of beam directions using simulated annealing and Ezzell (1996) and Langer *et al* (1996) used genetic algorithms for treatment planning optimisation.

In this paper, we have described an algorithm, which aims at the generation of treatment plans, which obey prescribed ‘hard’ constraints for dose distributions in target and organs at risk (e.g.: target dose homogeneity, dose-volume constraints for organs at risk), while trying to reach the prescribed mean target dose. Although not limiting for the method, during this research, we have focused on coplanar treatments with uniform beams.

The automatic treatment plan generation selects beams (orientations) and corresponding weights sequentially. For each new beam selection, all orientations are scored regarding the optimally applied weight, and only that orientation, having the largest score, is added to the already existing treatment plan. The plan generation process is stopped when the prescribed target dose is reached or if any constraint is violated. If the plan generator is not successful, the importance factors of the score function are adapted and a next generation will be carried out. In this way the score function is adapted to force the plan generation as close as possible towards the dose prescription. A major difference with many methods presented so far is, that we do not use an objective function for the full plan, but a score function for each separate beam selection.

2.2 Method

2.2.1 Pre-calculation

Treatment plan generation is performed using sequential selection of beam orientations. In order to improve the speed of this process for each case, we have used pre-calculated single beam dose distributions for 36 orientations with 10 degrees interval on the full coplanar orientation range. These unit weight three-dimensional dose distributions $U_\theta(x, y, z)$ have the following properties:

1. BEV field shape with 0.5 cm margin around the projected target.
2. Coplanar, isocentric, flat intensity beams.
3. Heterogeneity corrected, using an effective path length method.
4. Unit beam weight is defined to be 1 Gy at d_{max} at source axis distance.

For treatment plans, a dose distribution is computed as a linear combination of weighted pre-calculated dose distributions, according:

$$D(x, y, z) = \sum_{\theta_i} w_{\theta_i} \cdot U_{\theta_i}(x, y, z) \quad (1)$$

From this dose distribution and the position of target and organs at risk, dose distribution quantities such as minimum and mean target dose: $D_{min,T}$, $D_{mean,T}$, maximum dose to normal tissue: $D_{max,N}$, mean and maximum dose to specified OARs: $D_{mean,Ri}$, $D_{max,Ri}$, and DVH-points, $D_{Vdef,Ri}$ i.e. the dose corresponding with a defined volume are extracted for use in the beam weighting, scoring, evaluation and selection process as described in the next section.

2.2.2 Plan generation

The plan generation algorithm is a sequential search method for the selection of beam orientations θ_k and weights w_k , where k is the sequential number of the selected beams, starting with $k = 1$ for the first beam. For each subsequent beam k , the plan generation algorithm uses a score function $S_k(\theta, w)$. $S_k(\theta, w)$ is constructed using the initial dose prescription and the dose distribution quantities of target and organs at risk due to the previous $k - 1$ beams and importance factors. Details on the selection and composition of $S_k(\theta, w)$ will be explained in section 2.2.3.

For the selection of the k th beam, the first step is the determination, for all θ in the interval $[0^\circ, 360^\circ]$, of the beam weight $w_{max}(\theta)$, which maximises $S_k(\theta, w)$. For each θ , this is done by addition of the unit dose distribution of orientation θ , multiplied by weight w , to the plan with the $k - 1$ previous beams, followed by weight optimisation until $S_k(\theta, w)$ reaches its maximum: $S_k(\theta, w_{max})$. This weight optimisation of $S_k(\theta, w)$ is performed using 3 subsequent numerical evaluations of $S_k(\theta, w)$ with refined resolution of the weight step size (final resolution: 0.1 Gy).

The second step is the determination of the specific orientation θ_k and $w_{max}(\theta_k)$, for which $S_k(\theta, w_{max})$ is maximum. The dose distribution of orientation θ_k and weight $w_{max}(\theta_k)$, is added to the plan followed by $S_{k+1}(\theta, w)$ definition and the selection of a new beam direction ($(k+1)$ th beam) can start. It may happen that the beam direction of the k th beam has already been chosen for a previous beam. In that case the beam weights are added together.

The beam selection (and addition) is repeated until the prescribed mean dose in the PTV has been reached within 1%, or a specified constraint for one or more organs at risk has been reached. In this latter case new importance factors are calculated based on the previously generated plan and a following plan generation process can start.

2.2.3 Score function

In order to optimise the weight for a beam orientation we need a function that balances the target dose against the dose to OARs, in relation to the dose prescription. Such a balance is very well present in score functions of the form as described by Mohan *et al* (1992):

$$F = P_{tc} \cdot \prod_i (1 - w_i \cdot P_{ntc,i}) \quad (2)$$

This function represents an increasing tumor control probability multiplied by many decreasing factors due to normal tissue complication probabilities. We have modified this type of function for a dose based weight optimisation and replaced the $P_{ntc,i}$ by the ratio between the dose distribution quantity and its constraint and the P_{tc} by the ratio of the mean target dose and the prescribed dose. We have put the importance factor as a power for each factor used. The modified function is shown in Equation (3).

$$\begin{aligned} S_k(\theta, w) = & \frac{D_{mean,T}^{(k)}(\theta, w)}{D_{pre,mean,T}^{(k)}} \cdot \left(1 - \frac{D_{dif,T}^{(k)}(\theta, w)}{D_{tol,dif,T}^{(k)}} \right)^{P_o P_{dif,T}} \cdot \left(1 - \frac{D_{max,N}^{(k)}(\theta, w)}{D_{tol,max,N}^{(k)}} \right)^{P_o P_{max,N}} \\ & \cdot \prod_{i=1}^{n_R} \left[\left(1 - \frac{D_{mean,R_i}^{(k)}(\theta, w)}{D_{tol,mean,R_i}^{(k)}} \right)^{P_o P_{mean,R_i}} \cdot \left(1 - \frac{D_{max,R_i}^{(k)}(\theta, w)}{D_{tol,max,R_i}^{(k)}} \right)^{P_o P_{max,R_i}} \right] \\ & \cdot \prod_{i=1}^{n_R} \left[\left(1 - \frac{D_{Vdef,R_i}^{(k)}(\theta, w)}{D_{tol,Vdef,R_i}^{(k)}} \right)^{P_o P_{Vdef,R_i}} \right] \end{aligned} \quad (3)$$

Only the first term of Equation (3) is due to the mean target dose and represents the increasing part of the score as function of beam weight w . All remaining terms are the decreasing terms due to the constraints. An advantage of this form of the score function is, that whatever dose quantity reaches its constraint, the score value will be 0. This is required to guarantee that none of the constraints will be violated. A requirement due to sequential search is, that for each new sequence number k , the score function must be redefined. The score function will account for the already existing dose distribution of the previously selected $k - 1$ beams and therefore also for the duty for beam k , to balance the target dose which is still to be applied, to the dose which is still allowed to burden the organs at risk. $D^{(k)}$ stands for the redefini-

tion. $D^{(k)}$ means that we consider the dose difference of a specific dose distribution quantity due to the k beams (k is the beam number of which the orientation is under selection) in the plan, minus the same dose distribution quantity due to the $k-1$ already existing beams in the plan. In formula for e.g. the maximum dose for OAR R_i we have:

$$D_{\max, R_i}^{(k)}(\theta, w) = D_{\max, R_i}^{(k)}(\theta, w) - D_{\max, R_i}^{(k-1)} \quad (4)$$

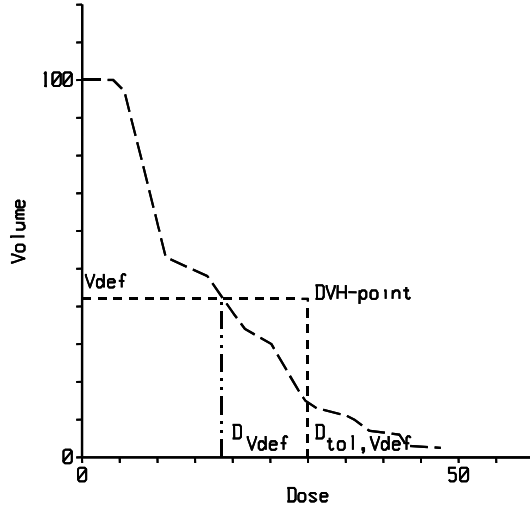


Figure 2.1 Dose volume histogram indicating the implementation of DVH constraints. A DVH-constraint is defined by a relative volume V_{def} and a dose value $D_{\text{tol}, V_{\text{def}}}$. The actual dose $D_{V_{\text{def}}}$ should be kept below the tolerance value $D_{\text{tol}, V_{\text{def}}}$.

defined volume V_{def} of organ R_i (see Figure 2.1). This dose value should always be kept below the constraint value $D_{\text{tol}, V_{\text{def}}, R_i}$.

In the same way, as for the considered dose distribution quantities we also have the constraints, e.g.: $D_{\text{tol}, \max, R_i}$ etc. These tolerances are redefined in the same way as the dose distribution quantities. For the first beam ($k=1$), $D_{\text{tol}, \max, N}^{(1)}$, $D_{\text{tol}, \max, R_i}^{(1)}$, and $D_{\text{tol}, \max, R_i}^{(1)}$ are the constraint values given by the physician. For the following beams ($k > 1$), e.g. $D_{\text{tol}, \max, R_i}^{(k)}$ is calculated as follows:

For the normal tissue N , i.e.: the tissue inside the body volume but outside the target and OARs, we only consider the maximum dose, $D_{\max, N}$. For the target we consider the mean dose and the homogeneity $D_{\text{dif}, T}$. $D_{\text{dif}, T}$ is the difference between the mean target dose and the minimum target dose. For the organs at risk we consider the mean dose and the maximum dose, respectively: D_{mean, R_i} , D_{\max, R_i} and a dose-volume constraint D_{V_{def}, R_i} : the dose level for a

$$D_{tol,max,R_i}^{(k)} = D_{tol,max,R_i}^{(1)} - D_{max,R_i}^{(k-1)} \quad (5)$$

$D_{pre,mean,T}^{(k)}$ is computed in a similar way as the constraint for mean dose in an organ at risk. $D_{pre,mean,T}^{(1)}$ is the target dose prescribed by the physician. Note, that $D_{pre,mean,T}^{(k)}$ does not play a real role in the selection of the beam direction and weight, because it does not influence the shape of the score function. $D_{pre,mean,T}^{(k)}$ is used to have a score that is without dimension.

The score parameter p_o and the importance factors p_{mean,R_i} , etc., control the plan generation process. Their introduction follows from two considerations on the score formula:

1. It should be possible to modify the balance between the increasing factor in the score due to the target dose and the decreasing factors due to the dose to the organs at risk. This is done by the introduction of the p_o -value, which is used as an overall score parameter and has the same value for all decreasing score factors.
2. It should be possible to modify the importance of a dose distribution quantity used in the score function, because we want to be able to emphasize specific factors in the decreasing part of the score function. This has led to the introduction of p_{mean,R_i} etc. The relative increase of a specific importance factor will force the algorithm to select orientations that avoid the growth of the accompanying dose distribution quantity. Because the number of the criteria used, is not allowed to change the mentioned overall balance in the score, their importance values have been ‘normalised’ according:

$$p_{max,N} + p_{dif,T} + \sum_i (p_{mean,R_i} + p_{max,R_i} + p_{Vdef,R_i}) = 1 \quad (6)$$

2.2.4 Iterative dose optimization

The prescribed target dose can only be obtained if the plan generation process is not stopped by a violation of one of the constraints. If the initial guess of importance factors has stopped the generation process too early by a constraint violation instead of reaching the target dose, apparently the dose distribution parameter for this violated

constraint should be even more reduced during the second generation. Therefore, the plan generation process has been included in an iterative procedure, where importance factors can be changed. This is in some way similar to the recent publication of Xing *et al* (1999). The importance factors are changed in such a way that the plan generation process is forced to reduce the dose to the limiting constraint and to spread the unwanted dose to other constraints that were not violated in the previous plan generation. A plan generation procedure may therefore consist of a few plan generations with improved importance factors.

The first plan generation starts with equal importance factors for all constraints used. If, by a constraint level hit, the prescribed target dose has not been reached, new importance factors are calculated, based on the dose values to the organs at risk of the previous plan generation. In order to evaluate the quality of the generated plan, we scale the generated dose distribution to the prescribed target dose, using:

$$D_{\text{scaled}}(x, y, z) = \frac{D_{\text{pre, mean, } T}}{D_{\text{mean, } T}} D(x, y, z) \quad (7)$$

where $D(x, y, z)$ and $D_{\text{mean, } T}$ represent the generated dose distribution and the mean target dose from the plan generation respectively. $D_{\text{pre, mean, } T}$ is the initially prescribed mean target dose. This scaling is carried out because of two reasons:

1. If the generation process has been stopped at the constraint hit, it is not known how far this constraint would have been violated for the prescribed target dose. These data are needed to estimate the dose reduction ratio for the corresponding dose quantity during the next generation.
2. Constraints that were not violated in the currently generated dose distribution may appear to be in violation when the distribution is scaled to the prescribed target dose. If this is the case, also for these dose quantities additional dose reduction factors must be estimated.

Using this scaled dose distribution, the scaled distribution quantities for all organs at risk, e.g.: $D_{\text{sc, mean, } Ri}$, etc, and their corresponding constraint violation rates: $D_{\text{sc, mean, } Ri} / D_{\text{tol, mean, } Ri}$ are derived and reviewed. Only if the violation rate for a considered dose distribution quantity is larger than 1, the corresponding importance factor is increased, assuming linearity between the importance factor and the required dose reduction ratio for a specific constraint. This assumption leads to the following expression:

$$p_{mean,Ri}^{(new)} = p_{mean,Ri}^{(old)} \times (1 + \gamma (\frac{D_{sc,mean,Ri}}{D_{tol,mean,Ri}^{(I)}} - 1)) \quad (8)$$

where γ is a relaxation parameter. If during the next plan generation the achieved target dose decreases compared with the previous one, the relaxation parameter γ is multiplied by a factor 0.5. Initial γ - values of 10 to 20 may be used.

The relaxation parameter is used to guide the iteration process. If a constraint is violated and the corresponding importance factor is increased too much, we observe a target dose decrease in the next generation caused by a more early violation of another constraint. Apparently the initial correction had been too large and therefore the value of the correction step size is reduced. The normalization of the importance factors (Equation (6)) will reduce the importance factor for the constraint, that was increased too much, when the importance factor for the other constraint is increased.

2.3 Results

2.3.1 Test cases

A theoretical case is used to illustrate various aspects of the plan generation process. The case (case 1a, shown in Figure 2.2) consists of a target volume and two organs at risk (R1 and R2). For the treatment plan, the requirement is to deliver 50 Gy to the target (T), while the maximum doses to R1 and R2 should be limited to 35 Gy and 45 Gy respectively. In addition, the maximum dose to the normal tissue (N) outside

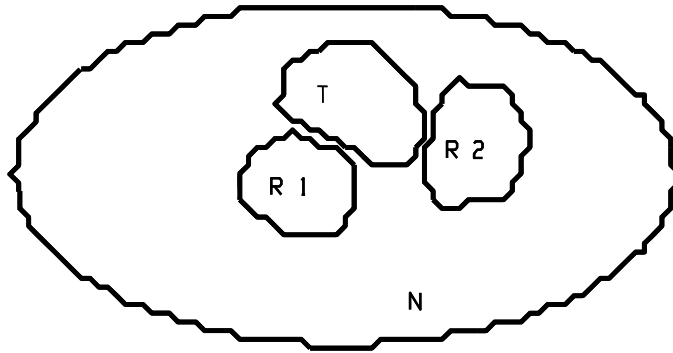


Figure 2.2 An artificial case with a target volume (T) and two organs at risk (R1 and R2) and normal tissue (N).

these regions should not exceed 55 Gy. The score function $S_I(\theta, w)$ with $p_o = 1$ and equal importance factors, as a function of beam weight w , for $\theta = 110^\circ$ and 300° , is given in Figure 2.3. This figure illustrates that the magnitude and the position of the maximum score

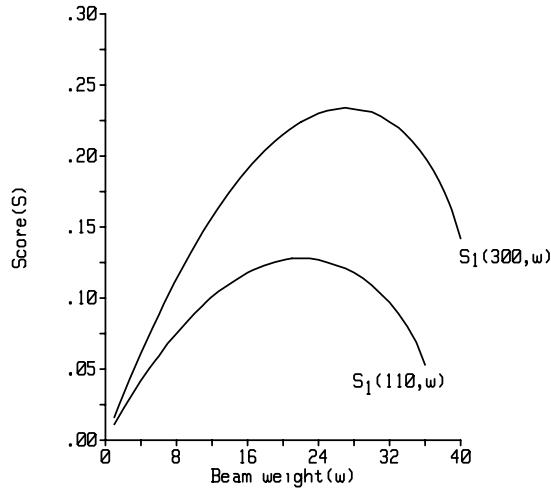


Figure 2.3 Score function as a function of beam weight for two orientations in case 1a.

sequential search for the selection of orientations. The solid line shows the maximum score due to weight optimization, $S_1(\theta, w_{\max})$ for each beam orientation. The orientation with the largest score ($\theta = 300^\circ$), together with its corresponding weight, is the first beam in the plan. Based on the dose distribution quantities resulting from the first beam, $S_2(\theta, w)$ is defined (see the score expressions (3), (4) and (5) in section 2.2.3). $S_2(\theta, w_{\max})$ is shown as a dashed line and has a shape which is significantly different from the one of $S_1(\theta, w_{\max})$ with an overall maximum at $\theta = 180^\circ$. This orientation is

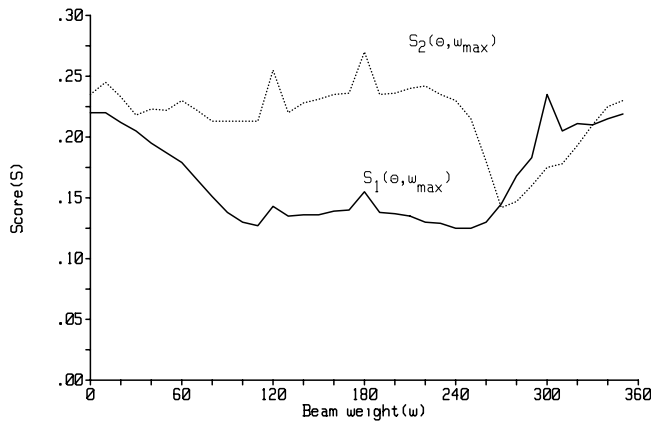


Figure 2.4 Maximum score patterns as function of the available orientations in case 1a for the first beam selection (solid) and for the second selection (dashed).

depends on the orientation of incidence. This dependency on beam orientation is caused by the fact that for each orientation a certain target dose is accompanied by different dose values in the organs at risk. Figure 2.3 does also show that $S_1(\theta, w)$ has a single maximum. This maximum represents the balance between the consequences of an increasing target dose and the increasing dose to the organs at risk. Figure 2.4 shows the procedure of

added to the plan and $S_3(\theta, w)$ is defined to determine the orientation of beam 3 etc.

A drawback of the sequential search may be, that the obtained results are dependent on the initial beam selections. To reduce this effect, the p_o -value was introduced. A large p_o -value

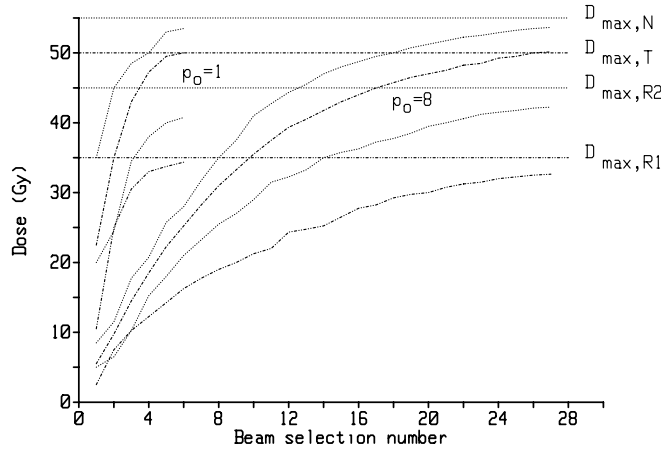


Figure 2.5 Gradual dose growth during plan generation of two values of the overall parameter for case 1a.

orientations to be built gradually and more precisely. In Figure 2.5, dose results for two plan generations for case 1a with equal importance factors and different p_o -values are shown. Due to the relatively large dose step size ($p_o=1$), the observed dose distribution quantities may grow rather irregularly, resulting in a final unequal ‘free space’ (dose difference between the finally generated dose distribution quantities and their constraints). In this example for $p_o=1$, this dose difference for region 1 is much smaller than that for region 2. This free space can be distributed more equally between the dose distribution quantities if a smaller dose step size is used for plan generation. For $p_o=8$, the differences between D_{\max} in R1 and D_{\max} in R2 and their respective constraint levels are more equal than for $p_o=1$. Consequently, more beam selections are needed to achieve the prescribed target dose, improving the possibility to avoid

reduces the weight and thereby the dose step size, which is applied during each beam selection. A consequence is that, if favourite orientations exist for a plan generation, these orientations will be found more times with relative low weight, enabling the total weight of these

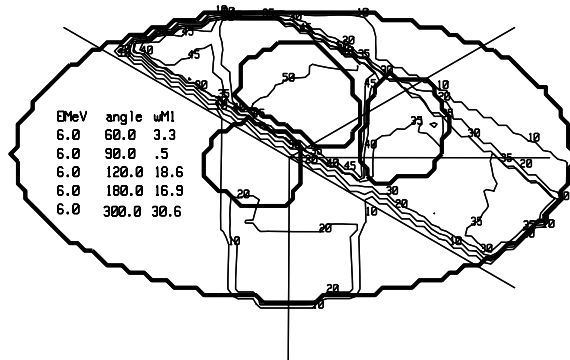


Figure 2.6 Derived distribution for the prescription of case 1a.

violation of the constraints. A repeated selection of the same orientation may occur more frequently. However beam orientations with a relatively low weight may appear in the plan as well. The results of both plan generations are summa-

	Orientations and total weights					Dose distribution quantities		
	60	90	120	180	300	$D_{\max,N}$	$D_{\max,R1}$	$D_{\max,R2}$
$w,(p_o=1)$	4.1		15.0	21.0	29.5	53.5	34.4	40.8
$w,(p_o=8)$	3.3	0.5	18.6	16.9	30.6	53.6	32.6	42.4

Table 2.1 Plan data and dose quantities from two different plan generations.

risied in Table 2.1. The treatment plan for $p_o=8$ is shown in Figure 2.6. For this case, the enforced decrease in dose step-size per selected beam has only led to the introduction of one extra orientation with low weight and to a weight redistribution for the orientations obtained at $p_o=1$.

For case 1a, the dose prescription was quite simple and the target dose could be reached using only one single plan generation as described in section 2.2.2. To show the use of the importance factors in the iterative procedure, mean dose constraints were added. These mean dose levels for regions 1 and 2 were set to values of 18.5 and 20 Gy respectively, while the maximum dose in these regions should be kept below 45 Gy (case 1b). This appeared to be such a strong requirement, that the plan generator could hardly achieve the prescribed target dose. Figure 2.7 shows the effect of p_o on the iteration procedure. The clear disadvantage of $p_o=1$ is that the iteration procedure is not very well controllable. Even after 9 iterations the prescribed mean target dose cannot be achieved within 1% (48.9 Gy). Better results are obtained using p_o -

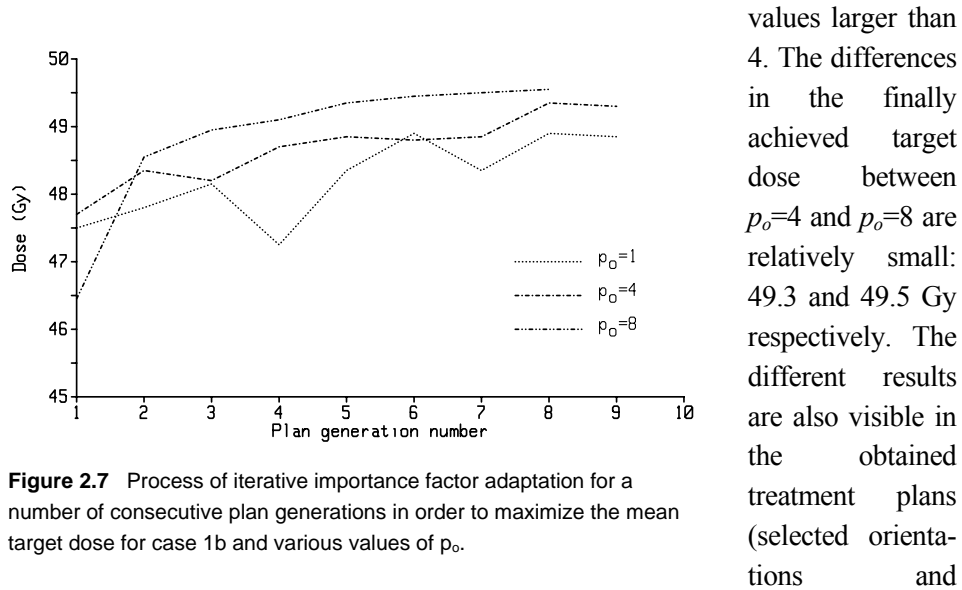


Figure 2.7 Process of iterative importance factor adaptation for a number of consecutive plan generations in order to maximize the mean target dose for case 1b and various values of p_o .

values larger than 4. The differences in the finally achieved target dose between $p_o=4$ and $p_o=8$ are relatively small: 49.3 and 49.5 Gy respectively. The different results are also visible in the obtained treatment plans (selected orientations and

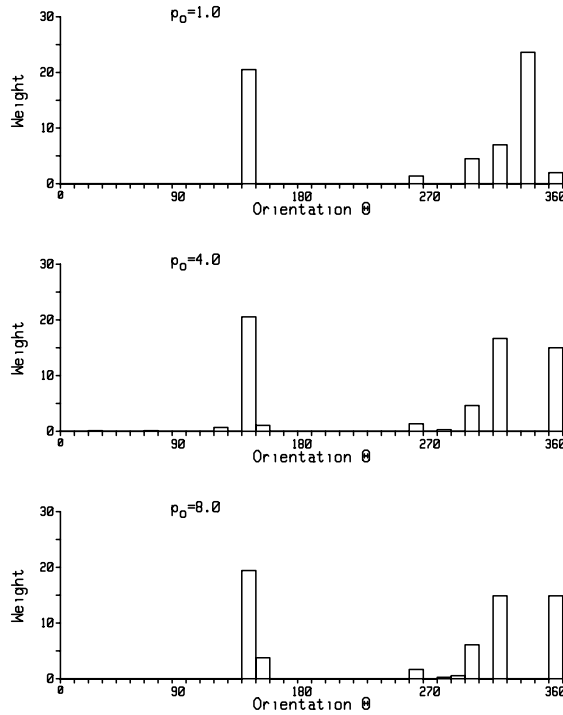


Figure 2.8 Final plan parameters (orientations and weights) for case 1b after iterative importance factor adaptation using various values of p_o .

weights), which are shown in Figure 2.8. It is shown that the orientations and weights obtained using $p_o=4$ and $p_o=8$ are almost the same, while for $p_o=1$, there is a significant difference especially in the obtained weights for the selected orientations.

Further investigation was made of the dependence of the initial importance factors on the outcome of the plan generation process. Although it is logical to start with equal importance factors, we

changed some importance factors in advance of the plan generation iteration to be twice or half of the other values. The results are shown in Figures 2.9 and 2.10. In Figure 2.9 is shown, that despite the different initial guesses, the finally achieved target dose is more or less the same as well as the obtained plan parameters (orientations and weights) as shown in Figure 2.10. In conclusion: when the constraints are very tight so that the prescribed target dose cannot be reached, the algorithm using a rather low dose step size for plan generation tends to find the prescribed dose independent of the initial choice of the importance factors. Moreover for this case the common stable subset of beam directions is large.

2.3.2 Clinical cases

Finally, to evaluate some clinical cases, we have used a simple prostate and a pancreas anatomy. For the prostate we used a simple anatomy, with the rectum clearly separated from the target. The femur contours have been set to 1.2 g/cc density and 23MV dose distributions have been used. As a reference, we used the more or less standard

beam geometry in our clinic with an AP and two lateral beams. In order to reduce the

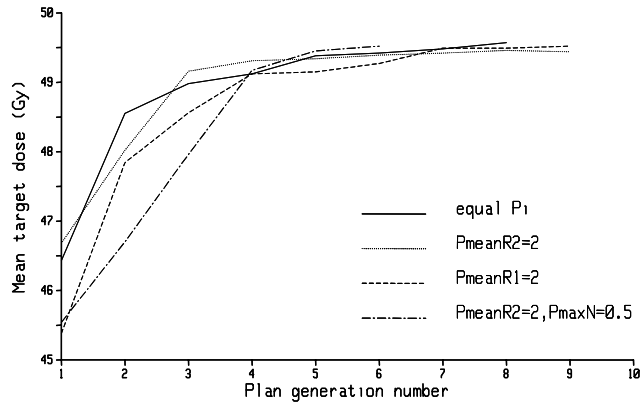


Figure 2.9 Process of iterative importance factor adaptation for a number of consecutive plan generations in order to maximize the mean target dose for case 1b for different initial guesses of importance factors.

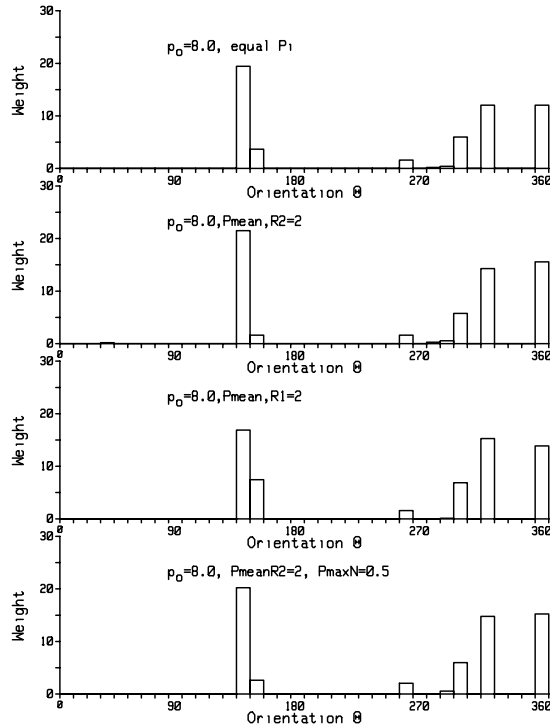


Figure 2.10 Final plan parameters (orientations and weights) for case 1b after iterative importance factor adaptation and different initial guesses of the importance factors.

dose to the rectum the relative weight of the AP beams is 0.8. The laterals have weight 1.0. These relative weights were scaled to arrive at an absolute mean target dose of 70 Gy. We have used the dose distribution quantities of this standard plan (mean and max value and a dvh-point of the rectum and femur heads) as input constraints for the optimization algorithm. For the DVH-points we have used for rectum: $V_{\text{def}} = 0.22$, $D_{\text{tol}, V_{\text{def}}} = 43$ Gy and for the femur heads: $V_{\text{def}} = 0.82$, $D_{\text{tol}, V_{\text{def}}} = 50$ Gy. The results of the constrained plan generation are shown in the Figures 2.11 and 2.12. Figure 2.11 shows the dose volume histograms of target, rectum and left and right femur head and compares the standard technique against the generated plan. Because we have prescribed the dose

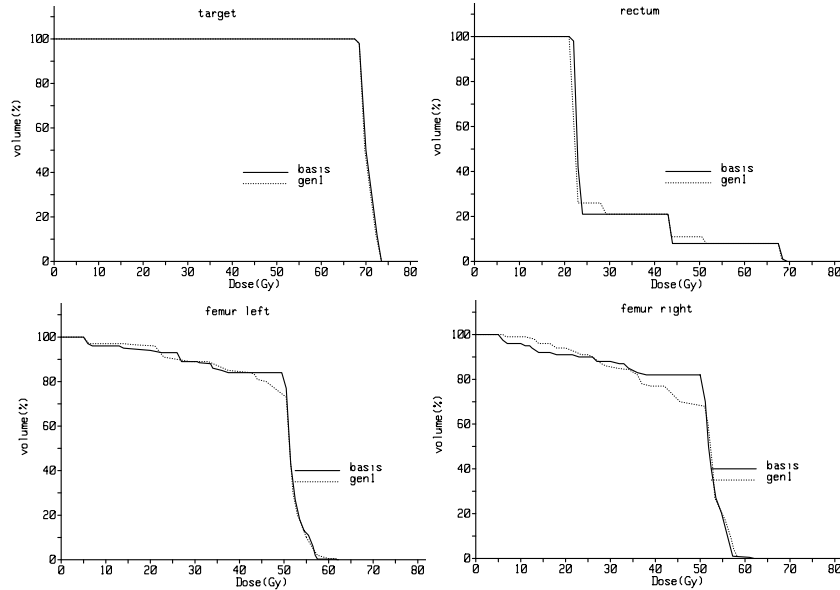


Figure 2.11 Dose-volume histograms for standard prostate irradiation (basis) compared with a generated distribution (gen1).

distributions to rectum and femur heads with mean and maximum dose and a DVH-point, the distribution in the conflicting OARs (rectum against femur heads) are quite well defined. The relatively small gain to the femur heads is made on the expense of a

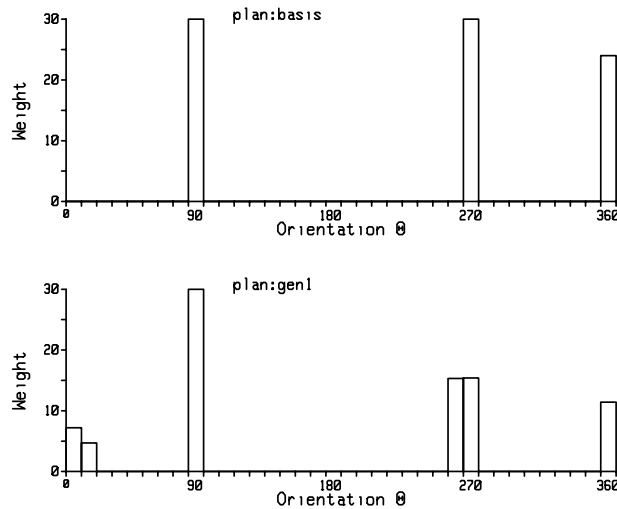


Figure 2.12 Plan parameters for the standard prostate irradiation and the generated distribution (gen1).

small compromise to the rectum, which in its turn is corrected by a spread of dose contributions from the AP direction. This is shown in Figure 2.12, where the orientations and weights of both plans are compared. Although the gain in dose distribution is little in this case, the dose distribution of the generated plan shows that a comparable plan can be found automati-

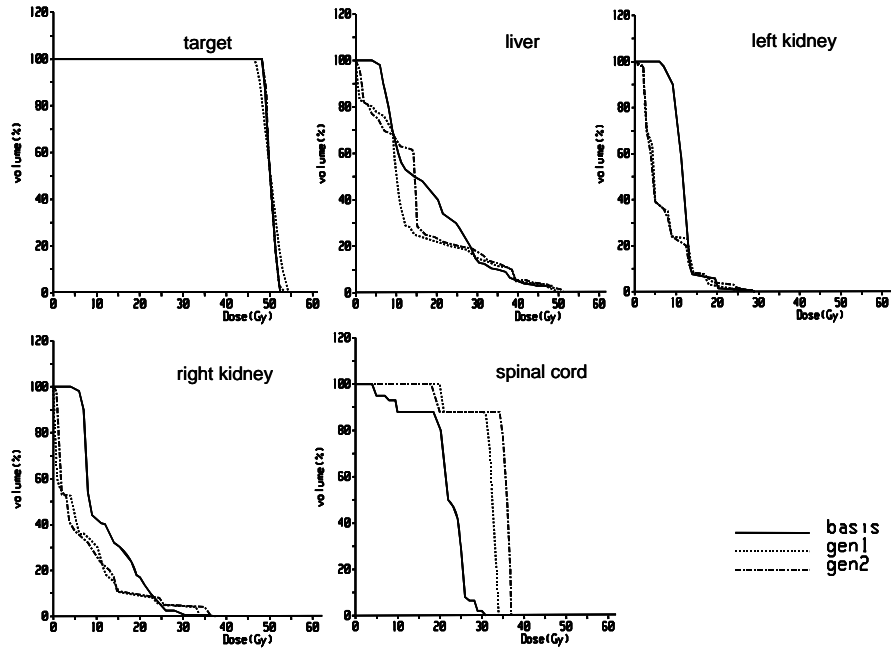


Figure 2.13 Dose-volume histograms for target, liver, kidneys and spinal cord for a clinical pancreas plan (basis) compared with two generated distributions (gen1 and gen2).

cally using only the dose distribution quantities of the standard plan as constraints. Especially the laterals and their weights agree rather well with the standard distribution. The fact that the right laterals are distributed on two orientations may indicate a required orientation resolution of 5 degrees instead of 10.

Finally we have used a multi-2D anatomy of the pancreas consisting of 9 slices with 1.5 cm spacing. For this case we have used the clinical plan as a reference. The clinical plan is shown as a solid line in Figure 2.13 and is called ‘basis’. In this plan wedges were used in two of the four orientations. This ‘basis’ plan looks good, however one might have asked to spare the kidneys even better on the expense of somewhat more dose to the spinal cord. This was the task for the first generation, where we put an additional dose volume constraint on both kidney’s: $V_{\text{def}} = 0.10$, $D_{\text{tol},V_{\text{def}}} = 20$ Gy, because in the clinical plan 18% of the right kidney got a dose more than 20 Gy. We used the mean and max dose to the liver of the ‘basis’ plan as constraints and widened the constraints for the spinal cord (mean and max dose) to 50 Gy. The mean dose to the kidneys was lowered to such a level (7 Gy), that the prescribed target dose (50 Gy) could hardly be achieved. The result of this generation (gen1) is also shown in Figure 2.13. The distribution to the kidneys meets the DVH

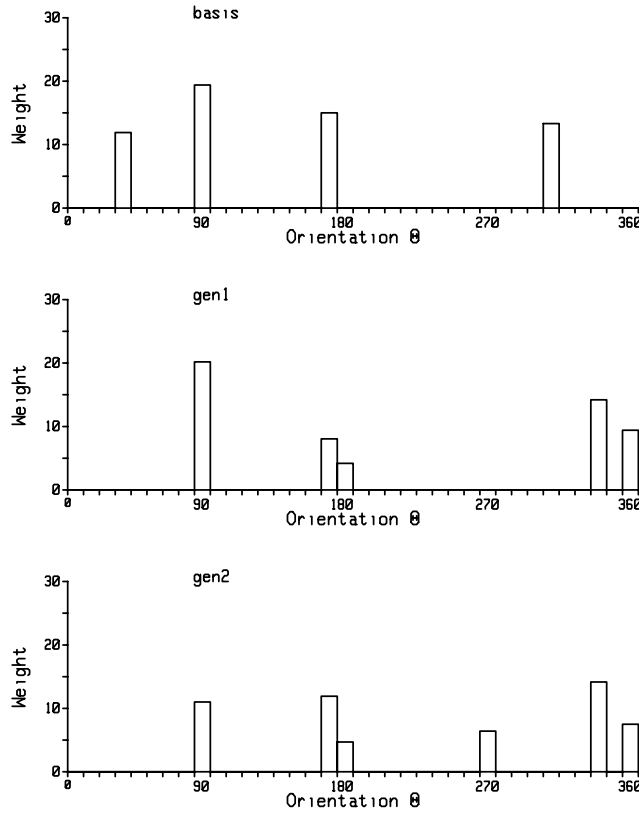


Figure 2.14 Plan parameters for the clinical pancreas irradiation and the two generated distributions.

prescription while in addition the mean dose is reduced significantly as well. The mean dose to the liver is reduced and somewhat more dose is allowed to the spinal cord (max 35 Gy). However the target dose homogeneity worsened. In the last generation (gen 2) we kept all the previous constraints but put an additional constraint on the target dose homogeneity: the minimum dose should not be less than 95% of the mean target dose. The results are shown in Figure 2.13 as well. In the DVH of the target the gen2 curve

can hardly be distinguished from 'basis'. The dose to the kidneys does not change too much but the dose to the liver and spinal cord increase, but still remain under the given tolerance values.

These results show that using the plan generator the dose to the kidneys can be reduced significantly compared with the clinical plan at the cost of some tolerable dose to the spinal cord. A comparable target dose homogeneity can be achieved, yielding a comparable dose to the liver but maintaining the gain of kidney dose reduction. The changes from gen1 to gen2 can be understood from Figure 2.14 as well where we have shown the plan parameters of the three plans. The largest difference between gen1 and gen2 is the transition from the heavily weighted left lateral beam ($\theta = 90^\circ$) to the 'opposed laterals' ($\theta = 90^\circ$ and $\theta = 270^\circ$) yielding a dose increase to the liver but still below the constraints. Finally the orientation 170° receives somewhat

more dose yielding an increased dose to the spinal cord but below the constraints.

2.4 Discussion

In this paper we have presented an algorithm for automated simultaneous evaluation of beam angles and weights. The algorithm aims at the delivery of the prescribed target dose, without any violation of prescribed constraints for the dose distributions in the target and organs at risk. This requirement for the dose prescription links up with the demands on treatment plans that we regularly encounter in clinical practice and is similar to the MDVL approach of Morrill *et al* (1991). Because the algorithm only aims to reach the solution space, it means that if a solution space exists the result will be somewhere within this space and not necessarily in the optimum position within this space. Another well-known aspect of optimization, which is not addressed in this paper, regards the compromise between dose distribution quality and the number of beams.

The plan generator uses sequential beam selection: new beam angles or beam weight increases of previously selected beam angles are determined while taking into account the dose distribution of already selected beams. The calculation time required for plan generation is rather short. A plan generation using 36 input orientations takes about 10 minutes.

One may criticize that sequential search has very limited possibilities regarding the freedom of weight and orientation selection, which is needed to handle the correlated beam weights and orientations of a treatment plan. In this way the described method is not comparable with other more general techniques like simulated annealing or genetic algorithms, where at any time weights and orientation changes can be made in reverse directions. Although the severity of this problem is somewhat reduced by the introduction of a small dose step size (p_o -value), this drawback is not inherently solved. An example of this fact is given in Figure 2.7, where the generator even when using $p_o=8$ will not immediately find the plan within the constraints, but only after a number of iterative plan generations.

Therefore, in order to overcome the drawback of sequential search, a very essential and even indispensable step in the plan generation procedure is the iterative change of the importance factors. In summary the described algorithm consists of two basic elements:

1. Plan generation using sequential search: This is a systematic way to generate a plan, considering a number of independent hard constraints and importance factors. A large p_o value refines the sequential plan generation but does not break the sequential character. It reduces the errors that should be made when using large dose step sizes, but in essence yet there is no way back and selections of weights and orientations cannot be ‘undone’.
2. Iterative plan generation using adapted importance factors: The sequential character of the complete process is only broken during a following generation where importance factors are changed and a new generation is started with an empty plan. During this generation a significantly different plan can be made, based on the new importance factors.

In other words: the sequential plan generation produces a ‘track’ through the beam parameter space (orientations, weights and the number of beams). This track is more refined as we decrease the dose step size but is yet inherently a sequential procedure on which a correction is not possible. The ‘direction’ of the track is purely determined by the plan constraints and the importance factors. At the end of the track the ‘distance’ between the track endpoint and the solution space is ‘measured’ and the generator is steered into the direction of the solution space, using importance factors based on the difference between the previously generated plan and the solution space. A remarkable property of the plan generator is that steering appears to be possible.

For large p_o , i.e. for $p_o \geq 4$, which corresponds to relatively small target dose increases during plan generation, the stability of the iteration result will be better than for low p_o values. The use of too small p_o -values may hamper the selection of an acceptable plan. Large p_o -values may, however, result in inclusion of some beam orientations with very low weight. If very low weight orientations exist, a next run of the described algorithm using only those beam orientations that initially had a substantial weight, will generally yield a clinically feasible plan.

It is remarkable to see that if the prescription is set to a severe level and therefore more plan generations are needed to reach the prescribed target dose, the results of the plan generation tend to converge to the same plan, independent from the initially set importance factor values (case 1b and Figures 2.9 and 2.10). This may indicate that severe prescription requirements of hard constraints transform the solution space in a way that the global maximum becomes more pronounced and therefore can be found more easily.

In case a prescribed mean target dose results in a plan that is substantially off from violation of any of the prescribed constraints, there is room for dose escalation. Sequential application of the described method for beam angle and weight selection with increasing prescribed tumour doses may then result in a final treatment plan that has a higher tumour dose while just not exceeding the constraints.

In this paper our method for automated beam angle and weight selection was demonstrated using uniform beams. However, inclusion of wedged fields and a form of intensity modulation as described by Webb (1991) is straightforward. The proposed algorithm is independent of the applied dose calculation model and can be used for any type of single beam dose distributions.

Acknowledgements

The authors wish to acknowledge Dr. M. Keijzer, Technical University Delft, who allowed us to use their basic treatment planning software, mr. B.A.v.d. Leye who modified this basic code for more easy use and Dr. B.J.M. Heijmen for valuable comments and discussion on the manuscript.

References:

1. Bortfeld Th, Bürkelbach J, Boesecke R and Schlegel W 1990 *Methods of image reconstruction from projections applied to conformation radiotherapy*, *Phys. Med. Biol.* **35** 1423-34
2. Bortfeld T and Schlegel W 1993 *Optimization of beam orientations in radiation therapy: some theoretical considerations* *Phys. Med. Biol.* **38** 291-304
3. Brahme A 1988 *Optimization of stationary and moving beam radiation therapy techniques* *Radiother. Oncol.* **12** 129-140
4. Ezzell G A 1996 *Genetic and geometric optimization of three-dimensional radiation therapy treatment planning* *Med. Phys.* **23** 293-305
5. Langer M, Brown R, Morrill S, Lane R and Lee O 1996 *A generic genetic algorithm for generating beam weights* *Med. Phys.* **23** 965-71
6. Mageras G S and Mohan R 1993 *Application of fast simulated annealing to optimization of conformal radiation treatments* *Med. Phys.* **20** 639-47
7. Mohan R, Mageras G S, Baldwin B, Brewster L J, and Kutcher G J 1992 *Clinically relevant optimization of 3-D conformal treatments* *Med. Phys.* **19** 933-44
8. Morill, S M, Lane R G, Jacobson G and Rosen I I 1991 *Treatment planning optimization using constrained simulated annealing* *Phys. Med. Biol.* **36** 1341-61
9. Morrill S M, Lam K S, Lane R G, Langer M, and Rosen I I 1995 *Very fast simulated reannealing in radiation therapy treatment plan optimization* *Int.J. Rad. Onc. Biol. Phys.* **31**, 179-88

10. Rowbottom C G, Webb S and Oldham M 1998 Improvements in prostate radiotherapy from the customization of beam directions *Med. Phys.* **25** 1171-79
11. Rowbottom C G, Oldham M and Webb S 1999 Constrained customization of non-coplanar beam orientations in radiotherapy of brain tumors *Phys. Med. Biol.* **44** 383-99
12. Söderström S and Brahme A 1993 Optimization of the dose delivery in a few field techniques using radiobiological objective functions *Med. Phys.* **20** 1201-10
13. Spirou S V and Chui C 1998 A gradient inverse planning algorithm with dose volume constraints *Med. Phys.* **25** 321-33
14. Wang X-H, Mohan R, Jackson A, Leibel S A, Fuks Z and Ling C C 1995 Optimization of intensity-modulated 3D conformal treatment plans based on biological indices *Radiother. Oncol.* **37** 140-52
15. Webb S 1989 Optimization of conformal radiotherapy dose distributions by simulated annealing *Phys. Med. Biol.* **34** 1349-70
16. Webb S 1991 Optimization by simulated annealing of three-dimensional conformal treatment planning for radiation fields defined by a multileaf collimator *Phys. Med. Biol.* **36** 1201-26
17. Webb S 1992 Optimization by simulated annealing of three-dimensional, conformal treatment planning for radiation fields defined by a multileaf collimator: II. Inclusion of two dimensional modulation of the x-ray intensity *Phys. Med. Biol.* **37** 1689-1704
18. Webb S 1994 Optimizing the planning of intensity-modulated radiotherapy *Phys. Med. Biol.* **39** 2229-46
19. Xing L, Li J G, Donaldson S, Le Q T and Boyer A L 1999 Optimization of importance factors in inverse planning *Phys. Med. Biol.* **44** 2525-36

CHAPTER 3

**AUTOMATED BEAM ANGLE AND WEIGHT SELECTION IN
RADIOTHERAPY TREATMENT PLANNING APPLIED TO PANCREAS
TUMORS**

E. Woudstra and B.J.M. Heijmen, *Int. J. Rad. Oncol. Biol. Phys.* **56**, 878-888, 2003

ABSTRACT

Purpose: To extend and investigate the clinical value of a recently developed algorithm for automatic beam angle and beam weight selection for irradiation of pancreas tumors.

Methods and Materials: The algorithm aims at generation of acceptable treatment plans, i.e. delivering the prescribed tumor dose while strictly obeying the imposed *hard* constraints for organs at risk and target. Extensions were made to minimize the beam number and/or to escalate the tumor dose. For five pancreas patients, the clinical value and the potential for beam number reduction and dose escalation were investigated. Comparisons were made with clinical plans and equi-angular plans.

Results: Compared to clinical plans, the generated plans with the same number of beams yielded a substantial reduction in the dose to critical tissues. Using the algorithm, an escalated tumor dose of 58 Gy could be achieved for two cases. Maximum dose escalations required a minimum of 3-4 beam orientations. For 13 CT-slices and an in-slice resolution of 0.5 cm, the total calculation times were 23-55 minutes, including pre-calculation of 180 input dose distributions (15 minutes).

Conclusions: The algorithm yielded acceptable treatment plans with clinically feasible numbers of beams, even for escalated tumor doses. Generated plans were superior to the clinically applied plans and to equi-angular setups. Calculation times were clinically acceptable. The algorithm is now increasingly used in clinical routine.

3.1 Introduction

Automated beam angle, beam weight and wedge filter selection in radiotherapy treatment planning has been studied by several groups (1-23). The technical aspects of the method implemented in Rotterdam have been described in detail in Ref. (22), and will be summarized in ‘Methods and Materials’. The algorithm aims at the generation of an ‘acceptable’ treatment plan, i.e. a plan that delivers the prescribed target dose, while strictly obeying the imposed *hard* constraints on the dose delivery to the target and the organs at risk. In general, there may be several acceptable solutions. The aim is to find one of them. To optimize the probability of finding an acceptable plan, the applied score function has been designed to favor (sequential) selection of beam orientations that best avoid approaching the imposed constraints. The algorithm has an intrinsic drive to generate solutions that stay away as far as possible from all imposed

Case	V _{PTV} (cc)	Number of beams
1	496	3
2	455	4
3	744	3
4	164	5
5	391	4

Table 3.1 PTV volumes and numbers of beams in the clinical plan of the 5 patient cases in this study.

constraints: good dose homogeneity in the tumor and limited dose delivery to organs at risk. If the algorithm does not succeed in generating an acceptable plan, it does give the beam orientations and beam weights for maximum dose delivery to the tumor, while still obeying all constraints. The dose limiting constraints are then also shown. The radiotherapy team may then decide to stay within the original constraints and to treat the patient with a lower tumor dose, or to relax one of the limiting constraints. This is followed by a second attempt to automatically generate a plan that does succeed in delivering the prescribed tumor dose. We have found that automatic treatment plan generation with the published algorithm does often result in treat-

ment plans with 6-9 beam directions. Although this is a rather low number compared to the initial 36 orientations (see ‘Methods and Materials’), it is more than what we normally use clinically.

The goal of this paper is to extend and investigate this algorithm for clinical application. If the automatically generated plan for a patient stays well away from the imposed constraints, it may be possible to generate an alternative acceptable plan with less beams; dose escalation may then also be an option. To investigate this, we have implemented features, resulting in acceptable treatment plans that have fewer treatment beams, or have an escalated tumor dose, both at the cost of approaching more closely the prescribed constraints. The algorithm has also been modified in order to allow the inclusion of wedge fields for four different collimator angles. Evaluations have been performed using treatment planning studies for five patients with a pancreas tumor that were previously treated in our institution. Automatic beam angle selection has been compared with the clinically delivered plan, and with equi-angular plans. Calculation times for automatic treatment plan generation have been assessed.

Each year about 15 of our pancreas patients are treated with radiotherapy. The clinical outcome is poor and protocols are being developed to intensify treatment. One aspect under study is the use breathing control to reduce geometrical uncertainties. The automated beam angle and weight selection as described in this paper allows for better individualization of treatment plans. The pancreas is a challenging site to test inverse planning algorithms because of its geometry. It has a target of varying size and

position, surrounded by a number of organs at risk (kidneys, small bowel, spinal cord, and liver).

3.2 Methods and Materials

3.2.1 Pancreas cases, tumor dose prescription and constraints

The patient material consists of CT data sets of five patients who were previously treated in our clinic (Table 3.1). For each patient case, thirteen CT-slices were used for our studies. In Figure 3.1, patient outlines with delineated structures are presented for the central plane of the clinical treatment plan, showing the geometric complexity of the problem. The patients were treated with a dose of 50 Gy. In agreement with ICRU-50 (24), the tumor dose was prescribed to the isocenter, which was always located in the center of the target. The allowed minimum and maximum PTV-doses were 95% and 107% respectively. During design of the clinical plan for patient 1, the desired sparing of both kidneys, while also delivering a tumor dose of 50 Gy, turned out to be unfeasible. Therefore, a plan was made to optimally spare the right kidney, while accepting a less favorable dose delivery to the left kidney. The patients in this study were treated by different physicians, and there was no (standard) treatment planning protocol for design of the clinical plans and for evaluation of dose delivery to the critical tissues.

For automatic plan generation, the following normal tissues were considered: liver, small bowel, kidneys, spinal cord, and all other tissue outside the target volume, designated OTAR (other tissue at risk). The applied constraints for the PTV (ICRU-50) and the normal tissues are summarized in Table 3.2. All constraint parameters in this table are <1 in case the plans are within the constraints and >1 when constraints are violated. The constraints for the liver, the kidney, the small bowel, and the spinal cord were based on published data (25-27) and on the clinical practice in our institution. A constraint on the maximum dose in the OTAR was used to avoid occurrence of significant hot spots in these tissues. Regions of overlap between the PTV and healthy tissues were considered as PTV.

3.2.2 Precalculated input dose distributions

Automatic beam angle selection is based on pre-calculated, three-dimensional single

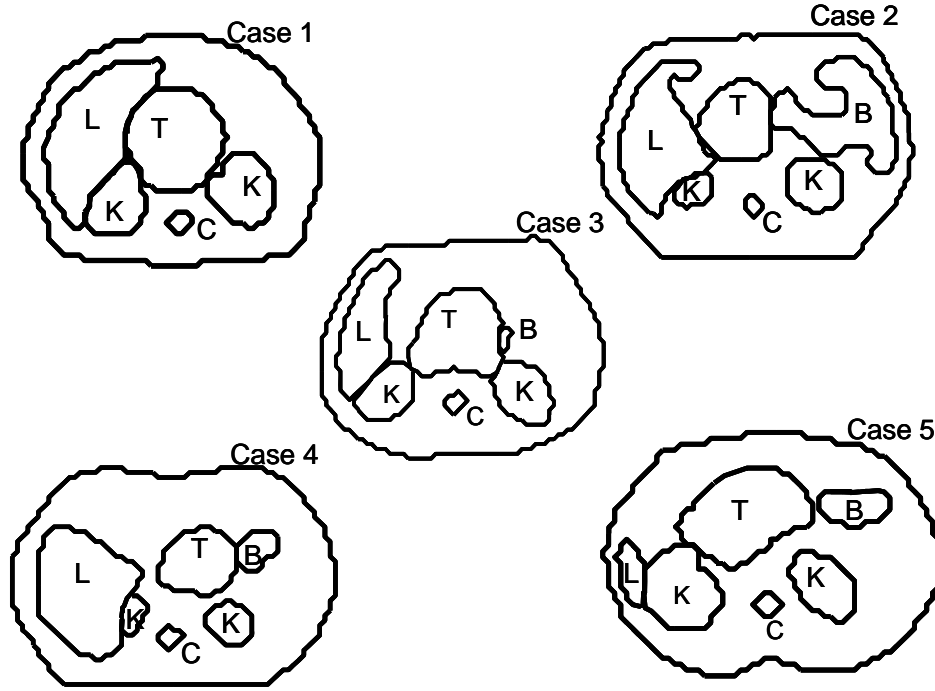


Figure 3.1 The central CT slice of the 5 pancreas cases in this study. T = target, L = liver, B = small bowel, C = spinal cord. The small bowel delineations were not used for the production of the clinical plans. They were added afterwards for the purpose of our study. For case 1, the small bowel outline does not show up, because in the central slice, it was completely contained in the PTV.

beam dose distributions for 36 angles of incidence θ with 10 degrees intervals. Beam's-eye-view (BEV) is used for field shape definition with a 0.5 cm margin around the projected target. For each θ , the uniform field distribution $U_{\theta u}(x, y, z)$ and four 60°-wedge distributions $U_{\theta 60, \phi}(x, y, z)$, for collimator angles ϕ of 0°, 90°, 180° and 270° are involved. The dose distributions are calculated using the CT-data of the patient.

For the investigations in this paper, 23 MV X-ray fields were used. The dose calculation algorithm is based on the percentage depth dose (PDD) for a typical field size for pancreas treatment, on three-dimensional ray tracing, and the effective path length method for correction of inhomogeneities. The penumbra and the dose level outside the field edges have been parameterized to fit with measurements.

Unit beam weight has been defined to be 1 Gy at d_{max} at the source-to-axis distance. Only coplanar beams were included in the analyses. However, in geometric sense the algorithm is truly three-dimensional, allowing the calculation of non-coplanar dose

j	Organ	Constraint	Constraint parameter Cj
1	PTV	$D_{\min} > 0.95 \cdot D_{\text{isoc}}^{\text{pre}}$	$(D_{\text{isoc}} - D_{\min}) / (0.05 \cdot D_{\text{isoc}}^{\text{pre}})$
2	PTV	$D_{\max} > 1.07 \cdot D_{\text{isoc}}^{\text{pre}}$	$(D_{\max} - D_{\text{isoc}}) / (0.07 \cdot D_{\text{isoc}}^{\text{pre}})$
3	OTAR	$D_{\max} > 1.1 \cdot D_{\text{isoc}}^{\text{pre}}$	$(D_{\max} - D_{\text{isoc}}) / (0.1 \cdot D_{\text{isoc}}^{\text{pre}})$
4	Liver	$V_{D>40\text{Gy}} < 33\%$	$V_{D>40\text{Gy}} / 33$
5	Liver	$D_{\text{mean}} < 20\text{Gy}$	$D_{\text{mean}} / 20$
6	Small bowel	$V_{D>50\text{Gy}} < 5\%$	$V_{D>50\text{Gy}} / 5$
7	Small bowel	$D_{\max} < 55\text{Gy}$	$D_{\max} / 55$
8	Left Kidney	$V_{D>25\text{Gy}} < 33\%$	$V_{D>25\text{Gy}} / 33$
9	Left Kidney	$D_{\text{mean}} < 15\text{Gy}$	$D_{\text{mean}} / 15$
10	Right Kidney	$V_{D>25\text{Gy}} < 33\%$	$V_{D>25\text{Gy}} / 33$
11	Right Kidney	$D_{\text{mean}} < 15\text{Gy}$	$D_{\text{mean}} / 15$
12	Spinal cord	$D_{\max} < 50\text{Gy}$	$D_{\max} / 50$

Table 3.2 Constraints for automatic beam orientation and beam weight selection and corresponding constraints parameters for evaluation.

distributions as well. For calculation times, see ‘Results’.

For comparison of clinical plans with automatically generated plans, the clinical plans were re-calculated with the dose calculation algorithm that is also used for automatic treatment plan generation.

3.2.3 The algorithm for automatic beam angle and beam weight selection

Precalculated single-beam dose distributions at every 10° angle of incidence are used as input (see above). Starting with an empty plan without beams and as long as none of the imposed hard constraints has been violated, the algorithm sequentially adds one of these beams to the treatment plan until the prescribed target dose has been reached. As described in detail in the next section, a ‘dynamic’ score function is used to sequentially select beam orientations and weights; before selection of the next beam the score function is adapted to account for the dose delivery by the previously

selected beams.

Initially, the score function has equal penalty factors (p_j) for approaching each of the various constraints. In case these initial factors do not result in a plan that delivers the prescribed tumor dose without violating constraints, there is an automatic recalculation of these factors followed by a new run of the algorithm for beam angle selection. Because of this re-scaling, the penalties for approaching constraints that were hit in the previous run wield a larger influence over the score function, i.e. approaching such a constraint will result in a stronger decrease of the score function value. Consequently, in the new run, the algorithm will favor selection of orientations that better avoid approaching these particular constraints (for details see next section and Ref. (22)).

The program has been written in FORTRAN and runs on a UNIX workstation.

3.2.4 The applied score function and selection of the next beam

The score function S_k , used for selection of the orientation, θ_k , and weight, w_k , of the next beam, k , while accounting for all imposed constraints, j , and the dose distribution resulting from the first selected $k-1$ beams, is described by Equation 1:

$$S_k(\theta, w) = \frac{\Delta D_{PTV}(\theta, w, k)}{\Delta D_{PTV}^{pre}(k)} \cdot \prod_j \left(1 - \frac{\Delta P_j(\theta, w, k)}{\Delta P_{j,tol}(k)} \right)^{p_0 \cdot p_j} \quad (1)$$

with the following:

$\Delta D_{PTV}(\theta, w, k)$, the increase in the delivered PTV dose (isocenter) because of addition of a beam k with angle of incidence θ and weight w to the previously selected beams.

$\Delta D_{PTV}^{pre}(k)$, the prescribed PTV dose minus the dose delivered by the first $k-1$ beams.

$\Delta P_j(\theta, w, k)$, the increase in the dose distribution parameter P_j (e.g. the maximum delivered dose in an organ at risk), due to addition of a beam k with θ and w .

$\Delta P_{j,tol}(k)$, the tolerance value for parameter P_j (e.g. the maximum allowed dose in an organ at risk) minus the value resulting from the first selected $k-1$ beams.

p_0 , to balance the favorable increase in PTV dose if the beam weight of the next beam.

risks, against the unfavorable approach of constraint levels (See also below). In this study p_0 was always 4.

p_j , penalty factors that determine the penalties for approaching the various constraints j (previous section and below).

For each angle of incidence θ , the term $\frac{\Delta D_{PTV}(\theta, w, k)}{\Delta D_{PTV}^{pre}(k)}$ in Equation 1 goes up if the

beam weight w rises due to the resulting increase in PTV dose. The extent of the

increase depends on θ . All penalty terms $\left(1 - \frac{\Delta P_j(\theta, w, k)}{\Delta P_{j,tol}(k)}\right)^{p_0 \cdot p_j}$ (one for each hard

constraint j), decrease if w goes up, because of a closer approach of the constraint parameters. This decrease is dependent also on the angle of incidence. For each of the 36 potential beam directions θ for selection of the next beam k , the score function $S_k(\theta, w)$ has a single maximum $S_k(\theta, w_{max}(\theta))$ at the θ -dependent weight, designated $w_{max}(\theta)$. The angle of incidence θ with the highest maximum score is selected as the next direction θ_k , with the beam weight $w_k = w_{max}(\theta_k)$. Due to the multiplication of penalty terms in Equation 1, in case of equal p_j for all constraints j , the algorithm for automatic beam angle and weight selection tends to generate acceptable plans with an equal spread of unwanted dose over to the various constraints.

With sequential beam angle selection, there is a danger that non-optimal selection of the first beams results in a situation that an acceptable plan (i.e. a plan with the prescribed tumor dose and not violating the imposed constraints) is not generated, while in reality such an acceptable solution does exist. To reduce the risk that this situation occurs several measures were taken:

1. The value of the parameter p_0 in $S_k(\theta, w)$ was chosen large enough to ensure that all $w_{max}(\theta)$ are relatively small, resulting in a small w_k and therefore in a moderate dose addition due to the selected beam defined by θ_k and w_k . In case of a very favorable beam orientation, this beam will generally be selected several times in the overall process of sequential beam selection, increasing the overall dose delivery by this beam. However, it may also turn out that after 1 or 2 moderate dose increases from a certain angle of incidence, this direction becomes less favorable and other directions will then be selected. A too small value of p_0 would yield relatively large weights $w_{max}(\theta)$. Each newly selected beam k would then add a significant amount of dose to the treatment plan in a single step, which would limit the flexibility of the algorithm to

generate an acceptable plan. For $p_0=4$ as used in this study, isocenter dose increases were always smaller than 5 Gy.

2. Each plan generation starts with a run with equal penalty factors p_j . In case an acceptable treatment plan cannot be obtained, there is an automatic rescaling of the parameters p_j to increase the penalty on approaching the limiting constraints, followed by a new run of the algorithm (See also previous section).

3.2.5 Reduction of the number of selected orientations

As mentioned under ‘Introduction’, we have observed that treatment plans generated with our published algorithm for beam angle selection do generally consist of a relatively low number of beams (6-9); that is however somewhat higher than what we prefer to use clinically. We have now modified this algorithm to investigate whether the number of beams may be reduced, perhaps at the expense of approaching more closely (one of) the constraints. For this purpose we have extended the plan generation routine with an option to generate a treatment plan using an arbitrary subset of the 36 possible beam orientations.

The procedure for reduction of the number of selected angles of incidence is as follows. First, a treatment plan is generated using the original algorithm with all 36 beam directions available for beam selection. Next, the selected orientation with the smallest weight is removed from the set of selected orientations and the reduced set (instead of the 36 orientations) is now input for the option to generate a plan from a pre-selected set of orientations. If again a solution exists, the beam angle that now has the lowest weight is then removed and again a new plan generation is performed. This iterative process of successive exclusion of the lowest weight angle of incidence is continued until, due to the plan constraints, the achievable target dose has reduced to 99% of the prescribed dose.

3.2.6 Dose escalation

If the prescribed target dose can be (easily) delivered without violating the constraints, there is room for reduction of the number of selected beam orientations (previous section). Alternatively, the prescribed tumor dose may then be increased. An option to maximally increase this dose while not violating any of the constraints has been added to our algorithm for automatic beam angle and weight selection. The target dose is

then increased in small steps, each followed by an automatic treatment plan generation for beam angle and weight selection. This iterative procedure is stopped when the dose cannot be further increased without violation of constraints. When the maximum tumor dose has been found, beam number reduction with the procedure described above may then be applied to find escalated plans with low numbers of beams.

3.2.7 Comparison with equi-angular setups

For the five pancreas cases in this study, plans designed with full beam angle selection (36 input directions, 10° angular resolution) were compared with equi-angular plans consisting of 3, 5, 7 or 9 beams with 120°, 70°, 50° or 40° intervals, respectively. For each of these intervals, two sets of angles of incidence were investigated; compared to the first set, in the second set all beams were rotated over 180°. The beam weights for the equi-angular combinations were automatically determined using the option to generate a treatment plan using an (arbitrary) subset of the 36 possible beam orientations (see above). For all generated plans, the imposed dose distribution constraints were the same.

3.2.8 Comparison of treatment plans

As mentioned above, for each case in this study several acceptable treatment plans were generated (e.g. with different numbers of beam orientations). For mutual comparison of these plans, and for comparison with the clinical plan, we have used the constraint parameters C_j , as defined in Table 3.2. In an acceptable plan, C_j is less than for all j . The smaller a C_j value is, the larger is the distance from the corresponding constraint level. To summarize the quality of a plan regarding avoidance of constraint levels, we have also introduced the DIP ('distance-from-ideal plan'), defined as follows:

$$DIP = \sqrt{\frac{1}{N} \sum_{j=1}^N (C_j)^2} \quad (2)$$

The summation in Equation 2 is for all constraint parameters C_j mentioned in Table 3.2. For (non-realizable) ideal plans (i.e. a perfectly homogeneous dose distribution in the PTV equal to the prescribed tumor dose, and no dose delivery at all to the healthy

tissues), the DIP is equal to 0. In case each of the individual constraints is about to be violated, the DIP approaches the value 1.

There is no formal validation of the DIP. However, we do think that the DIP may be of relevance for comparing treatment plans generated with imposed hard constraints. This is certainly true if all hard constraints have equal importance, and if a larger ‘distance’ from a constraint is considered more favorable than closely approaching the constraint. In that case a plan with a lower DIP is always better than a plan with a higher DIP. Apart from the C_j -values and the DIP, also dose volume histograms (DVH) were used for plan evaluations.

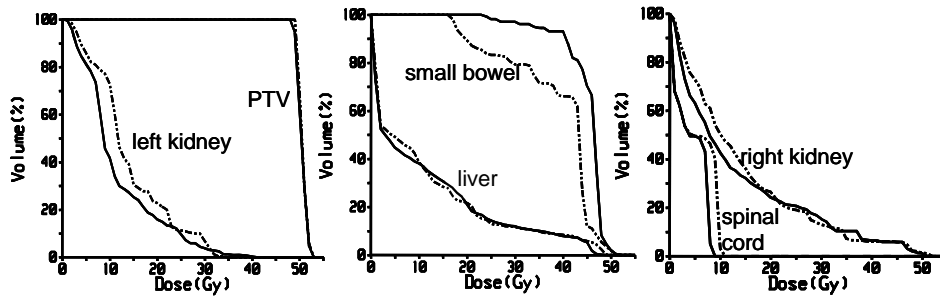


Figure 3.2 Dose volume histograms of automatically generated acceptable treatment plans for case 5, with 6 beams (solid lines) and 3 beams (dashed curves). The prescribed tumor dose was 50 Gy.

3.3 Results

3.3.1 Treatment plans for the prescribed clinical tumor dose (50 Gy)

For each case, a 50 Gy treatment plan was generated using full automatic beam angle selection, i.e. 36 input directions with 10° angular resolution. The number of selected beams was then gradually reduced with the procedure described in ‘Methods and Materials’. In agreement with the production of the clinical plan, the plans generated for case 1 were designed while ignoring constraints 8 and 9 in Table 3.2 for the left kidney (See ‘Methods and Materials’).

Full beam angle selection resulted in plans with 8, 6, 4, 6 and 6 beams for the Cases 1 to 5, respectively; the minimum numbers of beams required to generate an acceptable plan were 3, 2, 2, 2 and 3. For some cases, this reduction in beam orientations was

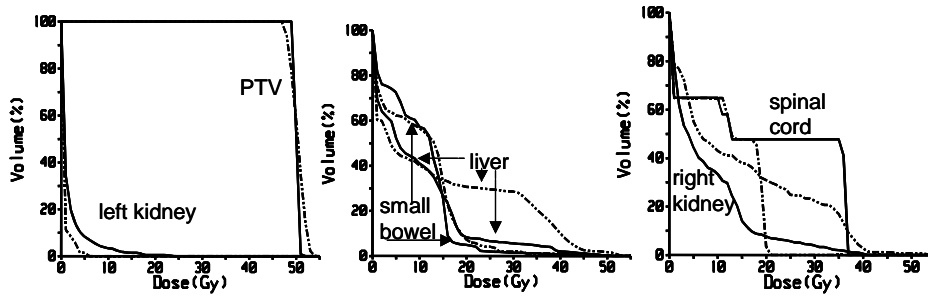


Figure 3.3 Dose volume histograms of automatically generated acceptable treatment plans for case 2, with 6 beams (solid lines) and 2 beams (dashed curves). The prescribed tumor dose was 50 Gy.

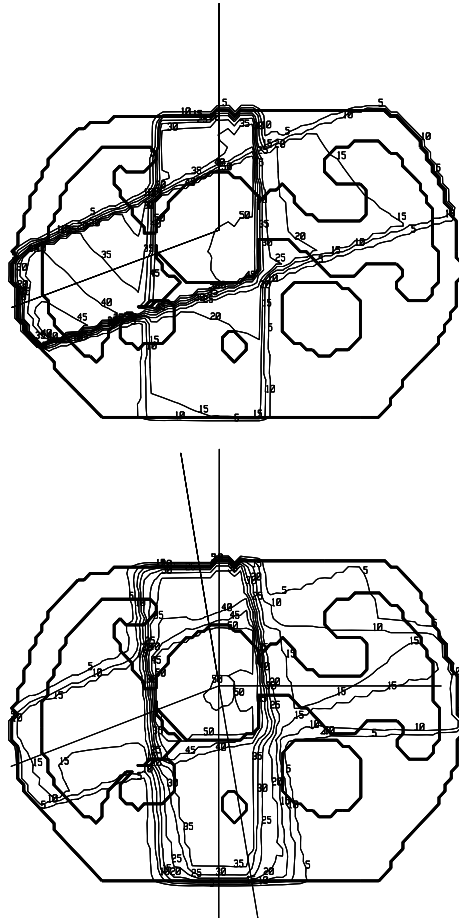


Figure 3.4 Dose distributions of (a) 2 field plans and (b) 6-field plan for case 2. Isodoses are in Gy.

possible with only minor changes in the C_j values (Table 3.2), i.e., without approaching more closely the imposed constraint tolerance levels. For Case 5, for example, the number of beams could be reduced from six to three, whereas there were only small differences regarding the avoidance of imposed constraint levels. As a consequence, by going from 6 to 3 beams the DIP ('distance-from-ideal plan', equation (2)) increased from 0.61 to only 0.63. Figure 3.2 shows that the differences are also small between the 6- and the 3-beam plans in the dose volume histograms (DVH) of the PTV and the critical organs.

For other cases, reduction of the number of involved beams yielded significant increases in

j	Organ	Constraint	Dose parameters 2-beam plan	Dose parameters 6-beam plan
1	PTV	$D_{\min} > 0.95 \cdot D_{\text{isoc}}^{\text{pre}}$	$D_{\min} = 0.96 \cdot D_{\text{isoc}}$	$D_{\min} = 0.99 \cdot D_{\text{isoc}}$
2	PTV	$D_{\max} > 1.07 \cdot D_{\text{isoc}}^{\text{pre}}$	$D_{\max} = 1.06 \cdot D_{\text{isoc}}$	$D_{\max} = 1.02 \cdot D_{\text{isoc}}$
3	OTAR	$D_{\max} > 1.1 \cdot D_{\text{isoc}}^{\text{pre}}$	$D_{\max} = 1.09 \cdot D_{\text{isoc}}$	$D_{\max} = 1.02 \cdot D_{\text{isoc}}$
4	Liver	$V_{D>40\text{Gy}} < 33\%$	$V_{D>40\text{Gy}} = 10\%$	$V_{D>40\text{Gy}} = 2\%$
5	Liver	$D_{\text{mean}} < 20\text{Gy}$	$D_{\text{mean}} = 12.3\text{Gy}$	$D_{\text{mean}} = 7.7\text{Gy}$
6	Small bowel	$V_{D>50\text{Gy}} < 5\%$	$V_{D>50\text{Gy}} = 0.1\%$	$V_{D>50\text{Gy}} = 0.1\%$
7	Small bowel	$D_{\max} < 55\text{Gy}$	$D_{\max} = 51.7\text{Gy}$	$D_{\max} = 50.5\text{Gy}$
8	Left Kidney	$V_{D>25\text{Gy}} < 33\%$	$V_{D>25\text{Gy}} = 0.0\%$	$V_{D>25\text{Gy}} = 0.0\%$
9	Left Kidney	$D_{\text{mean}} < 15\text{Gy}$	$D_{\text{mean}} = 0.5\text{Gy}$	$D_{\text{mean}} = 1.0\text{Gy}$
10	Right Kidney	$V_{D>25\text{Gy}} < 33\%$	$V_{D>25\text{Gy}} = 21.0\%$	$V_{D>25\text{Gy}} = 4.0\%$
11	Right Kidney	$D_{\text{mean}} < 15\text{Gy}$	$D_{\text{mean}} = 11.2\text{Gy}$	$D_{\text{mean}} = 5.6\text{Gy}$
12	Spinal cord	$D_{\max} < 50\text{Gy}$	$D_{\max} = 20.4\text{Gy}$	$D_{\max} = 36.4\text{Gy}$

Table 3.3 Comparison of dose parameters for 2- and 6- field plans for case 2

the C_j -values, and consequently also in the DIP. For case 2, for example, going from an acceptable plan with 6 beams to an acceptable 2-beam plan resulted in an increase in the DIP from 0.39 to 0.62. This was caused mainly by a deteriorated dose homogeneity in the PTV (constraints 1 and 2, Table 3.2), a higher maximum dose in the OTAR (constraint 3), and increased dose deliveries to the liver (constraints 4 and 5) and to the right kidney (constraints 10 and 11). Regarding dose delivery to the spinal cord and the left kidney, the 2-beam plan is (somewhat) more favorable than the plan with 6 beams. The corresponding DVHs for case 2 are shown in Figure 3.3. Dose distributions for the 2- and 6- beam plans in the plane through the isocenter are depicted in Figure 3.4. The corresponding dose parameters are shown in Table 3.3.

For each case, we have compared the dose distribution of the clinical plan with the distribution from the automatically generated plan with the same number of beams as the clinical plan. Apart from two minor deviations for case 3, all clinical plans were within the constraints, i.e. $C_j < 1$. Generally, the C_j -values for the automatically

Case	Clinical	Generated
1	0.74	0.54
2	0.60	0.39
3	0.73	0.51
4	0.51	0.36
5	0.75	0.63

Table 3.4 DIP-values for the comparison of clinical plans and automatically generated plans with the same number of beams and 50 Gy prescribed tumor dose.

generated plan are lower than the corresponding values for the clinical plan, indicating that the clinical plans do more closely approach the imposed constraint levels. This is also reflected by the substantial differences in the ‘distance-from-ideal-plan’ (DIP) values as shown in Table 3.4. The differences in difficulty as expected from viewing Figure 3.1 seem to be reflected in the DIP values of the clinical plans as well as in the automatically generated plans. The DVHs for case 3 as shown in Figure 3.5 illustrate the significantly better sparing of critical tissues by automatic beam angle and weight selection. For this case the automatic generation has chosen to deliver a relatively larger dose to the spinal cord, providing the possibility to significantly reduce the dose to the kidneys, liver and small bowel.

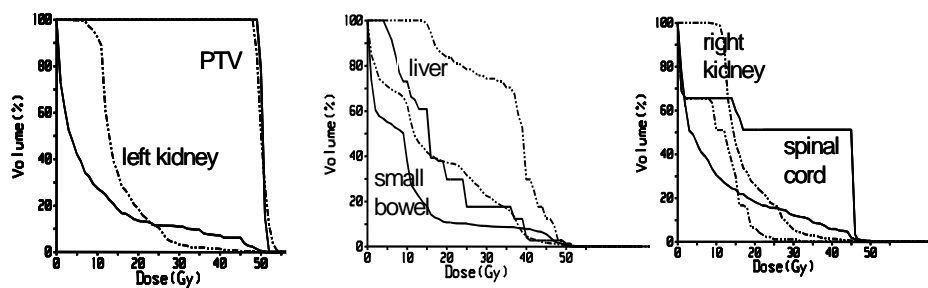


Figure 3.5 Dose volume histograms for case 3. Dashed lines represent the clinical plan; solid lines belong to automatically generated plans with the same number of beams (3) and the same prescribed tumor dose (50 Gy).

3.3.2 Dose escalation

For the cases 2-5, the prescribed tumor dose was stepwise increased until the generator could not achieve anymore a plan without violation of constraints. For the esca-

lated dose, the number of selected orientations was then reduced to the lowest possible number.

Using full beam angle selection, the target dose could be escalated to 58, 57, 58, and 54 Gy for the cases 2, 3, 4, and 5, respectively; the selected numbers of beams were 9, 8, 7, and 5. For each escalated plan, at least 2 dose distribution parameters approached their constraint level; the maximum small bowel dose was always one of the limiting constraints for dose escalation.

The procedure of beam number reduction resulted in escalated acceptable plans with 4, 4, 3, and 4 beams. For the cases 2, 4 and 5, this minimum number of beams needed for the maximum dose escalation was less than, or equal to the clinical plan with a prescribed dose of only 50 Gy (compare with Table 3.1).

3.3.3 Comparison with equi-angular beam setups

For the cases 2-5, the prescribed tumor dose for automatic generation of the equi-angular plans was equal to the maximal achievable dose as mentioned in the previous section. For case 1, the prescribed dose was 50 Gy, and also here constraints 8-9 in Table 3.2 for the left kidney were ignored (see above). For the cases 3 and 5, even with 9 equally distributed beams it was not possible to realize the prescribed (escalated) tumor dose without violating constraints. For cases 2 and 4, acceptable equi-angular plans could be generated with minimum beam numbers 7 and 3, respectively (of the five case in the study, case 4 had by far the smallest target volume, Table 3.1). However, compared to the corresponding plans with the same numbers of beams, but automatically generated with full beam angle selection, followed by iterative beam number reduction (previous section), the DIP went up from 0.62 to 0.67 and from 0.61 to 0.65, respectively. For case 4, the reduced sparing of critical tissues is also illustrated in Figure 3.6. For this case, compared to the equi-angular setup, the combination of three freely selected orientations has moderate improvements in the dose delivery to the left kidney, the small bowel and the liver, and results in a major improvement in the sparing of the right kidney, all at the expense of somewhat increased dose delivery to the spinal cord (but still far below the constraint level).

3.3.4 Calculation times

Even though the developed software has not yet been optimized for speed, the time to

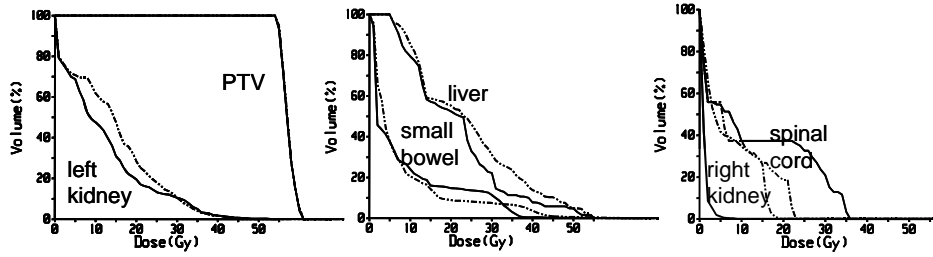


Figure 3.6 Dose volume histograms for case 4 for escalated dose prescription. Solid lines represent free beam angle selection after reduction to 3 beams. Dashed lines represent the 3 equi-angular plan.

automatically generate an acceptable plan is 23-55 minutes using a workstation, with about twice the speed of a modern PC with a comparable amount of memory, including 15 minutes for pre-calculation of 36x5 input dose distributions (13 CT-slices, in-slice resolution 0.5 cm). These pre-calculated dose distributions require about 90 MB disk space. The overall calculation times scale linearly with the applied number of CT-slices.

One single plan generation takes about 8 minutes. Generally, after the second generation with adjusted penalty factors, it is clear whether an acceptable plan will be generated or not. For the cases 2-5 and a prescribed tumor dose of 50 Gy, 1 or 2 generations (8-16 minutes) were needed to arrive at an acceptable plan. Difficult problems may require 5 generations (40 minutes) to assure that no solution will be found within the constraints. If after two generations the PTV dose is larger than 95% of the prescribed dose, it is useful to wait for the outcome of the next three generations.

Automatic plan generation with a reduced number of input directions (e.g. to reduce the number of beams obtained by selection from all 36 input directions) is much faster (typically 2-3 minutes per generation). For case 3, 50 Gy prescribed dose, and 36 input orientations, one plan generation (8 minutes) resulted in an acceptable plan with 5 orientations. The subsequent three plan generations to reduce the beam number to 2 took only 5 minutes.

3.4 Discussion

In this paper we have investigated clinical implications of a recently described algorithm (22) for automatic beam angle and weight selection for treatment of pancreas patients. The algorithm uses dose and dose-volume based parameters for

beam selection, such as minimum, mean and maximum organ doses, and dose-volume-histogram points. These parameters are also used in our daily routine treatment planning and for reporting in clinical trials. Beam angle selection with this algorithm may probably also be based on more biology oriented dose distribution parameters such as calculated tumor control probabilities (TCP) and normal tissue complication probabilities (NTCP). However, this was not the subject of the presented investigations.

Several published methods (12, 15) for inverse planning aim at the design of an 'optimal' plan, using an objective function with a user-defined numerical weighting of different treatment objectives (e.g. tumor coverage versus irradiation of critical tissue). In our algorithm such an a priori weighting is not required.

Similar to the methods described in (7, 8, 9, 16), our algorithm searches for an acceptable plan within all imposed hard constraints for the tumor and the critical tissues; constraint violations are not allowed at all. In case the prescribed tumor dose cannot be delivered without constraint violation, the patient may be treated with a lower dose or the radiotherapy team may decide to relax a limiting constraint followed by a new automatic plan generation.

For the cases studied in this paper we have observed that often a variety of acceptable plans exists with sometimes quite different combinations of beam numbers, beam weights and beam orientations. These acceptable plans may also have quite different balances between the approach of the various constraints. It remains to be investigated whether for a large group of similar patients the algorithm would lead to some type of class solution, i.e. similar plans for similar patients.

In this study we have observed that the applied algorithm may generate treatment plans that deliver the prescribed tumor dose while staying at some distance from all prescribed constraints. We have demonstrated that a new plan may then be generated with fewer treatment beams or with a higher tumor dose, while still not violating the constraints. Another possibility may then be to tighten the constraint on one or more critical dose distribution parameters, followed by a new plan generation.

When using a large number of input beam orientations for inverse planning, the generated plan may contain as many orientations with a non-zero weight, as has been shown by several authors (5, 9). It was suggested to then sequentially reduce the involved number of beams to arrive at a clinical plan. Other attempts to automatically generate plans with clinically feasible numbers of beam orientations were based on

the use of a limited number of fixed, equi-angularly distributed input orientations, as it was shown that for prostate cases that when the number of beams increases, equi-angular orientations provide a suitable solution (17). Exhaustive search (13, 14) and simulated annealing (11, 12) have been used to optimize both the beam angles and the beam weights for a fixed, limited number of beams. The algorithm described in this paper has 36 input beam orientations and there is no explicit objective to arrive at plans with a low numbers of beam orientations with a non-zero weight. Nevertheless, in our experience, even without the described routine for automatic beam number reduction, the generated plans do hardly ever have more than 9 orientations, which is only a little bit more than what we clinically use. This result could be because of the sequential character of the algorithm.

To complement DVHs for plan evaluation, we have introduced the DIP-value (distance-from-ideal plan). This DIP is similar to the well-known ‘root mean square difference’ objective function, which quantifies the differences between prescribed point doses and realized doses (1, 15, 17, 18). In the DIP, the differences between prescribed and realized doses are replaced by ratios of dose distribution parameters (such as the maximum dose in an OAR) and the allowed tolerance level for this parameter.

In strict mathematical terms the developed algorithm is not an optimization technique. However, there is an intrinsic drive to generate treatment plans that stay away from all imposed constraints. For the pancreas patients in this study it was always possible to generate a plan with the clinical tumor dose of 50 Gy that obeyed all constraints. Based on the DIP- and DVH-analyses, it was concluded that the quality of an automatically generated plan was generally higher than that of the corresponding clinically applied plan, which was generated with conventional manual forward planning. The algorithm is now increasingly used for the design of clinical treatment plans, also for other sites, especially when we do not succeed in designing an acceptable plan by forward treatment planning. After design of the plan, the final (forward) dose calculation is performed in our treatment planning system (Cadplan, manufactured by Varian). Because of the difference in beam model between the two systems, small modifications in the automatically designed plan have sometimes to be made, based on the dose calculations by the treatment planning system.

The developed method for beam angle and weight optimization has become a powerful tool in our clinical practice. Automatic plan generation has resulted in acceptable treatment plans in less than an hour computation time for cases that could

not be solved by our dosimetrists after days of manual forward treatment planning. We have not yet quantitatively investigated the success rate of finding an acceptable plan if such a plan does indeed exist. This is a topic for future research. Preliminary exhaustive search studies point at a high probability of finding acceptable plans.

3.5 Conclusions

The investigated algorithm for beam orientation and beam weight selection features automatic generation of treatment plans with clinically feasible numbers of treatment beams, even for escalated tumor doses. The generated plans deliver the prescribed tumor dose while strictly obeying the imposed hard constraints on dose delivery to the tumor and the organs at risk. For the pancreas patients in this study, the automatically generated plans were superior to the clinically applied plans and to equi-angular set-ups. Calculation times were clinically acceptable; automatic plan generation is generally much faster than the manual, forward planning approach. The algorithm is now increasingly used in our daily clinical routine. Extensions for non-coplanar beam set-ups and IMRT are being developed.

References

1. Bortfeld T, and Schlegel W. Optimization of beam orientations in radiation therapy: Some theoretical considerations. *Phys Med Biol* 1993; 38:291-304.
2. Ezzell GA. Genetic and geometric optimization of three-dimensional radiation therapy treatment planning. *Med Phys* 1996; 23:293-305.
3. Langer M, Brown R, Morrill S, et al. A generic genetic algorithm for generating beam weights. *Med Phys* 1996; 23:965-971.
4. Li JG, Boyer AL, Xing L. Clinical implementation of wedge filter optimization in three-dimensional radiotherapy treatment planning. *Radiat Oncol* 1999; 53:257-264.
5. Mageras GS, Mohan R. Application of fast simulated annealing to optimization of conformal radiation treatments. *Med Phys* 1993; 20:639-647.
6. Mohan R, Mageras GS, Baldwin B, et al. Clinically relevant optimization of 3-D conformal treatments. *Med Phys* 1992; 19:933-944.
7. Morrill SM, Lane RG, Jacobson G, et al. Treatment planning optimization using constrained simulated annealing. *Phys Med Biol* 1991; 36:1341-1361.
8. Morrill SM, Lam KS, Lane RG, et al. Very fast simulated reannealing in radiation therapy treatment plan optimization. *Int J Radiat Oncol Biol Phys* 1995; 31:179-188.
9. Powlis WD, Altschuler MD, Censor Y, et al. Semi-automated radiotherapy treatment planning with a mathematical model to satisfy treatment goals. *Int J Radiat Oncol Biol Phys* 1988; 16:271-276.

10. Rowbottom CG, Webb S, Oldham M. Improvements in prostate radiotherapy from the customization of beam directions. *Med Phys* 1998; 25:1171-1179
11. Rowbottom CG, Oldham M and Webb S. Constrained customization of non-coplanar beam orientations in radiotherapy of brain tumors. *Phys Med Biol* 1999; 44: 383-399
12. Rowbottom CG, Khoo VS and Webb S. Simultaneous optimization of beam orientations and beam weights in conformal radiotherapy. *Med Phys* 2001; 28:1696-1702.
13. Söderström S and Brahme A. Optimization of the dose delivery in a few field techniques using radiobiological objective functions. *Med Phys* 1993; 20:1201-1210
14. Söderström S and Brahme A. Which is the most suitable number of photon beam portals in coplanar radiation therapy? *Int J Radiat Oncol Biol Phys* 1995; 33:151-159
15. Spirou SV Chui C-S. A gradient inverse planning algorithm with dose volume constraints. *Med Phys* 1998; 25:321-333
16. Starkschall G Pollack A and Stevens CW. Treatment planning using a dose-volume feasibility search algorithm. *Int J Radiat Oncol Biol Phys* 2001; 49:1419-1427.
17. Stein J, Mohan R, Wang X-H, et al. Number and orientations of beams in intensity-modulated radiation treatments. *Med Phys* 1997; 24:149-160.
18. Webb, S. 1989 Optimization of conformal radiotherapy dose distributions by simulated annealing. *Phys Med Biol* 1989; 34:1349-1370
19. Webb S. 1991 Optimization by simulated annealing of three-dimensional conformal treatment planning for radiation fields defined by a multileaf collimator. *Phys Med Biol* 1991; 36: 1201-1226.
20. Webb S. Optimization by simulated annealing of three-dimensional, conformal treatment planning for radiation fields defined by a multileaf collimator:II. Inclusion of two dimensional modulation of the x-ray intensity. *Phys Med Biol.* 1992; 37: 1689-1704.
21. Webb S. Optimizing the planning of intensity-modulated radiotherapy. *Phys Med Biol* 1994; 39: 2229-2246.
22. Woudstra E and Storchi PRM. Constrained treatment planning using sequential beam selection. *Phys Med Biol* 2000; 45: 2133-2149
23. Xing L, Hamilton RJ, Pelizarri C, et al. A three-dimensional algorithm for optimizing beam weights and wedge filters. *Med Phys* 1998; 25:1858-1865.
24. International Commission on Radiation Units and Measurements, Prescribing, Recording and Reporting Photon Beam Therapy. 1993.
25. Cassidy JR. Clinical Radiation Nephropathy. *Int J Radiat Oncol Biol Phys* 1995; 31:1249-1256.
26. Coia LR. Late effects of radiation therapy on the gastrointestinal tract. *Int J Radiat Oncol Biol Phys* 1995; 31:1213-1236.
27. Lawrence ThS. Hepatic toxicity resulting from cancer treatment. *Int J Radiat Oncol Biol Phys* 1995; 31:1237-1248.

CHAPTER 4

**AUTOMATED SELECTION OF BEAM ORIENTATIONS AND
SEGMENTED INTENSITY MODULATED RADIOTHERAPY (IMRT) FOR
TREATMENT OF OESOPHAGUS TUMORS**

E. Woudstra, B.J.M. Heijmen and P.R.M. Storchi, *Radiotherapy and Oncology* **77**,
(2005) 254-261

ABSTRACT

Background and Purpose: For some treatment sites, there is evidence in the literature that five to nine equi-angular input beam directions are enough for generating IMRT plans. For oesophagus cancer, there is a report showing that going from four to nine beams may even result in lower quality plans. In this paper, our previously published algorithm for automated beam angle selection (Cycle) has been extended to include segmented IMRT. For oesophagus cancer patients, we have investigated whether automated orientation selection from a large number of equi-angular input beam directions (up to 36) for IMRT optimisation can result in improved lung sparing.

Methods and Materials: CT-data from five oesophagus patients treated recently in our institute were used for this study. For a prescribed mean PTV dose of 55 Gy, Cycle was used in an iterative procedure to minimise the mean lung dose under the following hard constraints: standard deviation for PTV dose inhomogeneity 2% (1.1Gy), maximum spinal cord dose 45 Gy. Conformal radiotherapy (CFRT) and IMRT plans for a standard four-field oesophagus beam configuration were compared with IMRT plans generated by automated selection from 9 or 36 equi-angular input beam orientations. Comparisons were also made with dose distributions generated with our commercial treatment planning system (TPS), and with observations in the literature.

Results: Using Cycle, automated orientation selection from nine or thirty-six input beam directions resulted in improved lung sparing compared to the four field set-ups. Compared to selection from nine input orientations, selection from thirty-six directions did always result in lower mean lung doses, sometimes with even fewer non-zero weight beams. On average only seven beams with a non-zero weight were enough for obtaining the lowest mean lung dose, yielding clinically feasible plans even in case of thirty-six input directions for the optimisation process. With our commercial TPS we observed the same contra-intuitive, unfavourable results as reported in the literature; nine field equi-angular IMRT plans had substantially higher mean lung doses than plans for the conventional four field set-ups. For all cases, the Cycle plans generated from nine equi-angular input directions were superior compared to similar plans generated with our commercial TPS.

Conclusions: For the studied oesophagus cancer patients the best plans for IMRT were obtained with Cycle, using automated beam orientation selection from thirty-six input beam directions. The lowest mean lung doses could be obtained with, on average, a selection of only seven beams with non-zero weight.

4.1 Introduction

Investigations regarding the selection of beam orientations in combination with IMRT have started long ago. Theoretical considerations were given by Bortfeld and Schlegel [1]. Exhaustive search experiments have been carried out by Soderstrom and Brahme [14,15].

Based on case studies it was concluded that with IMRT adequate results would be obtained with 5 to 9 equi-angular beams directions; adding more beams would not significantly increase the quality of the plan [15,16]. Only for smaller numbers of beams, optimisation of the beam directions would result in improved plans.

Webb [17] and Mageras and Mohan [3] have described an approach to the problem of orientation selection that allows a large number of input orientations and they solve the problem using the beam weight space instead of using the phase space. Simulated annealing was used to find a solution and the results contained many beam orientations with a non-zero weight. Extrapolation of this method to IMRT may result in a search space that is too large to derive a solution within a reasonable time frame.

Beam orientation selection was also the subject of many more recent papers [2,4-13]. Practical methods for orientation selection and IMRT were proposed by Rowbottom *et al* [13] and later by Pugachev *et al* [6-9]: after the selection of the number of beams, a result may be obtained in a two-step process using e.g. fast simulated annealing for orientation sampling and fluence optimisation using a gradient technique.

Experiences with current IMRT-algorithms and pre-selected beam orientations have pointed at some unexpected problem for tumour sites, like head-and-neck and the thorax region. Compared to IMRT plans with 9 equi-angular beam arrangements, selection of fewer beams with properly chosen orientations, positively affected the dose distribution [4,5]. A possible explanation for this phenomenon has been given by Rowbottom *et al* [13], who mentioned that some IMRT algorithms have difficulty to reduce the dose in OARs in low dose regions.

Using the CT-data sets of five previously treated oesophagus cancer patients, and the CORVUS (v3.0), an inverse TPS, Nutting *et al* [5] investigated the use of IMRT for the conventional 4-field setup (anterior, posterior, and two posterior oblique beams), and for a 9-field equi-angular configuration. For the conventional beam setup, IMRT plans had lower mean lung doses than the corresponding conformal plans. However, compared to the IMRT plans for the 4-field configuration, the 9-field IMRT plans did unexpectedly result in higher mean lung doses.

In this paper we have extended our previously published algorithm for automated beam angle selection, designated Cycle, [18,19] to include segmented IMRT. Both for Cycle and for our commercial TPS (Cadplan/Helios), we have investigated, for oesophagus cancer patients, whether orientation selection from a large number of equi-angular input beam directions for IMRT optimisation, can result in decreased mean lung doses, compared to the standard 4-field setup. Comparisons were made with the study mentioned above by Nutting *et al* [5]. As our commercial TPS did not allow the use of a mean organ dose as a treatment objective, like in [5], minimisation of the lung volume receiving a dose higher than 18 Gy (V_{18}) was applied as an indirect means to reduce the mean lung dose. In Cycle, both minimisation of the mean lung dose as well as minimisation of V_{18} , are possible. Using Cycle, we compared these two optimisation schemes to investigate whether the rather poor results of our commercial TPS could be attributed to the use of this indirect lung dose minimisation (V_{18}).

4.2 Methods and Materials

In this study, treatment plans were designed for oesophagus cancer patients. The general objectives and constraints were similar to those in the study by Nutting *et al* [5]. The main objective was a minimum mean lung dose, while delivering the prescribed mean PTV dose without violation of the imposed hard constraints on the dose homogeneity in the PTV and the maximum dose in the myelum. The most important question to be addressed was whether IMRT optimisation with a large number of input beam directions (up to 36) can be used to improve on the mean lung dose obtained for the conventional beam setup, with an anterior beam, a posterior beam, and a left and a right posterior oblique beam. Plans were generated with our commercial TPS and with Cycle, an in-house developed package for automated beam angle selection [18,19].

4.2.1 Oesophagus patients

CT data sets were used of five patients with a tumour in the thoracic oesophagus, that were treated previously in our clinic. For each patient, 25 CT-slices (1 cm slice distance) were used. To provide for a setup margin, the inner outline of the vertebrae, designated spinal cord in this paper, was delineated instead of the myelum.

Treatment plans were generated with objectives and constraints similar to [5]. The main objective was to generate plans with a minimum mean lung dose. The prescribed mean PTV dose was 55 Gy. Regarding PTV dose homogeneity a maximum standard deviation of 1.1 Gy, (2% of mean PTV dose), was tolerated. The maximum acceptable spinal cord dose was 45 Gy. Both lungs were considered as one organ. Only the lung volume outside the PTV was considered for optimisation. In agreement with Nutting *et al* [5] no constraints were used for the mediastinum and the heart.

4.2.2 Dose calculation engine for Cycle and segmented IMRT

Automatic beam angle selection with Cycle is based on pre-calculated, three-dimensional single beam input dose distributions. Any number of input directions θ can be used. In this study the maximum was 36 with 10 degrees intervals. The input dose distributions were calculated with a dedicated dose calculation engine coupled to Cycle. This algorithm is based on 3D ray-tracing, and uses an effective path length method for correction of tissue heterogeneities. The CT-data of the patient is used as input. Unit beam weight has been defined to be 1 Gy at d_{max} at the source-to-axis distance. In a previous study [19] it was established that the resulting dose distributions agree well with the results obtained with our commercial TPS. The latter observation was confirmed in the study described in this paper. Instead of the dedicated dose calculation engine, input from any TPS may be used.

For each θ , the uniform field distribution $U_{\theta u}(x, y, z)$ and four 60°-wedge distributions $U_{\theta, 60, \varphi}(x, y, z)$, for collimator angles φ of 0°, 90°, 180° and 270° are involved. For the investigations described in this paper, the shapes of the fields were defined using the Beam's-eye-view (BEV) projections of the PTV plus a 0.5 cm margin. To include segmented IMRT, Cycle has been extended for the use of beam segments that do not fully encompass the PTV. In this study, two segments were used to obtain improved sparing of the spinal cord:

- the uniform BEV-shaped field, however with the projection of the spinal cord shielded.
- a complementary segment for segment 1, only irradiating the spinal cord.

To avoid significant lateral secondary electron transport, 6 MV X-ray beams were used.

4.2.3 Automated beam angle and weight selection with Cycle

Cycle has been described in detail elsewhere [18,19]. Here, a brief summary will be presented. For each patient, the algorithm uses pre-calculated three-dimensional dose distributions for a number of allowed input directions (generally 36, using 10 degrees intervals). Starting with an empty plan (no selected beams), the algorithm generates a treatment plan by *sequentially* adding beams from the potential input orientations until the prescribed target dose has been reached and as long as none of the imposed hard constraints has been violated. For the selection of each new beam to be added, *all* available 36 orientations are reviewed; the orientation to be selected has the best compromise between a PTV dose increase, and an unavoidable further approach towards the imposed hard constraints. To avoid generation of sub-optimal plans, new beams are added with a limited PTV dose contribution. A selected orientation may turn out to be very efficient in PTV dose delivery without approaching the constraints. As the selected orientation remains a candidate for the next selection, favourable beam directions are selected several times.

Sequential selection of beams is performed using a ‘dynamic’ score function. The meaning of the word ‘dynamic’ is twofold. Firstly, after each new beam selection the total dose distribution delivered so far is updated by adding the dose contribution from the new beam. Before selection of the next beam the score function is adapted to the updated dose distribution. Secondly, at the start of the beam selection process, the score function has equal penalty factors for approaching each of the various constraints. In case these initial factors do not result in a plan that delivers the prescribed tumour dose without violating constraints, the algorithm calculates new factors and generates a new plan. The new penalty factors favour selection of orientations that better avoid constraints that were violated in the previous run.

4.2.4 Mean lung dose minimisation with Cycle

As described in section 4.2.3, Cycle is an algorithm for generating a treatment plan that delivers the prescribed tumour dose without violating the imposed hard constraints. To minimise the mean lung dose for a patient and a specific input beam set, repeated runs of Cycle were automatically performed, with increasing demands on the maximum allowed mean lung dose. This automatic plan generation process was always started with a mean lung dose constraint level of 15 Gy. Because of the intrinsic drive of Cycle to stay away as far as possible from the constraints, in most

cases a solution was found with a lower mean dose result. Then, a new plan generation was automatically started with a constraint level set to 0.2-0.5 Gy lower than the result of the previous plan generation. This process of tightening the constraint level for the mean lung dose was stopped when generation of a plan with the prescribed mean tumour dose was no longer possible without exceeding any of the constraints. For plans selected from 9 or 36 input directions, a process similar to described in [19], was then performed to minimise the number of selected beam orientations, while not compromising the obtained minimum mean lung dose. This process is based on the successive removal of the beam with the lowest weight, followed by a new plan generation with the previously determined minimum mean lung dose (see above) as one of the constraints. The procedure was stopped when with the remaining orientations it was no longer possible to deliver the prescribed tumour dose with the previously determined minimum mean lung dose, and not violating any of the other constraints. This reduction in beams is generally obtained at the cost of more approaching (but not exceeding) one of these other constraint levels.

4.2.5 Treatment plans generated with Cycle aiming at minimal lung dose

Similar to Nutting et al [5] a variety of input beam arrangements was studied. For all these arrangements the mean lung dose was minimised, while delivering the prescribed tumour dose, and also maintaining the other dose constraint parameters within the prescribed tolerance levels.

First, Cycle was used to establish for all patients the optimal 4-field *conventional* beam arrangement with flat and wedged conformal fields (no IMRT segments for partial blocking of the myelum). For this purpose, for each patient a conformal plan was generated for each of three input sets of beam orientations. These sets all had pre-calculated anterior-posterior (AP) and posterior-anterior (PA) beams. The distinction was made through the (posterior-lateral) beams: two symmetric beams of 90°, 100° or 110°. Essentially, for each set, Cycle determined the beam weights to obtain a minimal mean lung dose. The set yielding the lowest minimised mean lung dose (section 2.4) for the patient was considered as optimal. The resulting dose plan, designated '4-CFRT', was used for further plan comparisons. The beam orientations as found for 4-CFRT were also used to generate plans ('4-IMRT') that include beam segments that allow protection of the spinal cord for further minimisation of the mean lung dose. Finally, segmented IMRT plans, designated '9-IMRT' and '36-IMRT', with minimal mean lung dose were generated using orientation selections from 9 or

36 equi-angular input beams. These plan generations were followed by a beam orientation reduction procedure as described in the previous section.

4.2.6 Comparison with a commercial TPS

For 9 equi-angular beam set-ups, IMRT plans for the 5 patients were also generated with our commercial TPS (Cadplan/Helios, version 6.4.7). As direct minimisation of the mean lung dose is not possible with this system, we indirectly minimised this dose by minimisation of V_{18} (as in [5]), by adjusting priority factors, profile smoothing factors, etc. For comparisons with the corresponding 9-IMRT Cycle plans, the optimal plan parameters (beam orientations, weights, BEV field shapes, BEV segments and segment weights) as obtained with Cycle were imported into the commercial TPS, and the dose distributions were re-calculated.

4.2.7 V_{18} minimization using Cycle

Often, commercial planning systems do not allow for direct minimisation of the mean lung dose. For this reason, Nutting *et al* [5] indirectly minimised this dose by minimisation of the lung volume with a dose higher than 18 Gy (V_{18}). With Cycle, direct minimisation of the mean lung dose, as well as indirect minimisation using V_{18} are possible. Section 4.2.4 describes the procedure for direct minimisation of the mean lung dose. A similar procedure was followed for minimisation of V_{18} , using the conventional four field orientations and 9 and 36 equi-angular input orientations and the resulting mean lung dose was compared with direct minimisation.

4.3 Results and discussion

4.3.1 Mean lung dose minimisation with Cycle

Table 4.1 gives an overview of the achieved mean lung doses and required numbers of beams in case of 9 and 36 input orientations (in between brackets) for the five patient cases in this study. In agreement with the observations of Nutting *et al* [5], the results show that 4-IMRT may yield a significantly lower mean lung dose than 4-CFRT (columns 2 and 4). Different from Nutting's observations with his commercial TPS, Table 4.1 shows that with Cycle further reductions are achieved with orientation

Table 4.1 Full overview of this study, regarding obtained mean lung dose values (Gy) for the 4-CFRT, the 4-IMRT, the 9-IMRT, and the 36-IMRT plans after minimization of the mean lung dose.

	Cycle								TPS	
	4 CFRT	4 IMRT		9 IMRT		36 IMRT		9 IMRT		
	mean	dvh	mean	dvh	mean	dvh	mean	Cy:mean	TPS:dvh	
1	13.7	12.3	12.3	12.1	11.1 (7)	11.6	9.1 (9)	11.7	17.2	
2	13.8	13.8	13.7	12.5	12.0 (7)	12.7	10.8 (7)	12.3	15.3	
3	14.7	13.0	13.0	11.9	12.6 (8)	11.9	10.2 (7)	12.3	15.5	
4	11.7	11.4	10.9	9.7	9.7 (9)	9.1	9.0 (7)	9.9	11.0	
5	14.1	14.2	14.1	13.9	12.3 (6)	13.3	10.8 (7)	12.3	18.8	

The mean lung dose was minimised using the mean dose parameter ('mean' columns) or the V_{18} parameter ('dvh' columns). For the 'mean' columns of the 9- and 36 IMRT-generations, the final number of selected beam orientations resulting from the procedure of beam orientation reduction is given in between brackets. The two 'TPS' columns for 9-IMRT on the right side of the table represent the results of the recalculation of the Cycle plans '9 IMRT-mean' using the TPS and indirect minimization of the mean lung dose using V_{18} by the algorithm of the TPS.

selection from 9 or 36 equi-angular input beams (columns 6 and 8). For the 36-IMRT plans, 4 patients have 7 beam orientations with a non-zero weight, one patient has a plan with 9 beams. For the cases 3 and 4, compared to 9-IMRT, the 36-IMRT plan has a lower mean lung dose, delivered with fewer beams.

The columns 6 and 8 of Table 4.1 show that using Cycle, the mean lung dose reduction may be improved when using orientation selection from many equi-angular (36) input orientations compared to 9. As also demonstrated in Table 4.1, generally, the use of more input directions did not result in plans with more orientations, but in a further optimised selection of the beams. Therefore, with Cycle there is no need to limit the number of input directions in order to obtain results with clinically feasible numbers of beams. Only the most efficient orientations will survive the selection procedure described in section 4.2.4.

Figure 4.1 shows optimised IMRT plans for case 1 using four and nine input orientations. The use of nine input orientations gives more freedom to avoid the lungs while maintaining the constraints on maximum spinal cord dose and PTV dose homogeneity. For the cases 3 and 5, the 36-IMRT dose distributions are depicted in Figure 4.2. All 36-IMRT plans have a large dose contribution from the 0° and 180° beams, as in the 4-CFRT and 4-IMRT plans.

Most other beams are posterior-oblique, also in agreement with the conventional beam set-up. However, for 4 out of 5 patients, also one or more anterior-oblique beams have been selected. Figure 4.2 shows some customisation of the selected orientations to the specific patient anatomy.

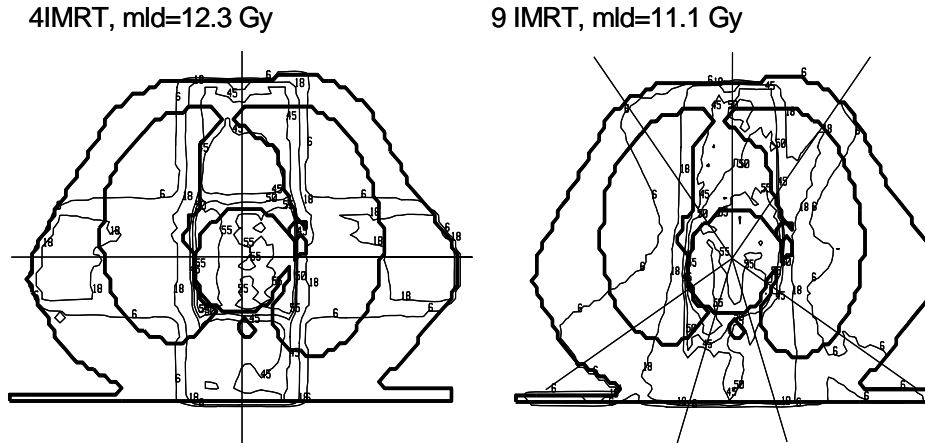


Figure 4.1 Central slice dose distributions of Cycle plans generated for case 1 using 4 and 9 input orientations, segmented IMRT and minimized mean lung dose. mld stands for mean lung dose. Isodose lines shown: 6, 18, 45, 50 and 55 Gy.

For the patients in this study, the main treatment objective was to achieve the prescribed tumour dose with a minimum mean lung dose, and not exceeding tolerance values of PTV dose homogeneity and the maximum spinal cord dose. For this reason, no constraints were used for the heart or the mediastinum. This explains the observed high weights for the anterior and posterior beams, and the relatively high doses in the

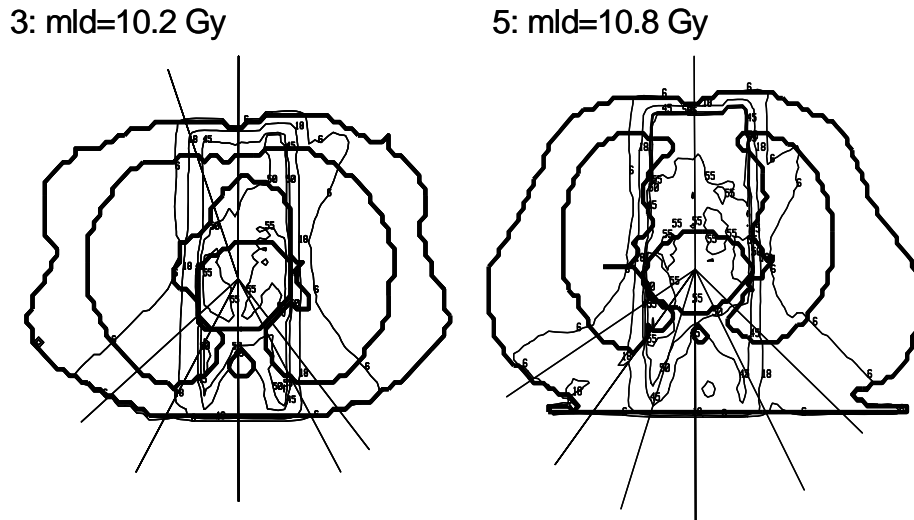


Figure 4.2 The 36-IMRT Cycle plans for the cases 3 and 5 in this study with minimized mean lung dose. Isodose lines shown: 6, 18, 45, 50 and 55 Gy.

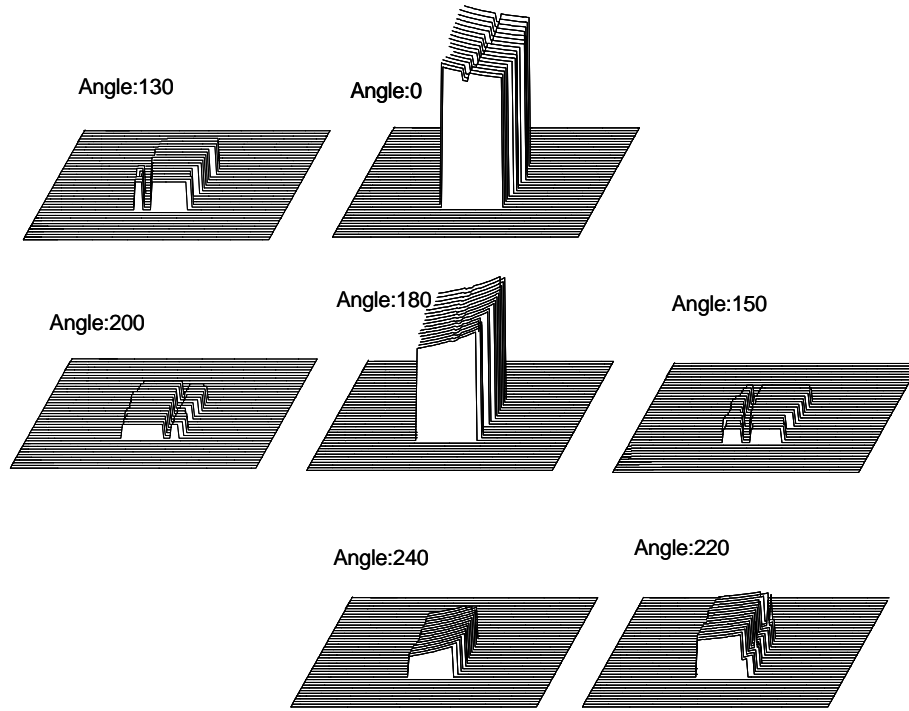


Figure 4.3 Fluence distributions for the 7 selected orientations in the 36-IMRT plan for case 5.

mediastinum and heart (Figures 4.1 and 4.2). To reduce these doses, constraints may be introduced for these organs. For one case we studied the attainable lowest mean lung dose as a function of the maximum allowed dose in the mediastinum. As to be expected, it was observed that the minimal mean lung dose went up with lower levels of the maximum tolerated mediastinal dose. Also in this test the smallest mean lung dose values were obtained using selection from 36 input orientations.

An example of fluence distributions obtained with Cycle is presented in Figure 4.3, showing the profiles for the 7 beams in the 36-IMRT plan of case 5. The figure clearly demonstrates the large weight of the anterior and posterior beams relative to the other beams. The 130°, 150° and 200° beams have complete shielding of the spinal cord. A customisation of beam orientations and weights to the specific patient anatomy and PTV delineation has been observed.

For case 1, dose volume histograms (DVH) for the lungs are shown for the 4-CFRT, the 4-IMRT, the 9-IMRT, and the 36-IMRT in Figure 4.4. The differences in mean lung as reported in Table 4.1 are reflected by corresponding differences in the lung DVHs. Similar to the mean lung dose reduction, a reduction of V_{18} can be observed.

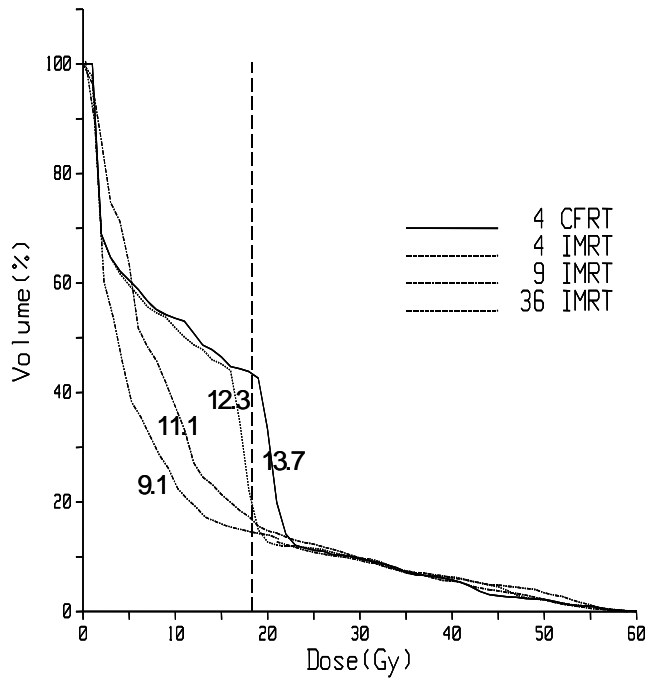


Figure 4.4 DVH comparisons for case 1, for the lungs outside the PTV and the various input orientation sets. The numbers correspond to the obtained mean lung doses.

As explained in section 4.2.4, a procedure was used to minimise the number of selected beam orientations while still delivering the prescribed tumour dose with the lowest achievable mean lung dose. Sometimes, this beam orientation reduction resulted in a plan with a somewhat higher maximum spinal cord dose or a somewhat less homogeneous PTV dose distribution (although always within the constraints for the cord and the PTV inhomogeneity).

The procedure for minimisation of the number of beams in the plan is an option within Cycle. If the lowest spinal cord dose or the highest PTV dose homogeneity are considered more important than dose delivery with the lowest number of beams, the option can be switched off.

4.3.2 Comparison with a commercial TPS

Table 4.1 also compares the mean lung doses obtained with Cycle, using direct mean lung dose minimisation and 9 equi-angular input beam orientations (column 6), but recalculated using our commercial TPS (column 9), with the doses in the corresponding 9-field plans generated with our commercial TPS and indirect minimisation based on V_{18} (column 10). Obviously, the Cycle plans have substantially lower mean lung doses.

The 9-field plans generated with our commercial TPS were always highly conformal, however at the expense of an unnecessary large mean lung dose level.

4.3.3 Direct lung dose minimization vs. V_{18} using Cycle

For indirect minimisation of the mean lung dose with Cycle using V_{18} (section 4.2.7), similar data, as was generated for direct minimisation, is also shown in Table 4.1 (see

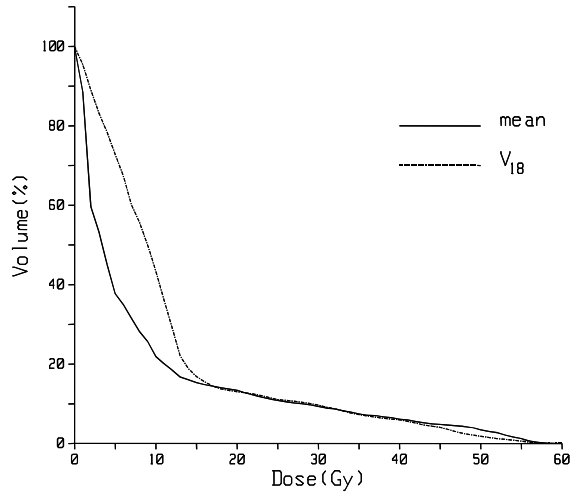


Figure 4.5 Typical result of a lung DVH comparison from direct mean lung dose minimisation and indirect minimisation using V_{18} and 36 input directions for case 1.

columns 3, 5 and 7). Like for direct minimisation, the achieved mean lung dose was in general lower for larger numbers of input beam directions. This finding demonstrates that the higher mean lung doses for higher numbers of input directions, as observed by Nutting et al [5], and by us for our commercial TPS (section 4.3.2), are not necessarily connected to the use of indirect mean lung dose minimisation with V_{18} .

This comparison between direct and indirect mean lung dose minimisation shows that direct lung dose minimisation is in general more effective especially with increasing number of input beam directions. As demonstrated in Figure 4.5, this reduction in mean lung dose stems from reduction in lung volumes exposed to low doses. Obviously, for the indirect optimisation process, for points with doses lower than 18 Gy, there is no drive for further dose reduction.

4.4 Conclusions

Using our algorithm for automated beam orientation selection and segmented IMRT, designated Cycle, the lowest mean lung dose is obtained for beam selection from 36 input orientations, compared to the standard 4-field setup and selection with only 9 equi-angular input directions. Due to a more refined orientation selection with 36 input beams instead of 9, the lower mean lung dose may even be obtained with a smaller number of non-zero weight beams in the final optimised plan. In contrast to the results obtained by Nutting *et al* [5], and to the observations for our commercial

TPS, going with Cycle from four to nine IMRT fields, does indeed yield a (to be expected) decrease in the mean lung dose. Using Cycle, also indirect minimisation of the mean lung dose by minimising V_{18} improves by going from the 4-field setup, to 9 and 36 input beam directions. Therefore, the unexpected increase in mean lung dose while going from a small number of beams to larger numbers of beams, as observed with the TPS used in [5] and with our own commercial TPS, is not necessarily due to the V_{18} minimisation applied with these systems. Plans generated with Cycle have lower mean lung doses than plans obtained with our commercial TPS.

Acknowledgements

We acknowledge the fruitful discussions with Dr. Mark de Langen on understanding, functionality and use of inverse planning using Helios in CadPlan.

References

1. Bortfeld Th, Schlegel W. Optimization of beam orientations in radiation therapy: some theoretical considerations. *Phys Med Biol* 1993; 38: 291-304.
2. Das S, Cullip T, Tracton G, et al. Beam orientation selection for intensity modulated radiation therapy based on target equivalent uniform dose maximization. *Int J Radiat Oncol Biol Phys* 2003; 55:215-24.
3. Mageras GS, Mohan R. Application of fast simulated annealing to optimization of conformal radiation treatments. *Med Phys* 1993; 20: 639-47
4. Nutting CM, Rowbottom CG, Cosgrove VP, et al. Optimisation of radiotherapy for carcinoma of the parotid gland: a comparison of conventional, three-dimensional; conformal and intensity modulated techniques. *Radiother Oncol* 2001; 60:163-72
5. Nutting CM, Bedford JL, Cosgrove VP, Tait DM, Dearnaley DP, Webb S. A comparison of conformal and intensity-modulated techniques for oesophageal radiotherapy. *Radiother Oncol* 2001; 61: 157-63
6. Pugachev A, Li JG, Boyer AL, et al. Role of beam orientation optimization in intensity-modulated radiation therapy. *Int J Radiat Oncol Biol Phys* 2001; 50: 551-60
7. Pugachev AB, Boyer AL, Xing L. Beam orientation optimization in intensity-modulated radiation treatment planning. *Med Phys* 2000; 27:1238-45
8. Pugachev A, Xing L. Computer assisted selection of coplanar beam orientations in intensity-modulated radiation therapy *Phys Med Biol* 2001; 46: 2467-76
9. Pugachev A, Xing L. Pseudo Beam's Eye View as applied to beam orientation selection in intensity modulated radiation therapy. *Int J Radiat Oncol Biol Phys* 2001; 51: 1361-70
10. Rowbottom CG, Webb S. Oldham M. Improvements in prostate radiotherapy from customization of beam directions. *Med Phys* 1998; 25: 1171-79

11. Rowbottom CG, Oldham M, Webb S. Constrained customization of non-coplanar beam orientations in radiotherapy of brain tumours. *Phys Med Biol* 1999; 44: 383-99
12. Rowbottom CG, Khoo VS, Webb S. Simultaneous optimization of beam orientations and beam weights in conformal radiotherapy. *Med Phys* 2001; 28: 1696-702
13. Rowbottom CG, Nutting CM, Webb S. Beam orientation optimization of intensity-modulated radiotherapy: clinical application of parotid gland tumours. *Radiother Oncol* 2001; 59: 169-77
14. Soderstrom S, Brahme A. Optimization of the dose delivery in a few field techniques using radiobiological objective functions. *Med Phys* 1993; 20: 1201-10
15. Soderstrom S, Brahme A. Which is the most suitable number of photon beam portals in coplanar radiation therapy? *Int J Radiat Oncol Biol Phys*. 1995; 33: 151-9
16. Stein J, Mohan R, Wang X, et al. Number and orientations of beam intensity-modulated radiation treatments. *Med Phys* 1997; 24: 149-60
17. Webb S. Optimization by simulated annealing of three-dimensional conformal treatment planning for radiation fields defined by a multi-leaf collimator: II Inclusion of two dimensional modulation of the x-ray intensity. *Phys Med Biol* 1992; 37: 1689-704
18. Woudstra E, Storchi PRM. Constrained treatment planning using sequential beam selection. *Phys Med Biol* 2000; 45: 2133-2149
19. Woudstra E, Heijmen BJM Automated beam angle and weight selection in radiotherapy treatment planning applied to pancreas tumors. *Int J Radiat Oncol Biol Phys* 2003; 56: 878-888

CHAPTER 5

COMPARISON OF AN ALGORITHM FOR AUTOMATED SEQUENTIAL BEAM ORIENTATION SELECTION WITH EXHAUSTIVE SEARCH AND SIMULATED ANNEALING

E. Woudstra, B.J.M. Heijmen and P.R.M. Storch, submitted

ABSTRACT

A few years ago we have developed and published a new deterministic algorithm (called Cycle) for automatic selection of beam orientations in radiotherapy. This algorithm is a plan generation process aiming at the prescribed PTV dose within hard dose and dose-volume constraints. In contrast with the most important published algorithms for orientation optimization, this algorithm does not require to specify the beam number in advance. The algorithm allows a large number of input orientations to be used and uses only the most efficient orientations, surviving the selection process.

In this paper we compare the capabilities of exhaustive search (ES), fast simulated annealing (FSA) and Cycle for cases where local optima are supposed to be present. Five pancreas and five oesophagus cases previously treated in our institute were selected for this comparison. Plans were generated by ES, FSA and Cycle, using the same hard dose and dose-volume constraints, and the largest possible achieved PTV doses as obtained from these algorithms were compared.

The largest achieved PTV dose values, were generally very similar for the three algorithms. In some cases FSA resulted in a slightly higher PTV dose than Cycle, at the cost of switching on substantially more beam orientations than Cycle. In other cases, when Cycle generated the solution with the highest PTV dose using only a limited number of non-zero weight beams, FSA seemed to have difficulty in switching off unfavourable directions. Calculation times for ES were clinically unacceptable. Cycle was faster than FSA, especially for large dimensional solution spaces.

5.1 Introduction

Simultaneous optimization of beam directions and beam weights remains a difficult subject for radiotherapy treatment plan optimization. This difficulty is caused by the ‘interdependence’ of beam orientations and beams weights. The selection of a specific orientation in a plan is meaningless without the knowledge of the corresponding beam weight.

Many investigations have been published regarding orientation optimization and the interdependence with beam weight, for simple CFRT (Bedford and Webb 2003, Morrill *et al* 1991,1995, Oldham *et al* 1995, Rowbottom *et al* 1998a, 1998b, 1999, and 2001, Woudstra and Storchi 2000, Woudstra and Heijmen 2003), for segmented

beam IMRT (Bortfeld and Schlegel 1993, Das *et al* 2003, Mageras and Mohan 1993, Webb 1991) and for full-blown IMRT (Djajaputra *et al* 2003, Gaede *et al* 2004, Nutting *et al* 2001a, 2001b, Pugachev 2000, 2001a, 2001b, 2001c, 2002, Rowbottom *et al* 2001, Soderstrom *et al* 1993, Soderstrom and Brahme 1993, Stein *et al* 1997, Webb 1989). In summary, it was concluded that orientation optimization (even for IMRT) is useful. Orientation optimized plans result in a better dose distribution (Nutting *et al* 2001a and 2001b, Pugachev 2002, Rowbottom 2001) or a comparable plan with fewer beams (Das 2003). The use of DVH constraints will certainly introduce local minima, of which the clinical effect will be more or less substantial (Deasy 1997, Llacer *et al* 2003, Rowbottom and Webb 2002, Wu and Mohan 2002 and Wu *et al* 2003).

The usual approach for the inverse problem of beam orientation optimization is to choose the number of beams in advance. Then, the selection of a combination of orientations is guided by a stochastic algorithm, e.g. simulated annealing. The next step is the optimisation of the beam weights or the fluences of this combination using an objective function and an inverse algorithm. Based on the resulting value of the objective function, a decision is taken to accept or reject the beam configuration (See: Nutting *et al* 2001, Pugachev and Xing 2002, Rowbottom *et al* 2001). Although attempts were taken to increase the speed, this technique is rather computation intensive. Compromises for calculation time reduction can be made to relax the stopping criterion with the risk of remaining in a local optimum. Consequences of errors due to convergence and local minima, were described recently by Jeraj *et al* (2003).

About five years ago we have developed and published (Woudstra and Storchi 2000) a new and rather fast approach to the inverse problem of orientation optimization, which we call 'Cycle'. Cycle is a non-stochastic automated beam angle and weight selection process based on sequential selection and addition of beams. The basic function of Cycle is the generation of an acceptable treatment plan, i.e. a plan yielding the prescribed tumour dose and simultaneously fully complies with all imposed hard constraints. Beam orientations are selected according to a score function after beam weight optimization for each considered orientation during a temporary placement in the already existing plan. In addition, Cycle was extended with an option for segmented IMRT. Using Cycle, it is not required to define the number of beams for the plan in advance. Only the most efficient orientations from the input set will survive the selection procedure. Selection from a larger set of input orientations does not necessarily result in a plan with more orientations but in a more proper orientation

selection. A priori assumptions regarding beam orientations are not required. Cycle uses pre-calculated dose distributions of various beam types to build a treatment plan. For conformal radiotherapy, uniform beams and 4 wedge beams (4 wedge directions) shaped to the target projection in the BEV are used and for segmented IMRT, beam segments may be added. These segments are defined by geometric projection of a selected organ at risk (OAR) in the direction of the beam orientation.

Inverse problems to search a prescribed PTV dose or the largest possible PTV dose within hard constraints can also be solved easily using stochastic search algorithms like e.g. fast simulated annealing (FSA). However, FSA could turn out to be time-consuming for large dimensional spaces. Contrary, the use of FSA could be mandatory especially when dose volume constraints give the feasible solution space a non-convex shape.

In order to study the capabilities of the mentioned algorithms, we have compared Cycle with Fast Simulated Annealing (FSA) for large dimensions of the feasible beam weight space and as an additional reference, we compared Cycle and FSA with an Exhaustive Search algorithm (ES) for low dimensional beam weight spaces. For all comparisons, sets of hard dose and dose volume constraints were defined. ES, FSA and Cycle were then used to search for plans with the largest achievable PTV dose within the imposed constraints. Apart from the achieved maximum PTV doses, the algorithms were also compared with respect to the selected number of non-zero weight beams, and calculation time.

5.2 Methods

5.2.1 *The feasible space and the objective*

The solution space of the inverse problems used in this paper with n isocentric input beams or beam segments, is the n -dimensional beam weight space. The part of this beam weight space, which is enclosed by constraint hyper planes due to the imposed hard constraints is called: the feasible space. The goal of this paper is to compare the mentioned algorithms (ES, FSA and Cycle) as to their ability to find the solution with the largest achievable target dose within this feasible space. Therefore, the objective was defined as the target dose at the isocentre or as the mean PTV dose. For fair comparisons, the definition of the solution space was always exactly the same for the algorithms involved, implying the use of the same input beam directions, the same

beam weight grid size, and the same maximum allowable beam weight for the various directions. Also, the pre-calculated dose distributions were exactly equal for input of the three algorithms, as well as the applied plan evaluation functions (DVH calculation, etc.). The only difference between the algorithms was the method for exploration of the solution space.

For comparisons involving Cycle and FSA only, the solution space had a discrete beam weight resolution of 0.01 Gy for all input beams (unit beam weight defined as 1 Gy at d_{max} at the source-to-axis distance), and the maximum beam weight was 50 Gy for all beams. To avoid excessive ES calculation times, comparisons involving ES, Cycle and FSA were performed in a 5 dimensional solution space with a beam weight resolution of 1 Gy and beam weight ranges of 0 to 30 Gy, again equal for all involved algorithms.

5.2.2 Calculation engine and beam types

For plan composition the algorithms have used the same pre-calculated, three-dimensional single beam dose distributions for a maximum of 36 angles of incidence θ with 10 degrees intervals. A beam's-eye-view (BEV) function is used for field shape definition with a 0.5 cm margin around the projected target. For each θ , the uniform field distribution $U_{\theta,u}(x, y, z)$ and four 60°-wedge distributions $U_{\theta,60,\varphi}(x, y, z)$, for collimator angles φ of 0°, 90°, 180° and 270° are involved. The dose distributions are calculated using the CT-data of the patient. Apart from conventional beams, beam segments for partial blocking of organs at risk could be used on top of the open and 4 wedged fields. Two segment types were used for improved sparing of the spinal cord for the oesophagus cases:

- the uniform BEV-shaped field with 0.5 cm margin around the PTV, however with the projection of the spinal cord shielded.
- a complementary segment for segment 1, only irradiating the spinal cord.

The dose calculation algorithm is based on 3D ray-tracing and uses an effective path length method for dose correction due to tissue heterogeneities. The engine was tuned regarding the heterogeneity correction, the penumbra and the dose level outside the field edges to fit with the dose distributions of our commercial TPS (CadPlan).

5.2.3 Algorithms

5.2.3.1 Exhaustive search

Exhaustive search (ES) was used by Soderstrom *et al* (1993), Soderstrom and Brahme (1993), and Stein *et al* (1997). They reported exhaustive search in the phase space. In this paper, exhaustive search is performed in the feasible space. Each point in the feasible space represents a treatment plan and a dose distribution. If all dose distribution parameters are within the prescribed constraint values, the plan is accepted and the objective value is equal to: the corresponding PTV dose. If the plan is violating one of the constraints, the objective is set to 0. The feasible space is exhaustively searched and the maximum objective value is retained as well as the corresponding beam weight combination.

5.2.3.2 Fast simulated annealing

Fast simulated annealing (FSA) as treatment planning optimization algorithm in radiotherapy was described in many papers and a large variety of implementations exists. The first applications of FSA for radiotherapy were described by Webb (1989, 1991) and Mageras and Mohan (1993).

The implementation in this paper is close to descriptions given by Oldham and Webb (1995) for the Cauchy distribution and Mageras and Mohan (1993) for the cooling schedule and the tuning procedure. Contrary to the usual search for a minimum objective, the FSA algorithm is used here to determine the largest PTV dose within the feasible space. For each new iteration, all beam weights are changed simultaneously. Because hard constraints are used, constraint violation results in an objective value equal to zero. If, after weight assignment to the beam weight vector, a constraint is violated, this vector is re-normalized. Re-normalization will guarantee that the most critical constraint is just touched and a feasible solution is found. This procedure is carried out to increase the speed and the efficiency of the search process.

An n-dimensional beam weight vector is used for iteration k: $\mathbf{x}^k = (x_1^k, x_2^k, \dots, x_n^k)$. The starting vector \mathbf{x}^0 is equal to $\mathbf{0}$. The i th element of the new beam weight vector at the k th iteration is determined by:

$$x_i^k = x_i^{k-1} + \Delta x_i^k \quad (1)$$

where Δx_i^k is determined with a Cauchy distribution:

$$\Delta x_i^k = W_k \tan(\pi(r-0.5)), \quad (2)$$

and:

- r is a random number between 0 and 1 from a uniform distribution.
- W_k is the width of Cauchy distribution: $W_k = W_0/(1+k/R)$.
- R represents the cooling parameter.

The beam weights are limited to values less than 50: $0 \leq x_i^k < 50$. Finally, when one or more constraints are violated, vector scaling to the most critical constraint is used: $\mathbf{x}^k \Rightarrow f_{sc} \cdot \mathbf{x}^k$, where f_{sc} is the scaling factor. Hereafter, the target dose D_{PTV} is recalculated. The new solution \mathbf{x}^k may be accepted with the probability:

$$P = \exp((D_{PTV}(\mathbf{x}^k) - D_{PTV}(\mathbf{x}^{k-1}))/T_k) \quad (3)$$

using $T_k = T_0/(1+k/R)$, where T_0 and T_k correspond to the initial temperature and the temperature of iteration k respectively.

The annealing parameters T_0 , W_0 and R have been tuned closely following the description of Mageras and Mohan (1993). This tuning resulted in: $W_0 = 1$, $T_0 = 0$ and $R = 200$. In fact, variation of R larger than 100, did not reveal any substantial influence on the results. The fact that the initial temperature was chosen to be zero, means that in the feasible space used in this study, hill climbing is considered less important than tunnelling. This is in agreement with observations of various investigators (Stein *et al* 1997, Mageras and Mohan 1993).

For the stopping criterion, initially, an expression was used, similar to the one used by Mageras and Mohan (1993) and Stein *et al* (1997), resulting in large iteration numbers for convergence. Later, the convergence criterion was somewhat relaxed to speed up the process without substantial loss of result. Initial observations showed that the required number of iterations strongly depends on the dimension of the beam weight space. The following suitable compromise between speed and convergence was made: the number of iterations was chosen to be 400 times the dimension of beam weight space. A comparable procedure was described recently by Bedford and Webb (2003). The tuning parameters W_0 , T_0 and R as obtained during the extensive tuning procedure and the stopping criterion described above, were used throughout all experiments described in this paper. For each case and input set of orientations, FSA was run using 5 different random series. The maximum value of the largest achievable PTV dose from these 5 series was used for comparison.

5.2.3.3 Sequential search (Cycle)

This algorithm was described previously in detail by Woudstra and Storchi (2000) and Woudstra and Heijmen (2003). In this paper a brief summary is given. Starting point is an empty plan where no beams are selected. Cycle *sequentially* adds beams (dose distributions) from the potential input orientations. Two criteria must be met to continue the process of selection and addition:

- the prescribed target dose has not been reached.
- none of the imposed hard constraints has been violated.

In order to select a new beam, all available orientations are reviewed, accounting for the already existing dose distribution from the previously selected beams. Each orientation of the input set is initially put into the plan and is evaluated by means of a beam weight increase. This beam weight increase causes a PTV dose increase and an unavoidable further approach to the imposed hard constraints for e.g. the organs at risk. The compromise between these conflicting effects is determined by the maximization of a score function. In this process of evaluation, first, each orientation obtains a temporary weight and a corresponding maximized score value. The orientation with the largest score value is then definitively selected for the plan with its corresponding weight. To avoid sub-optimal plans, new beams are added with relatively low weight. Consequently, favourable beam directions can be selected several times.

Cycle uses a dynamic score function for two reasons:

- to provide the possibility for sequential dose addition, the score function has to be re-defined to account for the new existing dose distribution, after each new beam addition.
- initially, the score function uses equal penalty factors for constraint approach. If a plan generation is not successful and stopped by a constraint hit, the algorithm calculates new penalty factors to better avoid the most critical constraints as observed in the previous generation.

Cycle produces tracks through the beam weight space towards the prescribed target dose within the hard constraints. An example to illustrate the above mentioned explanation is shown in Figure 5.1, which shows a simple 2-dimensional beam weight space of two uniform beams of the configuration shown in the upper right corner ($\theta = 10^\circ$ and $\theta = 300^\circ$). In the beam weight space, lines of equal target dose are represented as parallel lines. The level of the target dose lines increases in the direction of

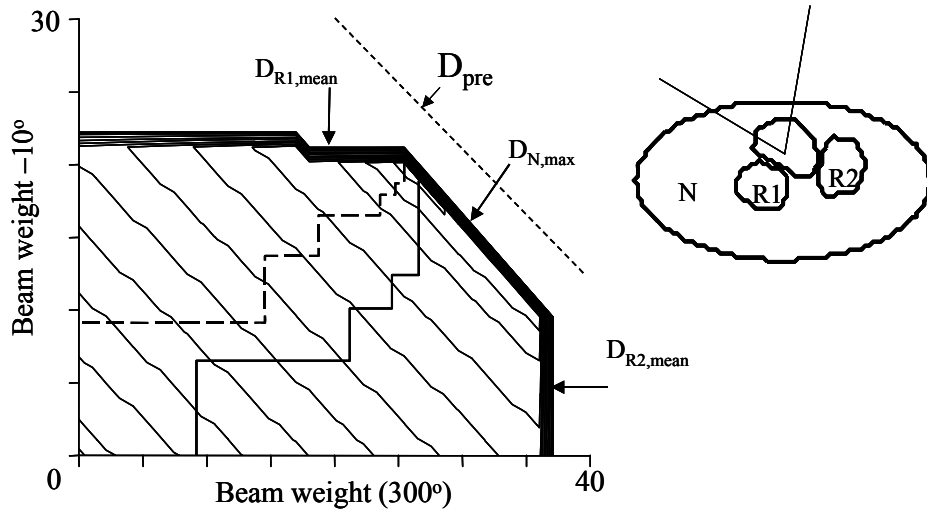


Figure 5.1 Two-dimensional beam weight space indicating the tracks produced by Cycle through this space. Solid line: first plan generation, dashed line: second plan generation after modification of the importance factors.

the enclosing three hard constraints: the mean doses $D_{R1,mean}$ and $D_{R2,mean}$ of the regions R_1 and R_2 , and the maximum dose of the normal tissue $D_{N,max}$. Each plan generation made by Cycle is represented as a ‘track’ in this feasible space. Each corner of the track represents a different orientation selection based on evaluation of both orientations and their respective beam weights. At these positions the score function is re-defined to account for the existing dose distribution. From the tracks, it is shown that both orientations are selected several times, thereby gradually increasing the total beam weight of the orientations. The constraints were selected to be too tight to achieve the prescribed target dose. The first generation ends with an N_{max} constraint hit (solid track). Recalculation of the penalty factor results in track 2 (dashed line), which ends in the corner of two conflicting constraints at closest distance from the prescribed target dose line (dashed line outside constraint area).

It should be noted that the score function as described in this section, should not be confused with the objective function for algorithm comparison in this paper. The score function in Cycle is used only to guide the plan generation process into the direction of the PTV prescription dose level while keeping the largest possible distance to the constraints. In the initial implementation of Cycle this generation process ends when the prescription level has been achieved.

For the comparisons in this paper, we modified this implementation in a way that, once the prescribed target dose is achieved, a new process starts with a 10% larger

prescription than the previous one, until Cycle is no more able to achieve the final prescription. This situation is equal to Figure 5.1, where the prescription level is outside the feasible space.

For each case and input set of orientations and the prescription outside the feasible space, Cycle was allowed to use 5 consecutive plan generations. In between these generations, the penalty factors were re-calculated aiming at avoidance of constraint violations as observed in the previous generation. Also here, the largest achieved objective value (PTV dose in isocentre or mean PTV dose) was used for comparison with the outcomes of ES or FSA. The parameter values as used by Cycle (see Woudstra and Storchi 2000), $p_o=4$ and $\gamma=20$, were not changed throughout all experiments described in this paper.

5.2.4 Cases and prescriptions

5.2.4.1 Pancreas (CFRT)

CT data sets of five patients were used. For this inverse planning comparison, the liver, small bowel, kidneys, spinal cord, and all other tissue outside the target volume, designated OTAR (other tissue at risk) were considered. The applied constraints for PTV (ICRU-50) and the normal tissues are summarized in Table 5.1. Constraints for kidney, small bowel and liver were derived mainly from the results of the SOMALENT conference (Cassidy (1995), Coia (1995) and Lawrence (1995)). These constraints were also used in our previous paper (Woudstra and Heijmen 2003). The target dose homogeneity constraints (see Table 5.1) are based on an initial PTV dose prescription of 50 Gy. As the prescription for the OARs contains DVH-constraints, local maxima are assumed to exist in the feasible space. The beam energy used by the calculation engine for these pancreas cases was 23 MV.

5.2.5 Oesophagus (segmented IMRT)

CT data sets of five patients with a tumour in the thoracic oesophagus were used. Applied constraints are shown in Table 5.2. The target dose homogeneity constraint (see Table 5.2) is 2% of an initial PTV dose prescription of 55 Gy. This prescription is similar to the one used by Nutting *et al* (2001). Both lungs were considered as one organ. Only the lung volume outside the PTV was considered for optimization. The beam energy used was 6 MV.

j	Organ	Constraint
1	PTV	$D_{\text{isoc}}^{\text{pre}} - D_{\text{min}} < 2.5 \text{ Gy}$
2	PTV	$D_{\text{max}} - D_{\text{isoc}}^{\text{pre}} < 3.5 \text{ Gy}$
3	OTAR	$D_{\text{max}} - D_{\text{isoc}}^{\text{pre}} < 5 \text{ Gy}$
4	Liver	$V_{D>40 \text{ Gy}} < 33\%$
5	Liver	$D_{\text{mean}} < 20 \text{ Gy}$
6	Small bowel	$V_{D>50 \text{ Gy}} < 5\%$
7	Small bowel	$D_{\text{max}} < 55 \text{ Gy}$
8	Left Kidney	$V_{D>25 \text{ Gy}} < 33\%$
9	Left Kidney	$D_{\text{mean}} < 15 \text{ Gy}$
10	Right Kidney	$V_{D>25 \text{ Gy}} < 33\%$
11	Right Kidney	$D_{\text{mean}} < 15 \text{ Gy}$
12	Spinal cord	$D_{\text{max}} < 50 \text{ Gy}$

Table 5.1 Prescription and constraints for the five pancreas cases used in this paper. Constraints are expressed using maximum organ doses D_{max} , minimum doses D_{min} , mean doses D_{mean} , or the relative organ volume with a dose value larger than a specified dose level $V_{D>a\text{Gy}}$. $D_{\text{iso}}^{\text{pre}}$ represents the prescribed tumor dose at the isocenter (initially set to 50 Gy).

For the oesophagus cases, 9 and 18 equi-angular BEV shaped segmented IMRT (uniform, wedged and segmented) beams were used as input beam sets for beam selection, generating comparisons in 63 and 126 dimensional spaces respectively (uniform beams, 4 wedge beams and 2 additional beam segments for each orientation).

5.2.6 Beam configurations

For the pancreas cases, initially 5 equi-angular orientations with BEV shaped field and uniform beam intensity were used to shape a 5-dimensional feasible space to provide a starting point for the comparisons between Cycle, FSA and ES. Beam input sets containing 9 as well as 18 equi-angular orientations, with BEV field shape and conventional (uniform and wedged) beam intensity were used for a comparison between Cycle and FSA regarding larger dimensional spaces. This comparison used 45- and 90-dimensional spaces respectively, built by 9 or 18 equi-spaced input orientations having a uniform beam and 4 wedge beams (5 beam weights).

j	Organ	Constraint
1	PTV	$\text{Std}_{\text{PTV}} < 1.1 \text{ Gy}$
2	Lungs	$V_{\text{D} > 18 \text{ Gy}} < 0.15$
3	Spinal cord	$D_{\text{max}} < 45 \text{ Gy}$

Table 5.2 Prescription and constraints for the five oesophagus cases used in this paper. Std_{PTV} is the standard deviation describing the dose inhomogeneity in the PTV. $V_{\text{D} > 18}$ is the patient dependent maximum relative lung volume receiving 18 Gy or higher.

5.2.7 Evaluation of the results

The most important criterion for the evaluation of the results is the largest achievable PTV-dose within constraints. Apart from this objective, the beam numbers of the generated plans and the required calculation times were evaluated.

5.3 Results

Patient	Cycle/ES	FSA/ES
1	0.989	0.966
2	0.997	0.984
3	0.998	0.971
4	0.988	0.989
5	1.000	0.985

Table 5.3 Ratios of maximum obtained PTV dose within constraints. Comparisons between ES, FSA and Cycle for a 5 dimensional beam weight space for the five pancreas cases.

5.3.1 Pancreas

5.3.1.1 Five equi-spaced uniform beams: comparison between ES, FSA and Cycle

As mentioned in section 5.2.1, for this experiment the resolution in the beam weight space was limited to 1 Gy for all three algorithms. In this way, the algorithms used the same grid points in the 5-dimensional beam weight space. As for FSA convergence is hard to achieve for a 1 Gy weight resolution, a large number of iterations was allowed (10000). Generally after 2000 iterations no further improvement was found for FSA. The results of the comparisons are shown in Table 5.3 as relative objective value ratios Cycle/ES and FSA/ES. Compared with ES, Cycle is almost equal (difference $< 1\%$) in 3 cases. Compared with FSA, Cycle is slightly better in 4 cases.

Orientation	70	140	220	290	360
Case 1					
ES	3	5	8	0	20
Cycle	9	5	5	4	13
FSA	8	5	5	1	16
Case 2					
ES	11	15	15	4	21
Cycle	11	15	15	5	20
FSA	11	14	13	7	20
Case 3					
ES	0	8	8	0	28
Cycle	1	8	8	0	27
FSA	3	6	7	4	23
Case 4					
ES	16	21	3	0	24
Cycle	17	26	1	1	19
FSA	20	19	5	3	17
Case 5					
ES	18	6	2	19	0
Cycle	18	6	2	19	0
FSA	21	7	0	16	0

Table 5.4 Positions of the solutions in the five dimensional feasible space as obtained by ES, FSA and Cycle for the five pancreas cases.

However for the three algorithms, the differences are small. Table 5.4 gives the beam weight combinations of the results. These combinations define the positions of the solutions in the 5-dimensional beam weight space. For the cases 2, 3 and 5, the positions of the solutions of the three algorithms are rather close to each other in the feasible space. For cases 1 and 4, both the Cycle and the FSA solution have a significant distance from the ES solution, although the differences between the objective values are rather small.

5.3.1.2 Pancreas, conventional plans (CFRT)

Table 5.5 presents the results as Cycle/FSA ratios of the five pancreas cases for coplanar beam configurations of 9 and 18 equi-angular orientations now applying uniform and wedge beams. Apart from a few somewhat larger deviations, generally the difference

in achieved PTV dose between the algorithms is small. A typical result is shown in Figure 5.2 for case 5 and 9 orientations. It is shown that both algorithms largely agree on the selected orientations and their beam weight. In this case FSA achieved 1.3% more PTV dose at the expense of using more low weight beams.

Patient	9 orientations	18 orientations
1	1.046	1.046
2	1.000	0.998
3	1.060	1.022
4	0.997	1.001
5	0.987	1.030

Table 5.5 Objective ratios Cycle/FSA for 9 and 18 equi-angular input orientations for the five pancreas cases.

5.3.2 Oesophagus (segmented IMRT)

For the five oesophagus cases, input beam sets of 9 and 18 equi-angular orientations were used. The comparison between FSA and Cycle is shown as Cycle/FSA ratio in table 5.6. Also for this comparison, apart from a few somewhat larger deviations, generally the difference in achieved PTV dose between the algorithms is small.

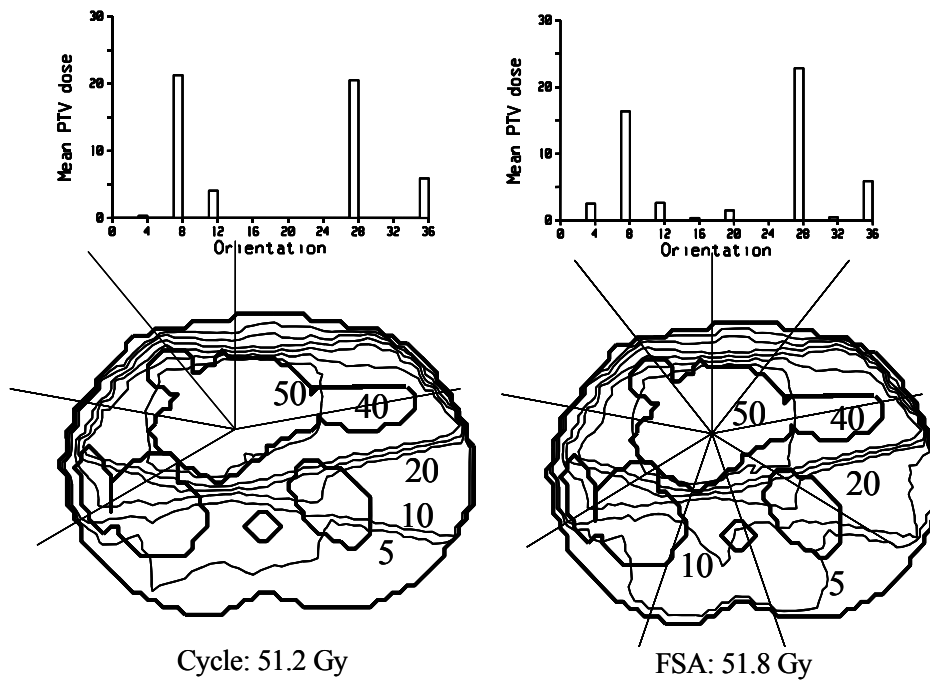


Figure 5.2 Treatment plans and dose distributions as obtained from Cycle and FSA for pancreas case 5 using 9 equidistant input orientations. Upper part: the applied mean PTV dose contribution through each orientation. Orientations are indicated counter clockwise. Lower part: corresponding dose distributions. Isodose lines: 5, 10, 20, 30, 40 and 50 Gy.

Patient	9 orientations	18 orientations
1	1.031	1.086
2	0.958	1.030
3	1.005	1.038
4	0.986	1.010
5	1.009	1.078

Table 5.6 Objective ratios Cycle/FSA for 9 and 18 equi-angular input orientations for the five oesophagus cases.

For most cases, Cycle yields a somewhat better result than FSA, except for case 2 and 9 orientations. A rather large difference is found for case 1 and 18 orientations. A typical case is shown in Figure 5.3 for case 3 and 18 orientations. Also from this figures it is clear that both algorithms largely agree on the selected orientations and their beam weight and FSA was not able to fully switch-off the ineffective orientations.

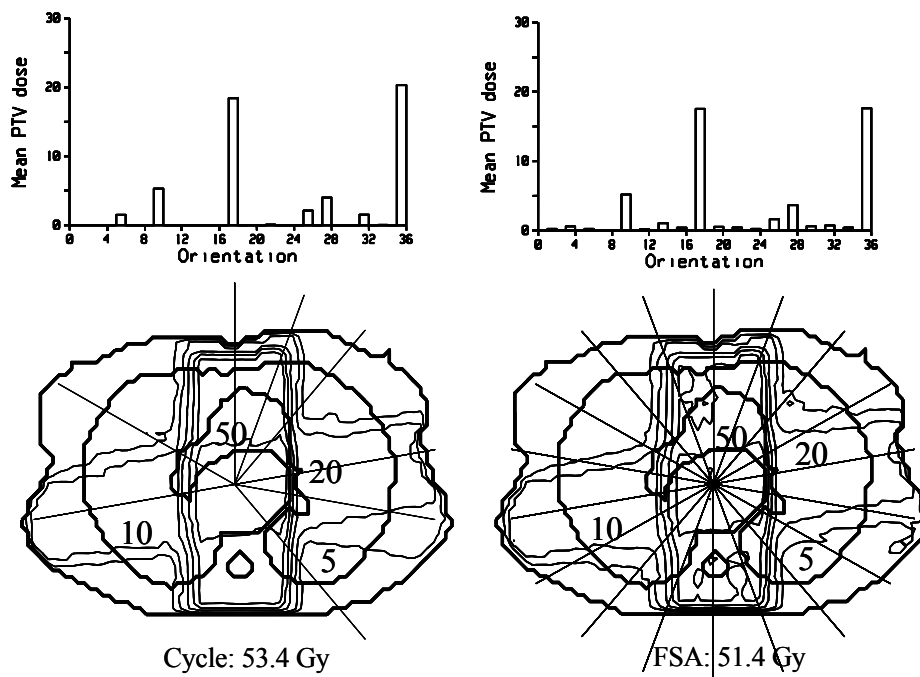


Figure 5.3 Treatment plans and dose distributions as obtained from Cycle and FSA for oesophagus case 3 using 18 equidistant input orientations. Upper part: the applied mean PTV dose contribution through each orientation. Orientations are indicated counter clockwise. Lower part: corresponding dose distributions. Isodose lines: 5, 10, 20, 30, 40 and 50 Gy.

	Calculation time (min)	
	Cycle	FSA
Dimension	5 generations	5 series
25	0.5	4
45	1	15
90	2	60
180	4	200

Table 5.7 Comparison of calculation time between FSA and Cycle.

5.3.3 Calculation time

The calculation time for exhaustive search in the five dimensional solution space is on the average 16 hours and is not very practical for clinical use.

Cycle and FSA have more clinically acceptable calculation times. Table 5.7 shows an overview of the calculation times for the pancreas cases in this study. For increasing dimensionality of the feasible

space, FSA appears to be increasingly time consuming. There are two possible reasons: A larger space dimension needs an increase in the number of iterations to achieve an acceptable convergence and secondly, the calculation of the dose distribution for each new iteration needs more time, because a larger number of dose distributions has to be combined. The calculation times mentioned in Table 5.7 do not include the time required for calculation of the input dose distributions. This pre-calculation takes about 5 minutes for 36 orientations and 7 beam types (1 uniform beam, 4 wedge beams and 2 segmented beams). For this work we have used a Xeon Server System with 3,2 GHz processor and 8 GB memory.

5.4 Discussion

It has been demonstrated that, apart from a few larger deviations, in general Cycle and FSA agree within a few percent on the achievable target dose within the imposed constraints. From this fact one might assume that, for those cases, the results of both algorithms are probably not far away from the global maximum target dose within constraints.

For FSA, we have carried out a few additional experiments such as the use of the multi-dimensional Cauchy distribution and the convergence criterion as described by Mageras and Mohan (1993). None of these experiments did substantially change our results.

The number of orientations from the Cycle plans could probably be minimized even further using the method described in a previous paper (Woudstra and Heijmen 2003). This reduction method has not been used in this paper, as this investigation deals with the strict mathematical exercise to find the maximum PTV dose within constraints in beam weight spaces of predefined dimension.

For oesophagus irradiation the use of a mean dose constraint for lung tissue would have been more useful from clinical perspective. However, instead, we have used a DVH-constraint to increase the probability for the algorithms to get trapped in local optima.

Selection from only 9 or 18 equi-spaced beams, as applied for comparisons between Cycle and FSA, may have an impact on the quality of the solutions, compared to selection from 36 beams, as we normally use for Cycle. In a previous paper (Woudstra and Heijmen 2003), we have compared plans selected from 9 and 36 equi-spaced orientations. Selection from 36 equi-spaced orientations resulted in better plans. In this paper we limited the number of input beams to avoid excessive calculation times with FSA.

The version of Cycle described in this paper, regards strictly coplanar beam orientations. A non-coplanar version has already been developed and is currently being tested. The non-coplanar search will certainly increase the dimension of the beam weight space and this will turn out to be beneficial for Cycle regarding calculation time and convergence in comparison with FSA.

In this study, we applied the equivalent path length method for inhomogeneity correction. The limited accuracy of this method is well known. As Cycle, FSA, and ES all used the same input dose distributions containing this correction, the application of this correction will not affect the comparison regarding the ability of finding the global maximum in the feasible search space. For clinical use we are aware of this deficiency and aim at the incorporation of Cycle in a modern TPS with accurate dose engine.

Using hard constraints instead of the more commonly applied strategy of minimizing an objective function to find a compromise solution for competing treatment goals has been described before (Morrill et al 1991 and Starkschall 2001, Bedford and Webb 2003). An advantage of the use of hard constraints in Cycle is, that the radiation oncologist first gets an answer whether or not the preferred constraints do allow generation of a plan with the requested PTV dose. In case that generation of a plan

with the prescribed PTV dose, while not violating the constraints, turns out to be not possible, the radiation oncologist may accept the plan as it is (with lower PTV dose) or select for the specific case which constraint may be relaxed and by how much, followed by a new plan generation. In Cycle, it is certain, that adaptation of a single constraint parameter will not result in a new plan that is not anymore acceptable for other constraints, whose levels were acceptable in the previous plan. In more commonly applied systems, based on finding a compromise solution based on an objective function, there is often not this guarantee.

The coupling of Cycle with the commercial treatment planning system XiO is currently being investigated.

5.5 Conclusion

In this paper comparisons have been made between Cycle, our algorithm for automatic beam orientation and weight selection, and fast simulated annealing (FSA) and exhaustive search (ES). The question was on the largest achievable target dose within constraints as obtained from the three algorithms. The largest achieved target dose values, in the feasible solution space of all plans obeying the imposed hard constraint levels, were generally very similar for the three algorithms. In some cases FSA resulted in a slightly higher PTV dose than Cycle, at the cost of switching on substantially more beam orientations than Cycle. In other cases, when Cycle generated the solution with the highest PTV dose using only a limited number of non-zero weight beams, FSA seemed to have difficulty in switching off unfavourable directions. Calculation times for ES were clinically unacceptable. Cycle was faster than FSA, especially for feasible large dimensional solution spaces.

References

1. Bedford J L and Webb S 2003 Elimination of importance factors for clinically accurate selection of beam orientations, beam weights and wedge angles in conformal radiation therapy *Med. Phys.* **30** 1788-804
2. Morrill S M et al. 1991 Treatment planning optimization using constrained simulated annealing *Phys. Med. Biol.* **36** 1341-61
3. Morrill S M et al. 1995 Very fast simulated reannealing in radiation therapy treatment plan optimization *Int.J. Radiat. Oncol. Biol. Phys.* **31** 179-188
4. Oldham M, Neal A and Webb S 1995 A comparison of conventional 'forward planning' with inverse planning for 3D conformal radiotherapy of the prostate" *Radio-*

- ther. *Oncol.* **35** 248-62
5. Rowbottom C G, Webb S and Oldham M 1998 Improvements in prostate radiotherapy from customization of beam directions *Med. Phys.* **25** 1171-79
 6. Rowbottom C G, Oldham M, and Webb S 1999 Constrained customization of non-coplanar beam orientations in radiotherapy of brain tumours *Phys. Med. Biol.* **44** 383-99
 7. Rowbottom C G, Khoo V S and Webb S 2001 Simultaneous optimization of beam orientations and beam weights in conformal radiotherapy *Med. Phys.* **28** 1696-1702
 8. Rowbottom C G, Webb S and Oldham M 1998 Improvements in prostate radiotherapy from customization of beam directions *Med. Phys.* **25** 1171-79
 9. Woudstra E and Storchi P R M 2000 Constrained treatment planning using sequential beam selection *Phys. Med. Biol.* **45** 2133-49
 10. Woudstra E and Heijmen B J M 2003 Automated beam angle and weight selection in radiotherapy treatment planning applied to pancreas tumors *Int. J. Radiat. Oncol. Biol. Phys.* **56** 878-88
 11. Bortfeld Th and Schlegel W 1993 Optimization of beam orientations in radiation therapy some theoretical considerations *Phys. Med. Biol.* **38** 291-304
 12. Das S et al. 2003 Beam orientation selection for intensity modulated radiation therapy based on target equivalent uniform dose maximization *Int. J. Radiat. Oncol. Biol. Phys.* **55** 215-24
 13. Mageras G S and Mohan R 1993 Application of fast simulated annealing to optimization of conformal radiation treatments *Med Phys* **20** 639-47
 14. Webb S 1991 Optimizing by simulated annealing of three-dimensional conformal treatment planning for radiation fields defined by a multi-leaf collimator *Phys. Med. Biol.* **36** 1201-26
 15. D. Djajaputra et al. 2003 Algorithm and performance of a clinical IMRT beam angle optimization system *Phys. Med. Biol.* **48** 3191-212
 16. Gaede S, Wong E and Rasmussen H 2004 An algorithm for systematic selection of beam directions for IMRT *Med. Phys.* **31** 376-88
 17. Nutting C M et al. 2001 Optimization of radiotherapy for carcinoma of the parotid gland: a comparison of conventional, three-dimensional; conformal and intensity modulated techniques *Radiother. Oncol.* **60** 163-72
 18. Nutting C M et al 2001 A comparison of conformal and intensity-modulated techniques for oesophageal radiotherapy *Radiother. Oncol.* **61** 157-63
 19. Pugachev A et al. 2001 Role of beam orientation optimization in intensity-modulated radiation therapy *Int. J. Radiat. Oncol. Biol. Phys.* **50** 551-60
 20. Pugachev A, Boyer A and Xing L 2000 Beam orientation optimization in intensity-modulated radiation treatment planning *Med. Phys.* **27** 1238-45
 21. Pugachev A and Xing L 2001 Computer assisted selection of coplanar beam orientations in intensity-modulated radiation therapy *Phys. Med. Biol.* **46** 2467-76
 22. Pugachev A and Xing L 2001 Pseudo Beam's Eye View as applied to beam orientation selection in intensity modulated radiation therapy *Int. J. Radiat. Oncol. Biol. Phys.* **51** 1361-70

23. Pugachev A and Xing L 2002 Incorporating prior knowledge into beam orientation optimization in IMRT *Int. J. Radiat. Oncol. Biol. Phys.* **54** 1565-74
24. Rowbottom C G, Nutting C M and Webb S 2001 Beam orientation optimization of intensity-modulated radiotherapy: clinical application of parotid gland tumours *Radiother. Oncol.* **59** 169-77
25. Soderstrom S, Gustafsson A and Brahme A 1993 The clinical value of different treatment objectives and degrees of freedom in radiation therapy optimization *Radiother. Oncol.* **29** 148-63
26. Soderstrom S and Brahme A 1993 Optimization of the dose delivery in a few field techniques using radiobiological objective functions *Med. Phys.* **20** 1201-10
27. Stein J, Mohan R, Wang X-H, Bortfeld Th, Wu Q, Preiser K, Ling C C and Schlegel W 1997 Number and orientations of beams in intensity modulated radiation treatments *Med. Phys.* **24** 149-60
28. S. Webb 1989 Optimization of conformal radiotherapy dose distributions by simulated annealing *Phys. Med. Biol.* **34** 1349-70
29. J.O. Deasy 1997 Multiple local minima in radiotherapy optimization problems with dose volume constraints", *Med. Phys.* **24** 1157-61
30. Llacer J et al 2003 Absence of multiple local minima effects in intensity modulated optimization with dose-volume constraints *Phys. Med. Biol.* **48** 183-210
31. Rowbottom C G and Webb S 2002 "Configuration space analysis of common cost functions in radiotherapy beam weight optimization algorithms", *Phys. Med. Biol.* **47** 65-77
32. Wu Q and Mohan R 2002 Multiple local minima in IMRT optimization based on dose volume criteria *Med. Phys.* **29** 1514-27
33. Wu C, Jeraj R and Mackie Th R 2003 The method of intercepts in parameter space for analysis of local minima caused by dose volume constraints *Phys. Med. Biol.* **48** N149-N157
34. Jeraj R, Wu C and Mackie Th R 2003 Optimizer convergence and local minima errors and their clinical significance *Phys Med Biol* **48** 2809-27
35. Oldham M and Webb S 1995 The optimization and inherent limitations of 3D conformal radiotherapy treatment plans of the prostate *BJR* **68** 882-93
36. Cassidy J R 1995 Clinical Radiation Nephropathy *Int. J. Radiat. Oncol. Biol. Phys.* **31** 1249-56.
37. Coia L R 1995 Late effects of radiation therapy on the gastrointestinal tract *Int. J. Radiat. Oncol. Biol. Phys.* **31** 1213-1236.
38. Lawrence ThS. 1995 Hepatic toxicity resulting from cancer treatment. *Int. J. Radiat. Oncol. Biol. Phys.* **31** 1237-12

CHAPTER 6
GENERAL DISCUSSION

6.1 Introduction

This thesis describes the development of Cycle, an algorithm for selection of beam orientations and weights to automatically generate radiotherapy treatment plans. Cycle aims at generation of an acceptable treatment plan, meaning that the prescribed tumor dose is delivered while strictly obeying the imposed hard constraints for organs at risk and PTV dose homogeneity. Generally, more acceptable plans may exist for a patient. There is not an explicit force to find the ‘best’ acceptable plan, although the plan generation process has a tendency to optimally avoid approaching constraint levels.

In Cycle beams are selected sequentially. For selection of each new beam to be added, all available orientations are reviewed by temporarily adding the beam to the already existing plan and optimising its weight; the orientation that is finally selected, has the best compromise between a PTV dose increase, and an unavoidable further approach towards the imposed hard constraints. This best compromise is determined by the applied score function.

Plan generation is carried out in an iterative way: at the start of the plan generation process, the score function has equal penalty factors for approaching each of the various constraints. In case these initial factors do not result in a plan that delivers the prescribed tumour dose without violating constraints, the algorithm automatically calculates new factors based on the dose distribution results of the previous generation and generates a new plan. The new penalty factors favour selection of orientations that better avoid constraints that were violated in the previous run.

A possible second iteration procedure gives Cycle an optimisation functionality. For example, an acceptable plan with the highest possible PTV dose can be generated by repeated generations of acceptable plans with increasing PTV dose prescription levels until an acceptable plan can no longer be obtained. Optimal sparing of a specific organ at risk can be realized by repeated plan generation with an increasingly strict constraint level, until the prescribed tumour dose can no longer be delivered without constraint violation. Finally, for optimisation, one may define an arbitrary objective function to be used as an additional hard constraint, followed by maximisation of this constraint for a specific PTV dose prescription.

6.2 Sequential beam selection

As Cycle is not an optimisation algorithm, it is meaningless to question whether the

best treatment plan has been found. In spite of this, one may criticize that sequential search has limited possibilities regarding the freedom of weight and orientation selection, which is needed to handle the correlated beam weights and orientations of a treatment plan. In essence there is no way to ‘undo’ the selections of weights and orientations.

This question was investigated in chapter 5. Here, for a group of patients, Cycle was compared with stochastic search and exhaustive search to find the largest possible PTV dose within constraints. In general, very similar results were obtained from the three algorithms. Because this comparison regards a limited number of patients and a limited number of constraints, future work should further clarify this point.

Nevertheless, experience with clinical cases has shown that Cycle is able to find substantially better solutions for cases, which were considered too difficult to find a solution in a long trial-and-error manual treatment planning process.

6.3 Hard constraints

Contrary to most commercial inverse planning systems, Cycle uses hard constraints during plan generation. The use of hard constraints has advantages as well as disadvantages:

- In the case that an acceptable solution cannot be found by Cycle, the program shows the maximum allowed PTV dose for the existing constraint levels, and a diagnosis on the conflicting constraints. The patient may then be treated with a lower dose or the radiotherapy team may decide to relax a limiting constraint followed by a new automatic plan generation. An *advantage* of this procedure is that a compromise to the dose prescription is made only when it has become clear that an acceptable solution does not exist. The user may then decide the level of compromise, instead of the algorithm. An additional advantage of *dose* based hard constraints is that the corresponding treatment plan and the dose distribution directly reflect the prescription. Based on this result, the clinician may decide on the compromise to the prescription. The current version of Cycle does not supply the user with data on the sensitivity of the achievable target dose for the various dose-limiting constraints. Future development may generate this data.
- The use of hard constraints may have some limitations as well: at this moment the clinical knowledge to define and describe the optimal treatment plan in terms of dose

distribution parameters is not yet available. In other words, it is not always known how to define a prescription (dose parameters and constraint levels) in order to find a treatment plan that is considered suitable from the perspective of clinical experience. Future clinical trial will extend our knowledge on this point.

- An acceptable solution may found to be far from all imposed constraints. This may indicate an ill-defined condition. The question arises, whether the corresponding solution is optimal regarding the distance to all constraints. Although Cycle tends to generate treatment plans with a more or less equal spread of unwanted dose over the various constraints, the sensitivity for dose addition to an OAR will decrease when the constraint levels are much too wide. Therefore the selection of orientations will become less accurate as well. The best way to achieve an acceptable treatment plan for such cases is to tighten the constraints, until Cycle needs a few iterations to achieve the prescribed target dose.

The current use of dose and dose-volume parameters to define a prescription for an acceptable treatment plan is not a limitation of Cycle. Although not yet implemented, Cycle can be extended easily with constraints having a biological basis.

6.4 IMRT and beam orientation selection

For several commercially available treatment planning systems it has been demonstrated that increasing the number of input orientations may deteriorate the quality of the optimised IMRT plan (Chapter 4). Obviously, the applied algorithms are unable to switch off less favourable beam orientations. In chapter 4 of this thesis Cycle is extended with segmented IMRT for partial shielding of organs at risk. Segmented IMRT plans have been generated for a group of oesophagus cancer patients. It was clearly demonstrated that the best plans are generated with the largest number of allowed input beam orientations, although most of these beams have zero weight in the final plan. This observation is in agreement with the general idea on optimisation problems that more degrees of freedom should result in better solutions. Also other investigators have pointed at the importance of selection of appropriate beam angles, also in case of IMRT. As explained in Chapter 4, the possibilities for IMRT plan generation with Cycle are limited. In future investigations Cycle will be extended with more advanced IMRT features. New planning studies should then be performed to find out for which cases and to what extent, automated beam orientation selection still results in better plans.

6.5 Clinical implementation

The calculation time needed for a treatment plan generation is determined by the time needed for pre-calculation of the input dose distributions, and the time for plan generation. Chapter 5 concludes that this time is acceptable for clinical application. At this moment, the pre-calculation uses a beam model that is considered to be too simple for large scale clinical application. However the plan generation algorithm is independent of this pre-calculation and may be connected to any pre-calculated dose distributions from whatever beam model. Therefore, this algorithm will be integrated in a commercial treatment planning system.

SUMMARY

This thesis describes the development of an algorithm (called: Cycle) for automated beam orientation and weight selection in radiotherapy treatment planning. The basic features are described in chapter 2. Extensions and evaluations are topics of the chapters 3, 4 and 5. The algorithm aims at delivery of the prescribed dose to the target volume without violation of constraints for target, organs at risk and the surrounding normal tissue. Pre-calculated dose distributions for all candidate orientations are used as input. Treatment beams are selected in a sequential way. A score function is used for the simultaneous selection of subsequent beam orientations and weights. In order to determine the optimum choice for the orientation and the corresponding weight of each new beam, the score function is first redefined to account for the dose distribution of the previously selected beams. During each selection the target dose is increased with relatively small dose quantities ($< 5\text{Gy}$). Addition of more beams to the plan is stopped when the target dose is reached or when no additional dose can be delivered without violating a constraint. In the latter case the score function is modified by importance factor changes to enforce better sparing of the organ with the limiting constraint and the algorithm is run again. Cycle is not an optimisation algorithm. Cycle aims to find one of the plans that deliver the prescribed tumour dose while strictly obeying the imposed constraints. By iterative use of Cycle, plans can however be optimised for a certain parameter, e.g. for minimization of the mean lung dose (chapter 4), or to maximize the delivered tumour dose (chapter 3).

In chapter 3 the clinical value of Cycle for irradiation of pancreas tumors was investigated. By repeated use of Cycle, beam numbers were minimized and/or the tumor dose was escalated. Comparisons were made with clinical plans and equi-angular plans. Compared to clinical plans, the generated plans with the same number of beams yielded a substantial reduction in the dose to critical tissues. Using the algorithm, an escalated tumour dose of 58 Gy could be achieved for two cases. Maximum dose escalations required a minimum of only 3-4 well selected beam orientations. Cycle resulted in acceptable treatment plans with clinically useable numbers of beams, even for escalated tumour doses. Generated plans were superior to the clinically applied plans and to equi-angular set-ups. Regarding the number of input orientations, selections from the largest number of orientations appeared to have the best dose escalation potential. Selection from a large set of input orientations does not necessarily result in a plan with more orientations but in a more proper orientation selection.

Chapter 4 describes an extension of Cycle for segmented IMRT. For oesophagus cancer patients, it was investigated whether automated orientation selection from a

large number of equi-angular input beam directions (up to 36) for IMRT optimisation could result in improved lung sparing. For a prescribed mean PTV dose of 55 Gy, Cycle was used in an iterative procedure to minimise the mean lung dose under the following hard constraints: standard deviation for PTV dose inhomogeneity 2% (1.1Gy), maximum spinal cord dose 45 Gy. Conformal radiotherapy (CFRT) and IMRT plans for a standard four field oesophagus beam configuration were compared with IMRT plans, generated by automated selection from 9 or 36 equi-angular input beam orientations. Comparisons were also made with dose distributions generated with our commercial treatment planning system (TPS), and with observations in the literature. Using Cycle, automated orientation selection from 9 or 36 input beam directions resulted in improved lung sparing compared to the 4-field set-ups. The study showed a further decrease of mean lung dose with increasing number of input orientations. On average only seven beams with a non-zero weight were sufficient to obtain the lowest mean lung dose, yielding clinically acceptable plans even in case of 36 input directions for the optimisation process. With our commercial TPS we observed the same contra-intuitive, unfavourable results as reported in the literature; 9-field equi-angular IMRT plans had substantially higher mean lung doses than plans for the conventional 4-field set-ups. For all cases, the Cycle plans generated from nine equi-angular input directions were superior compared to similar plans generated with our commercial TPS.

Finally, Cycle was compared with exhaustive search (ES) and fast simulated annealing (FSA), for cases where local optima are supposed to be present in the solution space (chapter 5). Five pancreas and five oesophagus cases previously treated in our institute were selected for this comparison. Plans were generated by ES, FSA and Cycle, using the same hard dose and dose-volume constraints, and the largest possible achieved PTV doses as obtained from these algorithms were compared.

The largest achieved PTV dose values were generally very similar for the three algorithms. In some cases, FSA resulted in a slightly higher PTV dose than Cycle, at the cost of switching on, substantially more beam orientations than Cycle. In other cases, when Cycle generated the solution with the highest PTV dose using only a limited number of non-zero weight beams, FSA seemed to have difficulty in switching off unfavourable directions. Calculation times for ES were clinically unacceptable. Cycle was faster than FSA, especially for feasible large dimensional solution spaces.

SAMENVATTING

Dit proefschrift beschrijft de ontwikkeling van een algoritme (Cycle genaamd) om bundelrichtingen en bundelgewichten automatisch te selecteren voor het maken van een bestralingsplan voor de radiotherapie. De basiseigenschappen van dit algoritme worden beschreven in hoofdstuk 2. Uitbreidingen van het algoritme en de evaluatie ervan zijn beschreven in de hoofdstukken 3, 4 en 5.

Het algoritme streeft naar de afgifte van de voorgeschreven dosis in het doelgebied, zonder het overschrijden van andere dosislimieten m.b.t. het doelgebied en dosislimieten m.b.t. de risico-organen en het verdere omgevende normale weefsel. Vooraf berekende dosisverdelingen van alle kandidaat richtingen worden als input gebruikt. De bundels worden na elkaar geselecteerd. Een score functie wordt gebruikt voor de gelijktijdige selectie van elke volgende bundel en het bijbehorende bundelgewicht. Om de optimale keuze te bepalen voor de richting en het bundelgewicht van elke nieuwe bundel wordt de scorefunctie eerst opnieuw gedefinieerd om de reeds bestaande dosisverdeling van de eerder gekozen bundels in rekening te brengen. Gedurende elke nieuwe selectie wordt de dosis in het doelgebied verhoogd met een relatief kleine hoeveelheid (< 5 Gy). Het toevoegen van bundels aan het plan wordt stopgezet wanneer de dosis in het doelgebied wordt bereikt of wanneer er geen dosis meer kan worden toegevoegd zonder het overschrijden van de dosislimieten. In het laatste geval, wordt de score functie gewijzigd d.m.v. verandering van de ‘importance’ factoren, om een sterkere sparing te bewerken van een orgaan, waarvan de dosislimiet werd bereikt, waarna het algoritme opnieuw kan worden uitgevoerd. Cycle is geen optimalisatie algoritme. Het doel is om één van de bestralingsplannen te vinden die de voorgeschreven dosis in het doelgebied kunnen leveren, waarbij bovendien strict voldaan wordt aan de opgelegde dosislimieten. Bij een iteratief gebruik van Cycle kunnen bestralingsplannen geoptimaliseerd worden wat betreft een bepaalde parameter, zoals het minimaliseren van de gemiddelde long dosis (hoofdstuk 4) of het maximaliseren van de toegediende tumordosis (hoofdstuk 3).

In hoofdstuk 3, wordt de klinische waarde van Cycle onderzocht wat betreft het bestralen van pancreas tumoren. Door het herhaald gebruik van Cycle, kan het aantal bundels geminimaliseerd worden en/of de toegediende dosis gemaximaliseerd worden. Vergelijkingen van Cycle zijn uitgevoerd met klinische plannen en plannen met gelijkmatig verdeelde bundelrichtingen. Vergeleken met klinische plannen, leverden de plannen van Cycle en een zelfde aantal bundels een aanzienlijke reductie van de dosis in kritieke organen. Met Cycle kon een verhoogde tumordosis van 58 Gy

worden bereikt in twee gevallen. Plannen met gemaximaliseerde dosis konden gemaakt worden met 3-4 goed gekozen richtingen. Cycle leverde acceptabele plannen met klinisch bruikbare aantallen bundels, zelfs bij gemaximaliseerde tumordosisniveaus. De plannen van Cycle waren beter dan de klinische plannen of de plannen met gelijkmatig verdeelde bundelrichtingen. Wat betreft het aantal richtingen waaruit gekozen kon worden, hadden selecties met keuze uit een groot aantal richtingen de beste mogelijkheden voor maximalisatie van de tumordosis. Selectie uit een groot aantal richtingen betekent niet noodzakelijk een resultaat met meer richtingen, maar leidt tot een nauwkeuriger keuze van de richtingen.

Hoofdstuk 4, beschrijft een uitbreiding van Cycle voor gesegmenteerde intensiteits gemoduleerde radiotherapie (IMRT). Voor patienten met slokdarmkanker werd onderzocht of automatische selectie van richtingen uit een groot aantal keuze richtingen (tot 36) bij gesegmenteerde IMRT zou kunnen leiden tot verbeterde longsparring. Bij een voorgeschreven gemiddelde dosis in het doelgebied van 55 Gy werd Cycle gebruikt in een iteratieve procedure om de gemiddelde longdosis te minimaliseren bij de volgende harde dosislimieten: standaarddeviatie van de dosis in het doelgebied kleiner dan 2% (1,1Gy) en de maximum dosis in het myelum kleiner dan 45 Gy. Conventionele plannen met conforme velden (CFRT) en IMRT plannen met een standaard 4-bundel configuratie werden vergeleken met gegenereerde IMRT plannen met 9 en 36 gelijkmatig verdeelde keuzerichtingen. Er werden ook vergelijkingen gemaakt met dosisverdelingen die gegenereerd werden door ons klinisch gebruikte planningsysteem en met waarnemingen uit de literatuur. Met het gebruik van Cycle leidde automatische richtingskeuze uit 9 of 36 keuze richtingen tot verbeterde longsparring in vergelijking met de standaard 4-bundel configuratie. De studie liet een verdere verlaging van de gemiddelde longdosis zien met een toenemend aantal keuze richtingen. Gemiddeld waren zeven richtingen voldoende om de laagste gemiddelde longdosis te bereiken. Hierbij werden klinisch acceptabele plannen gemaakt zelfs bij het gebruik van 36 keuze richtingen in het optimalisatieproces. Met het door ons klinisch gebruikte planning systeem werden dezelfde onbegrepen en ongunstige resultaten gevonden als in de literatuur: plannen met negen gelijkmatig verdeelde richtingen hadden een aanzienlijk hogere longdosis dan plannen met de conventionele 4-bundel configuratie. In alle gevallen waren de plannen uit Cycle met 9 hoeken beter dan die uit het door ons klinisch gebruikte planning systeem.

Tenslotte is Cycle vergeleken met andere algoritmen zoals: 'exhaustive search' (ES) en 'fast simulated annealing' (FSA) voor gevallen waarbij locale optima verondersteld worden aanwezig te zijn in de mathematische oplossingsruimte (hoofdstuk 5). De vijf

eerder genoemde pancreas patienten en de vijf slokdarm patienten werden gekozen voor deze vergelijking. Er werden plannen gegenereerd m.b.v. ES, FSA en Cycle, gebruikmakend van dezelfde harde dosis- en dosis-volume- limieten en de hoogst mogelijk bereikbare dosis in het doelgebied uit deze algoritmen werden met elkaar vergeleken.

De hoogste bereikte dosiswaarden lagen in het algemeen dicht bij elkaar voor de drie algoritmen. In sommige gevallen resulteerde FSA in iets hogere PTV dosiswaarden dan Cycle ten koste van het gebruik van meer bundelrichtingen dan Cycle. In andere gevallen waarbij Cycle de hoogste PTV dosis leverde en waarbij Cycle gebruik maakte van een zeer beperkt aantal bundelrichtingen, had FSA soms moeite met het uitschakelen van ongunstige richtingen. De rekentijden van ES waren klinisch onacceptabel. Cycle bleek sneller dan FSA vooral bij oplossingsruimten met hoge dimensie.

ACKNOWLEDGEMENTS

This work has turned out a fascinating journey, from a nice idea to generate a radiotherapy treatment plan, to the examination of multidimensional beam weight spaces. However, I did not make this journey on my own. Many persons have contributed to this work:

Marleen Keizer from the Technical University Delft (Mathematical Physics) allowed me to use the software of their dose calculation engine, which was previously developed by two students in cooperation with our radiotherapy department.

Pascal Storchi was always ready for stimulating discussions on this subject even long before the start of this project. His everlasting support and attention for this work and finally his thorough review of the algorithm have been very valuable to me.

Ben Heijmen has supervised this project and guided me to expand the development of the algorithm to the main topics of this work, always putting forward very critical questions during challenging discussions. His continuous support has motivated me to hold out especially in moments of set-back and disappointment.

Peter Levendag has always been an important drive for the technical innovations. As the head of this radiotherapy department, he has provided the necessary and indispensable conditions for this work to flourish.

Because this work was done partly in my spare time and partly during normal working hours, some of my colleagues have experienced the burden of this work as well. Especially, Henk Swarte, Henk v.d.Werf, and Huub Pennings have treated me with much understanding and patience.

The beauty and the burden of this work have also strongly influenced my private life. My dear wife Josien, my sons Evert-Jan, Jitse and Friso, and my only daughter Jantine have largely shared the joys and disappointments during this work. They allowed me to spend a lot of my spare time to this work and they have created an atmosphere of happiness at home, supporting me to recover from fatigue.

I also want to mention my parents, who have provided my life with many good things. Their interest, encouragement, support and advice have been very valuable to me.

Finally, I want to spend a few words to the rather uncommon Bible verse cited in the beginning of this thesis. Sarah, the wife of patriarch Abraham, used these words after she had given birth to a son. She and her husband had been promised by God to have innumerable many descendants. Sarah, however, appeared to be infertile and she had

come to an age, much too old for a pregnancy. After this miraculous birth of her only son, she expressed her gratefulness unto God with these words because of this amazing change of her life.

These words of Sarah remind me to the long period of time where I have struggled with basic ideas of treatment plan generation, without being successful from scientific perspective. After many attempts, I finally started to think of giving in and to consider myself as scientifically unproductive.

Then, in the afternoon of my life, suddenly, there was a change and I faced a breakthrough. I felt myself filled with creativity as never before. I was astonished about this sudden change of my life.

Therefore, with these words, borrowed from Sarah, I also want to express my gratefulness unto God, Who guides my life. I want to thank Him for this unexpected and joyful period in my life and for the creativity, the energy and the perseverance that He has given to me, to do this work.

CURRICULUM VITAE

Evert Woudstra was born on the 25th of May 1952 in The Hague. After a few years (1958), his family moved to Delft, where he visited various schools and education levels and finally studied Technical Physics at the Technical University of Delft. He decided to choose medical informatics as a main area of interest and obtained his masters degree in January 1976, after a study on pattern recognition of vector cardiograms.

Then, in a short break, he joined the army for military service and did some scientific work on pattern recognition and image processing. After this break, he continued to follow his main interest for medical physics with an appointment at the Rotterdam Radiotherapy Institute as a clinical physicist in October 1977.

In 1978, he married with Josien Pauw and in a period of 10 years, four children were born. Apart from the beauty of a growing family, the fascinating job as a clinical physicist resulted in a continuation of this work for a long period of almost 29 years, up to now.

Main areas of interest through these years have been: clinical application of high-energy electron beams, calculation models for photon and electron beams and the clinical use of treatment-planning systems. Parallel to these duties, the mechanism of the generation of dose distributions, especially applied to non-standard problems, became a main challenging subject for study. In 1997 such a study could be started and has finally resulted in this thesis.